VOLTAMMETRIC ANALYSIS OF PESTICIDES AND THEIR DEGRADATION: A CASE STUDY OF AMITRAZ AND ITS DEGRADANTS

A thesis submitted in fulfilment of the requirements for the degree of

MASTERS IN SCIENCE

of

RHODES UNIVERSITY

by

RORY DENNIS BRIMECOMBE

January 2006

ABSTRACT

Amitraz is a formamide acaricide used predominantly in the control of ectoparasites in livestock and honeybees. Amitraz hydrolysis is rapid and occurs under acidic conditions, exposure to sunlight and biodegradation by microorganisms. The main hydrolysis product of amitraz, 2,4-dimethylaniline, is recalcitrant in the environment and toxic to humans.

An electrochemical method for the determination of total amitraz residues and its final breakdown product, 2,4-dimethylaniline, in spent cattle dip, is presented. Cyclic voltammetry at a glassy carbon electrode showed the irreversible oxidation of amitraz and 2,4-dimethylaniline. A limit of detection in the range of 8.5×10^{-8} M for amitraz and 2×10^{-8} M for 2,4-dimethylaniline was determined using differential pulse voltammetry. Feasibility studies in which the effect of supporting electrolyte type and pH had on electroanalysis of amitraz and its degradants, showed that pH affects current response as well as the potential at which amitraz and its degradants are oxidised. Britton-Robinson buffer was found to be the most suitable supporting electrolyte for detection of amitraz and its degradants in terms of sensitivity and reproducibility.

Studies performed using environmental samples showed that the sensitivity and reproducibility of amitraz and 2,4-dimethylaniline analyses in spent cattle dip were comparable to analyses of amitraz and 2,4-dimethylaniline performed in Britton-Robinson buffer. In addition, the feasibility of measuring amitraz and 2,4-dimethylaniline in environmental samples was assessed and compared to amitraz and 2,4-dimethylaniline analyses in Britton-Robinson buffer. Amitraz and 2,4-dimethylaniline were readily detectable in milk and honey.

Furthermore, it was elucidated that 2,4-dimethylaniline can be metabolised to 3-methylcatechol by *Pseudomonas* species and the proposed breakdown pathway is presented. The biological degradation of amitraz and subsequent formation of 2,4-dimethylaniline was readily monitored in spent cattle dip. The breakdown of amitraz to 2,4-dimethylaniline and then to 3-MC was monitored using cyclic voltammetry.

ACKNOWLEDGEMENTS

- First and foremost I would like to extend my sincerest gratitude to my supervisor, Dr. Janice Limson, who nurtured my fascination for electrochemistry and exercised a great amount of understanding and patience, and who's in depth knowledge of the field has assisted in moulding my own fascination with the discipline.
- To my lab partners, Ronen Fogel and Nasheen Ragubeer I extend thanks for support and assistance in all aspects.
- Thank you to all my colleagues in the department.
- To Dr. Garth Cambray I extend my thanks for invaluable input.
- To my Mother and Father I extend my gratitude for being supportive. Recognising my ambition and assisting me in reaching my goals by both providing resources and emotional support. To my siblings for putting up with my 'tedious' discussions on electrochemistry.
- To the National Research Foundation I extend my gratitude, without who's funding this project would not have been possible.
- A special thanks goes to Bronwyn Moore, for her support and assistance in the proof reading of this thesis.
- And to the many friends I have made along the way, thank you for your support.

TABLE OF CONTENTS:

LIST OF ABBREVIATIONS:

In alphabetical order:

• 2,4-DMA	2,4-dimethylaniline
• 3-MBQ	3-methyl-*o*-benzoquinone
• 3-MC	3-methylcatechol
• A	Amps
• AE	Auxiliary electrode
• BAS	BioAnalytical Systems
• BR	Britton-Robinson buffer
• CVs	Cyclic voltammograms
• DMF	2,4-dimethylphenyl formamide
• DMPF	2,4-dimethylphenyl formamidine
• DMSO	Dimethyl sulphoxide
• DPV	Differential pulse voltammetry
• ECD	Electron capture detector
• ECECE	Electrochemical, Chemical
• GC	Gas chromatography
• GCE	Glassy carbon electrode
• HMDE	Hanging mercury drop electrode
• HPLC	High performance liquid chromatography
• I	Current
• *pa*	Anodic current
• *pc*	Cathodic current
• LLE	Liquid-liquid extraction
• LOD	Limit of detection
• MPC	metallophthalocyanine
• MS	Mass spectrometer
• MV/s	Millivolts per second
• NPD	Nitrogen-phosphorous detector
• O	Oxidation
• OD	Optical density
• PPM	Parts per million
• R	Reduction
• RE	Reference electrode
• RPM	Revolutions per minute
• SCE	Saturated calomel electrode
• SD	Standard deviation
• SPE	Screen printed electrode
• SPME	Solid-phase micro-extraction
• Spp.	Species
• TMB	Tetramethylbenzidine
• UV	Ultra violet
• V	Volts
• WE	Working electrode
• TCA	Tricarboxylic acid cycle

LIST OF FIGURES:

LIST OF SCHEMES:

LIST OF TABLES:

CHAPTER 1
OVERALL INTRODUCTION

1.1 BACKGROUND

One of the largest liabilities in the agricultural sector is the loss of crop and meat produce due to the action of insect pests, which target specific hosts, and can cause disease and lesions on fruit and vegetables. Ticks and mites cause substantial damage given that some are vectors for parasites that are lethal to livestock (McConnell *et al.* 2002, Hapeman *et al.* 2002, Rice *et al.* 1984). Even though pesticides are considered toxic and harmful to the environment, their utilisation as a means to control pests has continued due to a lack of an alternative, equivalent and effective method. Biological control methods are being researched and put into place, which involve genetic modification of fruits to withstand pests. However applications of these techniques are currently ethically controversial and a substantial amount of time will go by before they are utilised to the same extent as pesticides (Kagaruki 1996, Rule & Ianga 2005).

Through their ability to disperse in the environment, recalcitrant nature, and propensity for uptake into crops and residues in livestock meat and milk, pesticides and their components represent a significant risk in terms of air, water, soil and food contamination (Torres *et al.* 1996, Bogdanov *et al.* 2002, Korta *et al.* 2003, Arrebola *et al.* 2003, Pugliese *et al.* 2004). Humans are inevitably exposed to pesticides either through environmental contamination, or occupational use (pesticide formulation, manufacture and application) (Hodgson *et al.* 1991, Bolognesi 2003).

A possibility exists that components with no direct pesticidal activity, in the pesticide formulation, may have a higher degree of toxicity than the active ingredient itself (Osano *et al.* 2002, Bolognesi 2003). Pesticide formulations are produced to target a specific group of pests, although absolute specificity is difficult to achieve and human exposure to these formulations will be likely to have toxic contra-indications (Stewart *et al.* 1999, Bolognesi 2003).

Human intake of trace amounts of pesticide and their components is a growing health concern (Stewart *et al.* 1999, Bolognesi 2003). In the developing world, self-poisoning by pesticides is common. Worldwide, nearly 3 million cases of self-poisoning, of which 220 000 are fatal, are reported each year (Bolognesi 2003). In South Africa, 33% of all reported self-poisoning cases are due to agri-chemicals (Stewart *et al.* 1999). Certain pesticides, such as the group of organophosphates which include methidathion and dichlorvos, are structurally and functionally similar to nerve agents used in biological warfare. These pesticides are neurotoxic even in trace amounts. In addition, many pesticides and/or their components are potentially carcinogenic (Campbell & Needham 1984, Abu-Basha *et al.* 1999, Altobelli *et al.* 2001), teratogenic (Evans & Gee 1980, Abell *et al.* 2000, Bolognesi 2003), genotoxic (Hugnet *et al.* 1996, Kennel *et al.* 1996, Bolognesi 2003), hepatotoxic (Hsu & Kakuk 1984, Jorens *et al.* 1997, Aydin *et al.* 1997), neurotoxic (Costa *et al.* 1989, Ralide 1992) or a combination of these (Rojas *et al.* 2000, Zahm *et al.* 1997, Dearfield *et al.* 1999).

Cases of amitraz toxicity to humans have been reported, with symptoms including hyperglycemia, bradycardia, hypotension, headache, nausea, drowsiness, vomiting, polyuria, rash, stiffness, swelling and coma (Weissenberger *et al.* 1990, Kennel *et al.* 1996, Jorens *et al.* 1997).

Amitraz (N-(2,4-dimethylphenyl)-N'-[dimethylphenyl)-imino]methyl-N-methyline ethanimidamide) (figure 1.1) is a formamide pesticide with contact and respiratory action used predominantly against mites and ticks (*Boophilus microplus)* found on cattle, sheep and pigs (Foil *et al.* 2004, Li *et al.* 2004).

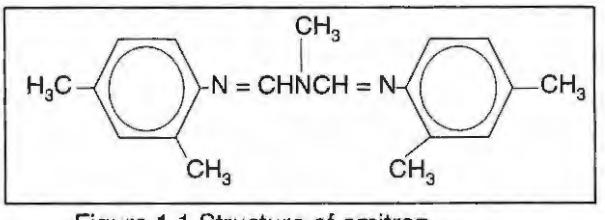

Figure.1.1 Structure of amitraz

Variants of the amitraz formulation are also used for the control of eriophyid mites, mealybugs, scale insects, whitefly, pear suckers, aphids and first instar larvae of Lepidoptera on citrus, cotton, strawberries, apples, hops, aubergines, tomatoes, and ornamental plants (Corta *et al.* 1999, Tseng *et al.* 1999). Additionally, amitraz has been

used against varroasis disease caused by the mite *Varroa jacobsoni* which affects *Apis mellifera* (honeybees) (Corta *et al.* 1999, Tseng *et al.* 1999, Bernal *et al.* 1997, Floris *et al.* 2001).

Under certain conditions, amitraz is believed to hydrolyse to formamidine and formamide intermediates, such as 2,4-dimethylphenylformamidine (2,4-DMPF) and 2,4-dimethylphenylformamide (2,4-DMF), with eventual hydrolysis to 2,4-dimethylaniline (2,4-DMA), which is genotoxic, teratogenic, potentially hepatotoxic and carcinogenic (Hall *et al.* 1975, Abu-Basha *et al.* 1999, Corta *et al.* 1999). In addition to its toxicity, 2,4-DMA is recalcitrant in a range of environmental matrices, which is a serious cause for concern.

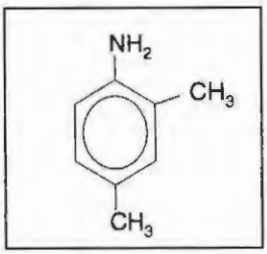

Figure 1.2 Structure of 2,4-dimethylaniline

The importance of the biological fate of 2,4-dimethylaniline

The biological degradation of 2,4-DMA has not been well characterised or understood, nor its degradants confirmed. However, theoretical pathways can be drawn from the breakdown of structurally similar aniline derivatives.

It is proposed that 2,4-DMA can be degraded to a methylcatechol derivative through oxidative deamination that is usually performed by *Pseudomonas* species (spp.) (Park *et al.* 1999, Pinheiro *et al.* 2004, Nachiyar & Rajakumar 2004, Jacques *et al.* 2005). Nachiyar & Rajakumar 2004 have postulated that *N,N'*-DMA derivatives degrade to *N*-methylcatechol, which can readily be degraded further. Pinheiro *et al.* 2004 focused on the biological breakdown of aromatic amines that result from degradation of azo dyes by soil microorganisms. In their studies on biodegradation of hydrocarbons in soil by a microbial consortium, Ghazali *et al.* 2004 emphasise the potential that exists for biodegradation of potentially toxic and recalcitrant compounds by microorganisms.

The monitoring of pesticides and their breakdown products has until very recently been a routine laboratory–based analysis. Such analyses would require field sampling of a potentially toxic site, and transportation to an approved quality assurance laboratory equipped with chromatographic equipment such as high performance liquid chromatography (HPLC) or gas chromatography coupled to a mass spectrometer (GC-MS) (Taccheo *et al.* 1988, Nakamura *et al.* 1989, Ameno *et al.* 1991, Lodesani *et al.* 1992, Ibrahim *et al.* 2001).

The sample would require pre-treatment prior to analysis and depending on its nature, pre-treatment would have to include several extraction and clean up steps. These procedures are time consuming and the operation of HPLC and GC-MS requires trained and skilled operators (Rossi *et al.* 2001, Jiménez *et al.* 2004) Given the extensive sample handling and the lag period from sampling to analyses, a high error margin is probable, in which time the composition of the target analyte could have altered (Wang & Mahmoud 1986, Ibrahim *et al.* 2001).

Little research has been done on the real time *in situ* monitoring of levels of amitraz and its metabolites in the environment. There exists a demand to monitor the concentrations of these xenobiotics. Despite the reliability and sensitivity offered by GC-MS and HPLC, they are not readily adaptable to on-site monitoring.

When designing an on–site monitoring device, the following criteria need to be addressed:

1. Portability of the analytical instrument
2. Ability to perform analyses in real time
3. Reproducibility and reliability of analyses
4. The sensitivity of the analytical device comparable to established laboratory - based analytical equipment
5. Cost-effectiveness of the device
6. Ease of operation
7. Minimal (if any) sample pre-treatment

(Rasooly & Rasooly 1999, Bilitewski & Turner 2000).

Electrochemistry is showing growing potential to be used as an analytical tool for portable analytical devices. Once the redox behaviour of an analyte of interest is known, the analyte can be detected within a complex matrix such as river water, soil or spent cattle dip with negligible interference from external factors. In addition, none or minimal pre-treatment is required, and current approaches in the field have seen the development of disposable screen-printed electrodes that are used for single analyses (Pritchard *et al.* 2004).

In this study the feasibility of using electrochemistry for the detection of amitraz and its degradants is assessed. Furthermore, the feasibility of using electrochemical methods for monitoring amitraz hydrolysis and clarification of the biological degradation of 2,4-DMA by *Pseudomonas* spp. is investigated. For ease of reference, chapter 2 shows the electrochemical characterisation of the major analytes examined, amitraz, 2,4-dimethylphenylformamide, 2,4-dimethylaniline and 3-methylcatechol (3-MC). The optimisation of key operational parameters for electrochemical detection of amitraz (chapter 3) and 2,4-DMA (chapter 4) were performed.

The degree of recalcitrance of 2,4-DMA was assessed and a potential breakdown product of 2,4-DMA, 3-MC was monitored electrochemically (chapter 5). Chapter 6 focuses on the detection and quantification of these analytes in environmental samples. The chemical hydrolysis of amitraz and the biodegradation of 2,4-DMA are investigated in chapter 7. The overall conclusions of this study and future recommendations are discussed in chapter 8. The second part of this chapter provides background to the theory behind electrochemistry and electroanalysis of relevance to this thesis.

1.2 ELECTROCHEMICAL PRINCIPLES AND TECHNIQUES

Electroanalysis entails the measurement of electrical variables such as current and potential (Kissinger & Heinemann 1996). Electrochemical analyses are classified into either static or dynamic systems. When equilibrium conditions are maintained by negligible interference of the solid-solution interface, the potential difference at zero current is measured. This system is said to be static (Kissinger & Heinemann 1996). Intentional disturbance of the equilibrium by alteration of the potential, current or time

makes up the basis of dynamic electrochemical analysis, where the response to the disturbance (such as current) is monitored (Rubinstein 1995).

Typically, a three electrode cell system is used in dynamic electroanalysis. Figure 1.3 is a representation of the three electrode system used in this study:

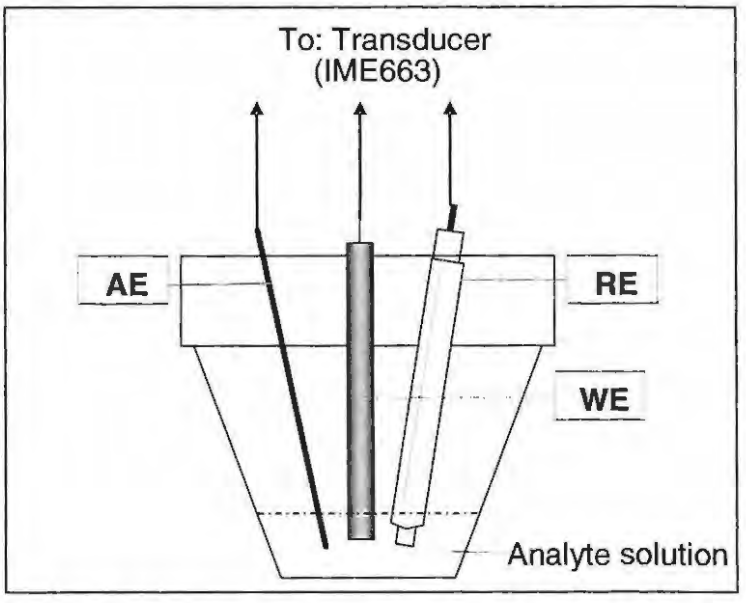

Figure 1.3 Three electrode electrochemical cell WE = working electrode (glassy carbon), AE = auxiliary electrode (platinum wire), RE = reference electrode (Ag/AgCl saturated with 3M KCl) (Adaptation: Kissinger & Heinemann 1996, Wang 1994).

The three electrode electrochemical cell is comprised of a reference electrode (RE) which can comprise of either a saturated calomel electrode (SCE) or alternatively a silver/silver chloride electrode (Ag/AgCl) (saturated with 3M KCl).

The reference electrode maintains a constant potential. The auxiliary electrode (AE) comprises an inert substance that functions to complete the electrical circuit in the solution. Typically, a platinum wire is used. The working electrode (WE) is the electrode at which electron transfer reactions occur. The WE material can be either metallic such as platinum, gold or mercury, or carbon-based. Glassy carbon electrodes (GCE) are commonly used given their cost effectiveness (Wang 1994).

The choice of WE is also based on the range of the potential window it can function within, its low electrical resistance, as well as its robustness under an array of conditions. Hydroxyl and carboxyl groups at the GCE surface also provide a means of

rapid modification to introduce chemical or biological molecules (Rubinstein 1995, Kissinger & Heinemann 1996).

1.2.1 Cyclic voltammetry

Cyclic voltammetry (CV) is a dynamic electrochemical technique and has been described as being widely utilised for the acquisition of qualitative information about electrochemical reactions (Wang 1994). CV provides useful insight into the redox reactions and involves the change in potential of a stationary working electrode. The resultant change in current is monitored as a function of the change in potential (Wang 1994).

In CV, the potential is scanned linearly from an initial potential to a desired potential within the potential range of the working electrode (which is beyond the oxidation or reduction potential of the analyte of interest), and then cycled back to the starting potential. Typically, during the oxidation/reduction potential scan, the analyte of interest is oxidised or reduced depending on its chemical properties.

During oxidation, a scan would typically start at a potential where no redox reactions occur. A linear increase in the potential at a given rate (i.e. a change in the potential at the working electrode surface towards a more positive potential) will result in oxidation of the electroactive species. Figure 1.4 is a graphical representation of oxidation and reduction occurring at the working electrode surface during cyclic voltammetry.

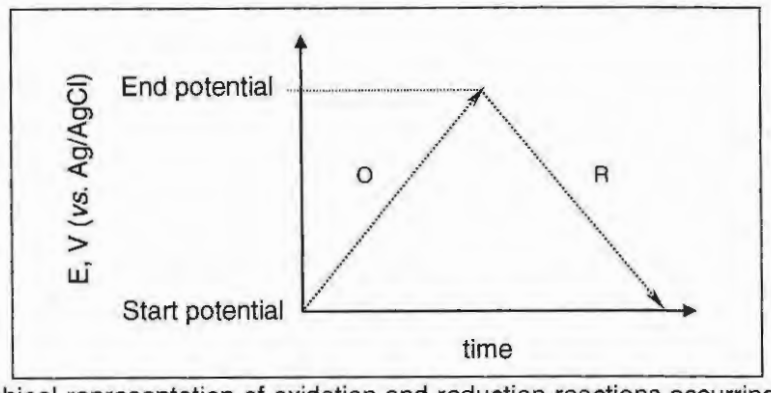

Figure 1.4 Graphical representation of oxidation and reduction reactions occurring at the working electrode surface during cyclic voltammetry. O = oxidation, R = reduction. (Adaptation: Wang 1994, Kissinger & Heinemann 1996).

Oxidation yields a positive current, as electrons diffuse from the electroactive analyte to the working electrode. Once the oxidation scan has reached a potential beyond the oxidation potential of the analyte, the scan is reversed. In this case, the potential is linearly decreased, resulting in the reduction of the analyte. Reduction yields a negative current as electrons defuse from the working electrode to the oxidised analyte (Wang 1994, Kissinger & Heinemann 1996).

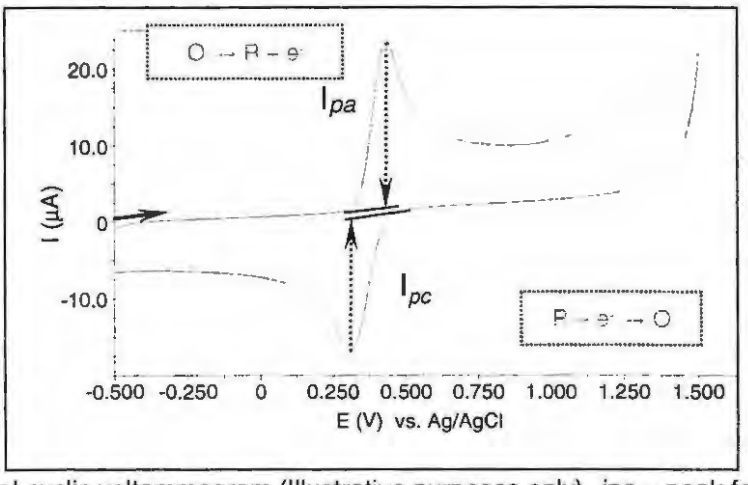

Figure 1.5 Typical cyclic voltammogram (Illustrative purposes only). *ipa* = peak for anodic current, *ipc* = peak for cathodic current.

As depicted in figure 1.5, once the potential of the working electrode approaches the oxidation potential of the electroactive analyte under consideration, the analyte becomes oxidised. This induces the migration of electrons from the electroactive species to the working electrode surface, which increase the current strength. Once all the electroactive species within the diffuse layer have undergone oxidation, the current magnitude decreases. The height of the resultant peak is the anodic peak current, *ipa*, the magnitude of which is directly proportional to the concentration of the electroactive analyte of interest. On the return scan, the oxidised species can be reduced, the height of this resultant peak being the cathodic peak current, *ipc*.

The number of peaks, their shape and the oxidation/reduction potentials provide information on the behaviour and structure of the analyte of interest, as well as the reversibility/ irreversibility of the redox reaction.

Reversibility

The reversibility of an electroactive species can be described as the efficiency of the charged moiety to rapidly exchange electrons with the working electrode, resulting in a

regeneration of the analyte. Typically, in a reversible couple, the rate of the forward reaction is equal to the rate of the reverse reaction, and a peak separation (ΔE_p) is no greater than 0.059 V/n (where n = number of electrons). The peak current is observed to increase with increasing square root of the scan rate (Wang 1994, Rubinstein 1995, Kissinger & Heinemann 1996).

Irreversibility

Irreversible couples typically show a single oxidation or reduction current peak with no (or very weak) corresponding reduction or oxidation current peak, indicating no regeneration of the starting reagent. This is characteristic of the formation of an electroinactive reduction/oxidation product. In accordance, $pa/pc \neq 1$, the rates of the forward and reverse scans differ and in the case of a weaker return peak, $\Delta E_p > 0.058$ V/n. The rate of electron transfer controls these reactions. A shift in the peak potential with a change in the scan rate is typically observed with irreversible systems (Wang 1994, Rubinstein 1995, Kissinger & Heinemann 1996).

Quasi-reversibility

In a quasi-reversible system, $pa < 1 > pc$. The peak potential separation of quasi-reversible systems is greater than 0.059 V/n and the resolution of the peaks is less distinct (i.e. the peaks are more rounded). In addition, peak current, i_p is not proportional to the square root of the scan rate. Typically, the current is controlled by mass transport and charge transfer (Wang 1994, Rubinstein 1995, Kissinger & Heinemann 1996).

Reproducibility

The accuracy of the CV analyses can be determined by calculating the standard deviation (S.D.) between multiple CV scans of the same analyte under identical conditions.

$$\% \text{ S.D.} = \frac{\text{S.D}}{\text{Mean (average) current}} \times 100$$

$$\text{Reproducibility (\%)} = 100 - \% \text{ S.D}$$

Limit of detection (LOD)

LOD is the lowest detectable concentration of the analyte of interest when compared to a baseline obtained from a solution void of the target analyte. LODs were calculated as the concentration that corresponds to the mean current of the baseline three times the standard deviations of the baselines (Kissinger & Heinemann 1996, Korta *et al.* 2003).

$$LOD = SD \times [3 \times Ip]$$

1.2.2 Differential pulse voltammetry (DPV)

The system for DPV measurement is similar to that of CV. Potential scanned between the working electrode and the reference electrode is changed as a pulse from the starting potential to an interlevel potential, remaining at the interlevel potential for between 5 and 100 milliseconds, after which it changes to the final potential (which is different from the starting potential). The pulse is repeated, with the final potential being changed. A constant difference is maintained between the starting and interlevel potential. The value of the current before and after the pulse is measured and plotted versus potential (Wang 1994, Kissinger & Heinemann 1996).

DPV is useful for the detection of trace amounts of analytes in that the effect of the charging current can be minimized, so high sensitivity is achieved. In addition, Faradaic current is extracted, making analyses of reactions occurring at the electrode more precise. DPV is typically characterized by reversible reactions which show symmetrical peaks, and irreversible reactions which show asymmetrical peaks. In addition, peak current is proportional to concentration of the analyte, and detection limits in the region of 10^{-8} M are obtainable (Wang 1994, Kissinger & Heinemann 1996).

1.2.3 Electrocatalysis

Not all compounds are readily electroactive. Some exhibit sluggish electron transfer kinetics and undergo a redox reaction at high overpotentials that might fall beyond the potential window of the working electrode. A catalyst can be employed to assist in the shuttling of electrons to and from the working electrode surface. The catalyst performs this duty by providing an alternative reaction pathway to the analyte avoiding a sluggish reaction rate. A catalyst is an inert substance that assists in increasing the rate at which a chemical reaction obtains equilibrium. It undergoes chemical transformation during the

redox process, but is regenerated to its initial chemical state (Wang 1994, Rubinstein 1995, Kissinger & Heinemann 1996).

Two modes of catalysis can occur. The mode of catalysis chosen is based on the type of catalyst used. The modes are: homogenous and heterogeneous catalysis. In homogenous catalysis, a complex is formed between the catalyst (reactant) and the target analyte (substrate). This complex migrates to the working electrode surface where a transfer of charge occurs. The deterioration of the complex allows for the regeneration of the catalyst to its original form (Bard & Faulkner 1980, Wang 1994, Rubinstein 1995, Kissinger & Heinemann 1996, Taylor & Schultz 2003).

In heterogeneous electrocatalysis, the catalyst is adsorbed onto the surface of the working electrode (via functional groups), and the substrate forms a complex with the adsorbed catalyst, and in so doing transfers electrons to the working electrode or receives electrons from the working electrode. The mediator function of catalysts is fundamental in assisting in increasing slow electron transfer kinetics (sluggish chemical response) and in so doing lower high overpotentials, as well as increase sensitivity of the current response.

Mediators such as potassium ferricyanide can also be used to assist the transfer of electrons between catalysts such as enzymes and the working electrode surface (Bard &Faulkner 1980, Wang 1994, Rubinstein 1995, Kissinger & Heinemann 1996, Taylor & Schultz 2003).

Scheme 1.1 illustrates the typical role of a mediator in transporting electrons to the working electrode surface.

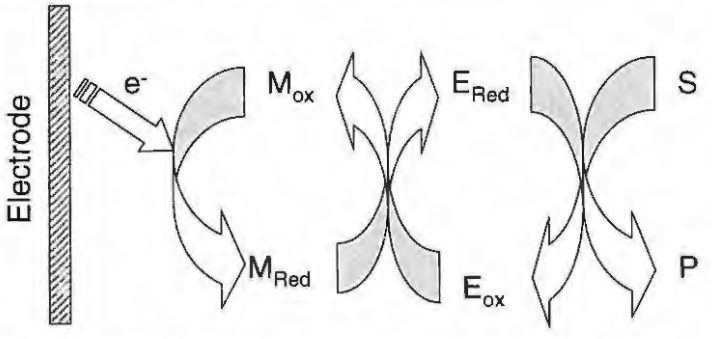

Scheme 1.1 Mediated electron transfer in the presence of a catalyst.
Legend: M = mediator, E = enzyme, S = substrate, P = product, ox = oxidation, red = reduction.

Poisoning of the working electrode surface (fouling phenomenon)

Poisoning of the working electrode surface occurs under a number of conditions:

1) Two reactants compete for the same surface active sites contributing to the deactivation of the electrode.
2) The desorption rate of one species is slower than the adsorption rate of another species.
3) Oxidation products become adsorbed to the electrode surface.

(Wang 1994, Kissinger & Heinemann 1996, Taylor & Schultz 2003).

Poisoning of the electrode results in a decrease in the amount of active sites on the working electrode surface. With consecutive runs, the current response decreases due to the inability of electroactive free analyte to associate with the electrode. This leads to electrode surface poisoning, also referred to as fouling or electrode passivation.

1.2.4 Effect of electrode surface fouling

The effect of fouling can be determined by successive scans of the electrode without cleaning in between runs. By assigning the current of the first scan a value of 100 %, all other peak currents can be expressed as a percentage of this current according to the equation.

The degree of fouling is then presented as a percentage of the original current response. Equation:

$$\text{Degree of fouling (\%)} = \frac{pa^{final}}{pa^{initial}} \times 100$$

Fouling of the electrode surface can be addressed through the use of appropriate modifiers and polymeric substances. For example, metallophthalocyanine (MPc) complexes have been frequently used in the modification of electrode surfaces. (Mafatle & Nyokong 1997). Phthalocyanines are a class of compounds structurally similar to the naturally occurring porphyrin and have a broad catalytic activity for a host of molecules (Mafatle & Nyokong 1997). MPc complexes contain a phthalocyaninato anion, $[C_{32}H_{18}N_8]^2$ and a ring structure comprised of four isoindole composites.

An alternative strategy to address fouling is the use of a single analysis, disposable screen printed electrode (SPE). SPEs show much promise in environmental monitoring given their ease of fabrication (and incorporation of chemical and biological mediators), user friendliness as well as comparative resolution of electroanalyses.

CHAPTER 2

CHARACTERISATION OF AMITRAZ AND ITS DEGRADANTS

2.1 INTRODUCTION

In the ensuing chapters, detailed characterisation and optimisation of the parameters for the cyclic voltammetric analysis of amitraz and its degradants, 2,4-dimethylphenylformamide (DMF) and 2,4-dimethylaniline (2,4-DMA) and 3-methylcatechol (3-MC), are provided. For ease of reference, the following brief chapter characterises the main anodic waves and peak potential for amitraz and its degradants.

2.2 INSTRUMENTATION AND METHODOLOGY

The electroanalytical analyses were performed using a Potentiostat/Galvanostat 30 (PGSTAT 30) from Autolab. Nitrogen purging was controlled using a Voltammetric Analytical stand (VA 663) obtained from Metrohm (Netherlands). The VA stand was coupled to the PGSTAT via an Autolab IME 663 interface (Swisslab).

pH measurements were performed using a WTW pH 330i pH meter (Germany), coupled to a SenTix 41 pH electrode.

2.2.1 REAGENTS

Analytes

Amitraz (99.4 %, PESTANAL, Sigma), 2,4-dimethylphenyl formamide (97.0 %, Sigma Aldrich), 2,4-dimethylaniline (98.0 %, Sigma Aldrich) and 3-methylcatechol (98.0 %, Sigma Aldrich) were prepared fresh prior to analysis in 20 % acetonitrile (99.9 %, Merck).

2.2.2 METHODS

Cyclic voltammetry

A three electrode system was employed for all cyclic voltammetric analyses. For all analyses using the PGSTAT 30, a glassy carbon electrode, 3 mm in diameter, BioAnalytical Systems (BAS) was employed as the working electrode. A Ag/AgCl electrode (saturated in 3 mM KCl) was used as the reference electrode for aqueous solution analysis. A platinum wire (BAS) was used as the auxiliary electrode in all analyses with the PGSTAT 30. Care was taken to ensure that the spacing between the electrodes was equidistant. A working volume of 2 ml was employed for all analyses unless otherwise stated.

All aqueous solutions were deoxygenated with nitrogen gas (instrument grade, Afrox) by purging for 5 minutes prior to the initial analysis, while a blanket of nitrogen was maintained over the solution during all analyses.

Glassy carbon electrode (GCE) preparation and cleaning

The GCE surface was cleaned thoroughly prior to analyses by rinsing sequentially with 70 % ethanol, triply distilled water, 5 % nitric acid followed by a final rinse with triply distilled water. The GCE surface was polished on a Buëhler felt pad (BAS) with a paste of alumina oxide powder (Sigma-Aldrich), rinsed with 20 % ethanol, and followed by triply distilled water. Unless stated otherwise, the GCE surface was cleaned and polished each time after a single run.

All glassware was washed thoroughly with warm soapy water and rinsed with triply distilled water. The electrochemical cells were thoroughly cleaned by an overnight soaking in a 5 % nitric acid bath, followed by rinsing with triply distilled water.

The above methods, reagents and instrumentation were used throughout the whole study unless otherwise stated.

2.3 RESULTS AND DISCUSSION

The following figures are representative cyclic voltammograms (CVs) of amitraz, DMF, 2,4-DMA and 3-MC.

2.3.1 Amitraz (N-(2,4-dimethylphenyl)-N'-[2,4-dimethylphenyl)-imino]methyl-N-methylinethanimidamide).

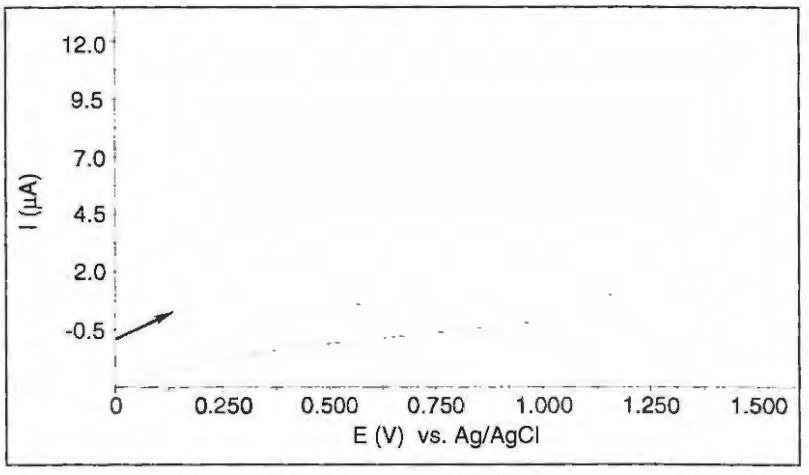

Figure 2.1 CV of amitraz (5 µM) in 0.2M BR buffer (pH 7.0). Scan rate = 100 mV/s.

The voltammetric analysis of pure amitraz yields a single anodic peak at an oxidation potential of between 1.10 V and 1.25 V, depending on the pH of the solution and the concentration of amitraz (as detailed in chapter 3), and is attributed to oxidation of the azomethine group (-N=CH-) of amitraz.

Amitraz is unstable, and starts to further hydrolyse to 2,4-DMA due to UV exposure and acidic pH (detailed in chapter 7). However amitraz can also degrade to intermediates such as DMF before degradation to 2,4-DMA (Bernal *et al.* 1997, Corta *et al.* 1999, Korta *et al.* 2003).

2.3.2. 2,4-dimethylphenyl formamide (DMF)

Figure 2.2 shows the CV for 5 µM DMF in 0.2 M BR buffer (pH 7.0)

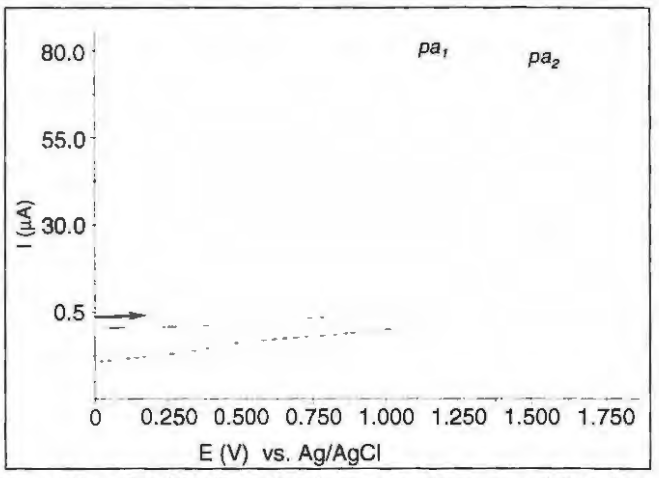

Figure 2.2 CV of DMF (5 µM) in 0.2 M BR buffer (pH 7.0). Scan rate 100 mV/s.

DMF yields a set of oxidation peaks on the anodic scan. The primary oxidation wave (pa_1) is observed between 1.15 V and 1.25 V, with a secondary anodic peak (pa_2) observed between 1.45 V and 1.55 V. The oxidation potential of the primary and secondary anodic peaks is dependent on the concentration of the DMF and the pH of the solution. No peak is observed on the return cathodic scan. The double anodic peaks observed at potentials > 1.15 V, correlate with values found in literature. DMF is unstable, and tends toward rapid hydrolysis, where the end product is 2,4-DMA.

2.3.3 2,4-dimethylaniline (2,4-DMA)

Figure 2.3 shows the CV for 8.7 µM 2,4-DMA in 0.2 M BR buffer (pH 7.0).

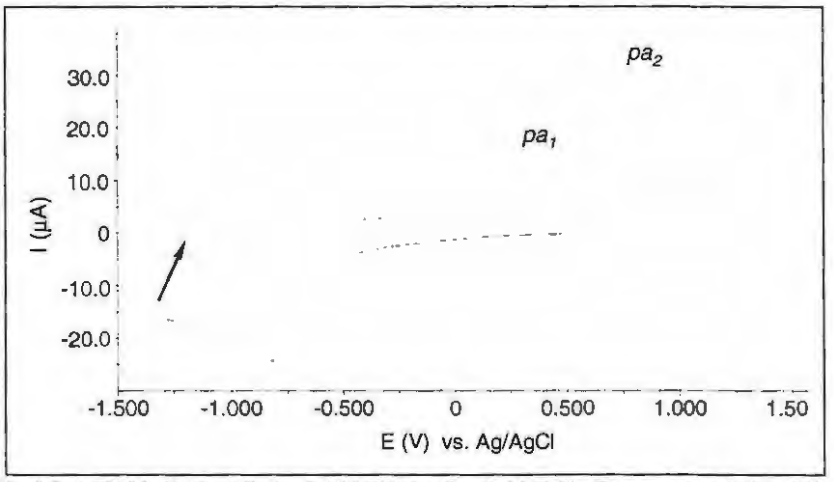

Figure 2.3 CV of 2,4-DMA (8.7 µM) in 0.2M BR buffer (pH 7.0). Scan rate: 100 mV/s.

The CV of 2,4-DMA, figure 2.3 shows two anodic waves at 0.50 V and 0.75 V. The potential and current strength of the primary (pa_1) and secondary (pa_2) peaks depend on the concentration and pH of the medium (detailed in chapter 4). On the cathodic scan a reduction wave at -0.85 V is observed. The secondary anodic peak at higher potentials was used as a measure of 2,4-DMA concentration given the strength and reproducibility of this wave.

Little reference to published information on the voltammetric behaviour of 2,4-DMA was found. CV studies by Marques *et al.* 1997, showed double anodic waves for 2,3-; 2.5-; 2,6-; 3,4- and 3,5-DMA only in anhydrous dimethylformamide solution and without any cathodic waves observed. These authors attribute the first oxidation wave to the formation of a cation radical following oxidation of the arylamine nitrogen and then followed by another one-electron oxidation to form a dication. Studies by Mizoguchi *et al.* 1962 showed CVs of N,N-Dimethylaniline (pH 2-3) with a reversible couple with $E_{1/2}$ approximately 0.5 V at a platinum electrode. In concurrence with Mizoguchi *et al.* 1962, Athawale *et al.* 1999 report that the oxidation of N,N-DMA involves the oxidation of the amine to produce a cation intermediate which reacts with unoxidised DMA to form tetramethylbenzidine (TMB). As proposed by these authors, TMB then oxidizes to produce a quinine diimine, TMBox, which may explain the origin of the double anodic waves observed in this study.

2.3.4 3-methylcatechol

The feasibility of the compound 3-methylcatechol (3-MC) as the primary degradant of 2,4-DMA is assessed in this thesis. Figure 2.4 is a representative CV scan for 3-MC.

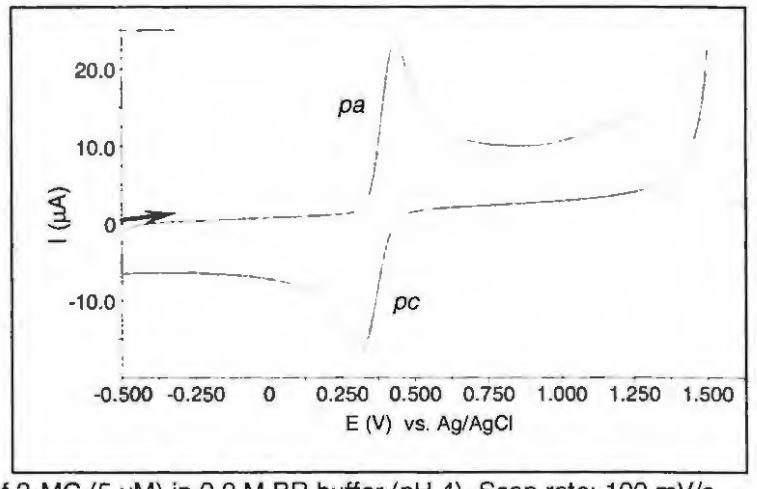

Figure 2.4 CV of 3-MC (5 µM) in 0.2 M BR buffer (pH 4). Scan rate: 100 mV/s.

The CV scan for 3-MC yields a quasi-reversible couple, with a difference in potentials being in the order of 0.125 V/n. E_{pa} = 0.375 V, E_{pc} = 0.250 V. The electrochemistry of 3-MC is well understood. A quasi-reversible couple of near unity is observed. These findings concur with those found in literature (Golabi & Nematollahi 1997). Chapter 3, 4 and 5 elaborate on the optimisation of the operational parameters for the characterisation and quantification of amitraz, 2,4-DMA and 3-MC respectively.

2.4 CONCLUSION

Cyclic voltammograms were obtained for amitraz, DMF, 2,4-DMA and 3-MC. The type of process and observe potential window for each are summarised in table 2.1.

Table 2.1 Characterisation data for each of the analytes examined in this study.

ANALYTE	TYPE OF PROCESS	POTENTIAL USED FOR ANALYSIS (V)
Amitraz	Irreversible (single anodic peak)	1.10 to 1.25
DMF	Irreversible (double anodic peaks)	1.15 to 1.25 1.45 to 1.55*
2,4-DMA	Irreversible (double anodic peaks)	0.42 to 0.78 0.52 to 0.93
3-MC	Quasi-reversible	0.30 to 0.50**

* High overpotential, therefore not considered for analyses
** Only observed at acidic pH (see Chapter 4.)

CHAPTER 3

OPTIMISATION OF OPERATIONAL PARAMETERS FOR THE CHARACTERISATION AND ANALYSES OF AMITRAZ

3.1 INTRODUCTION

Amitraz is widely used for the control of ticks and mites that target livestock, crops and honeybees. The potential of this pesticide to manifest in soil, waterways and in food products such as fruit, meat and milk is cause for concern. Analysis of the degradants of amitraz is of significant importance from an environmental and health perspective.

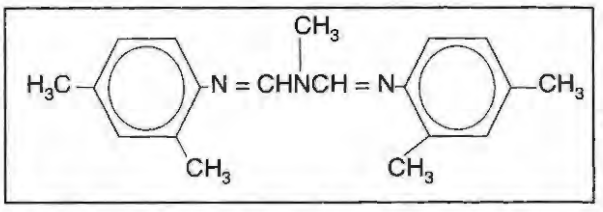

Figure 3.1 Structure of amitraz

In neutral solutions, amitraz hydrolysis occurs by initially degrading to 2,4-dimethylphenylformamide (DMF), which is further degraded to 2,4-DMA. Quantitative methods for amitraz detection in agricultural products exist, such as high performance liquid chromatography (HPLC) (Rice *et al.* 1984, Bernal *et al.* 1997, Pierpoint *et al.* 1997, Corta, *et al.* 1999, Tseng *et al.* 1999, Bogdanov 2003), gas chromatography (GC) equipped with a nitrogen-phosphorous detector (NPD) (Nakamura *et al.* 1989, Ameno *et al.* 1991), electron capture detector (ECD) (Hornish *et al.* 1984, Taccheo *et al.* 1988) and thermionic detector (Iwata *et al.* 1985, Queiroz *et al.* 2003). Most of these methods require complicated and time-consuming extraction procedures that use organic solvents for determining amitraz formulation (Tseng *et al.* 1999, Queiroz *et al.* 2003). Sample clean-up for HPLC and GC methods include steam distillation (Taccheo *et al.* 1988), liquid-liquid extraction (LLE) (Jiménez *et al.* 1997), supercritical-fluid extraction (Jiménez *et al.* 1997) or solid-phase extraction (SPE) (Bogdanov *et al.* 1998).

Authors such as Mester *et al.* 2001 and Queiroz *et al.* 2003 have utilised a simpler method for extracting amitraz from biological matrices. By making use of solid-phase micro-extraction (SPME), solvent-free amitraz extraction from biological materials has been made easier; however, this technique is still relatively time consuming and still needs to be analysed ideally by using GC coupled to thermionic specific detection, mass-spectroscopy or electron capture detection. Korta *et al.* 2003 had attempted to detect amitraz electrochemically in biological matrices prior to extraction and found that amitraz is not electroreducible at a mercury electrode, but is oxidisable at a glassy carbon electrode. The authors however do not present any values for the anodic potential of amitraz oxidation.

Stripping voltammetric studies of amitraz had been performed by Ibrahim *et al.* 2001 where a hanging mercury drop electrode (HMDE) was used as the working electrode. These authors observed an irreversible cathodic peak at highly negative potentials for amitraz after initial adsorption of amitraz onto a HMDE. In addition, it was observed that a shift in the potential as a result of the pH of the solution occurred. Even though this method resulted in sensitive analyses of amitraz (in the 10^{-8} M range) in a range of environmental matrices, given its toxicity, the utilisation of mercury in environmental analyses is not feasible.

3.2 AIMS

The overall objective of this section was the optimisation of operational parameters for the reproducible analysis of amitraz by cyclic voltammetry, in accordance with the validation of a voltammetric quantification method for amitraz. Factors which affect electroanalysis of target analytes include: type of supporting electrolyte, type of solvent, buffering capacity and pH of the solution (Perrin 1974, Wang 1994).

To achieve the overall objective, the following aims were addressed:

1. Assessment of the stability of amitraz in different solvents, and evaluation of the effect of solvent type on the magnitude and reproducibility of the electrochemical detection of amitraz.
2. Determination of the supporting electrolyte for accurate and reproducible amitraz detection.

3. Investigation of the behaviour of amitraz under different pH conditions. Assessment of the optimal pH for effective voltammetric analysis in terms of sensitivity, reproducibility and stability of amitraz.
4. Investigation of the effect of fouling. Assessment of the behaviour of amitraz at a GCE surface over sequential scans.
5. Investigation of the effect of scan rate on CV analysis of amitraz.
6. Assessment of the effect of pH on linearity and reproducibility of CV analyses for amitraz by standard curve generation.

3.3 METHODOLOGY

General methodology described in chapter 2 was applied. Specific methodology for this section is outlined further.

3.3.1 Assessing the effect of solvent type

Amitraz stock solution was prepared fresh prior to aqueous CV analyses in each of 20 % acetonitrile, 20 % dimethylsulphoxide (DMSO), 20 % methanol and 20 % ethanol.

3.3.2 Choice of supporting electrolyte

Buffers examined in this study were: 0.2 M sodium acetate buffer (pH 5.5), 0.2 M sodium carbonate buffer (pH 10.5), 0.2 M sodium phosphate buffer (pH 8) and 0.2 M Britton-Robinson buffer (BR). Reference is made in literature to the utilisation of 0.2 M BR buffer as the ideal supporting electrolyte to use for the electrochemical analyses of amitraz over a broad pH range (2–10) (Ibrahim *et al.* 2001). Results obtained from the electrochemical analyses of amitraz in the buffers were compared to those obtained from identical analyses of amitraz in 0.2 M BR buffer of equivalent pH. Aqueous electrochemistry was performed as outlined in chapter 2.2.

3.3.3 The effect of pH

CV of amitraz in the range pH 2 to pH 10 was performed in 0.2 M BR buffer.

3.3.4 Effect of fouling of GCE

Electrochemical scans were performed as outlined in section 1.5.1 with the exception that the GCE surface was not cleaned between scans. An equilibration time of 20 seconds was allowed between scans.

3.3.5 Effect of scan rate on amitraz

CV of amitraz (dissolved in 20 % acetonitrile) in 0.2 M BR buffer (pH 7.0) were assessed at scan rates of 25, 50, 100, 200 and 400 mV/s. GCE cleaning and polishing was performed between scans (outlined in chapter 2.2).

3.3.6 Generation of standard curves using optimised parameters

Linear standard curves of amitraz concentration versus current were set up at a range of pH values from 3.0–10.0 in 0.2 M BR buffer, at a scan rate of 100 mV/s.

3.4 RESULTS AND DISCUSSION

Amitraz oxidation at a GCE (*vs.* Ag/AgCl) yielded an irreversible anodic peak between 1.00 V and 1.25 V. Characterisation of amitraz was shown in chapter 2.3.1.

Optimisation of operational parameters for amitraz analysis

3.4.1 The effect of solvent type

Figure 3.2 is an overlay of the CVs showing the anodic peaks for 10 µM amitraz in 20 % acetonitrile, 20 % DMSO, 20 % methanol and 20 % ethanol. The anodic peak at pa_1 is attributed to amitraz, pa_2 to degradation of amitraz to DMF. The inset highlights anodic peaks attributed to 2,4-DMA formation. For the sake of clarity, the cathodic return waves are not shown.

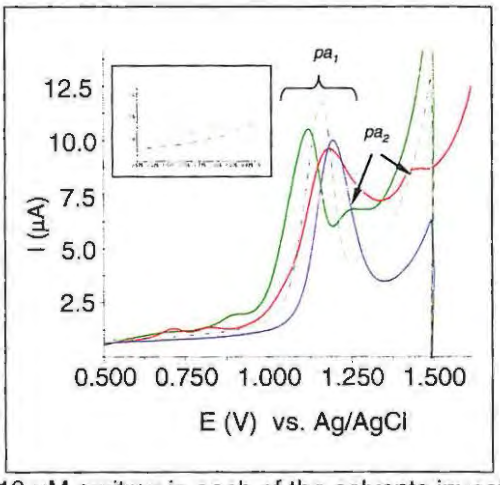

Figure 3.2 CVs generated for 10 μM amitraz in each of the solvents investigated: 20 % acetonitrile (black dotted line), 20 % DMSO (blue line), 20 % methanol (red line), 20 % ethanol (green line). Scan rate: 100 mV/s. *Legend:* pa_1= oxidation peak for amitraz, pa_2= formation of amitraz hydrolysis product, DMF. Inset= 2,4-DMA. Return scans not shown.

Table 3.1 summarises the current and potential values shown in figure 3.2 for amitraz oxidation in each of the solvents.

Table 3.1 Effect of solvent on current response and potential range of 10 μM amitraz, as assessed by CV.

SOLVENT	CURRENT, μA (Ipa_1)	POTENTIAL, V (Epa_1)
20 % acetonitrile	11.250 (± 0.100)	1.130 (± 0.003)
20 % ethanol	10.260 (± 1.000)	pa_1: 1.060 (± 0.010)
20 % methanol	9.000 (± 1.000)	pa_1: 1.150 (± 0.010)
20 % DMSO	10.000 (± 0.300)	1.200 (± 0.070)

Note: Current and potential values shown are the mean of 5 scans. Approximate error margins were calculated as the degree of deviation from the mean over 5 scans, shown in brackets. For 20 % ethanol and 20 % methanol, I and E values for pa_1 are shown.

Dissolution of 10 μM amitraz in 100 % of the solvents was inadequate due to a high degree of solvent volatilisation. Adequate dissolution of amitraz was shown in 20 % of the solvents, except in the case of 20 % ethanol, where the solution required moderate heating to aid amitraz dissolution.

As shown in figure 3.2 (and tabulated in table 3.1), amitraz detection in 20 % acetonitrile yielded a single anodic peak at a mean potential of 1.13 V (*vs.* Ag/AgCl), with ± 3 mV standard deviation. The oxidation potential obtained corresponds to the oxidation

potential at which amitraz was characterised (Chapter 2.3.1). A current of 11.25 µA (*vs.* Ag/AgCl) with a standard deviation from the mean of ± 0.1 µA was noted.

CV of amitraz dissolved in 20 % DMSO yielded an anodic peak at 1.20 V, which was 70 mV greater than the oxidation potential observed in 20 % acetonitrile. In addition, a greater standard deviation of ± 7 mV was observed in 20 % DMSO. A weaker current response of 10.00 µA (± 0.3 µA) in conjunction with a greater anodic potential for amitraz CV in 20 % DMSO could be attributed to sluggish electron transfer.

In the presence of 20 % ethanol, amitraz oxidation was observed to occur at 1.06 V (*vs.* Ag/AgCl). However, as can be seen in figure 3.2, formation of a broad anodic peak between 0.55 V and 0.70 V is observed which corresponds to the oxidation of 2,4-DMA as described in chapter 2.3.3. A secondary anodic peak (pa_2) at 1.24 V (*vs.* Ag/AgCl) was attributed to DMF, an intermediate hydrolysis product of amitraz (characterised in chapter 2.3.2).

CV of amitraz dissolved in 20 % methanol yielded a clear 2,4-DMA oxidation couple observed in 20 % ethanol (inset, figure 3.2), as well as a secondary oxidation peak (pa_2) at 1.45 V, attributed to DMF formation from amitraz hydrolysis. Findings regarding the hydrolysis of amitraz in methanol and ethanol solutions correlate with findings published by Bernal *et al.* 1997 who showed the lack of stability of amitraz in these solvents. Electroanalysis of amitraz dissolved in 20 % DMSO showed promising results with regards to sensitivity and reproducibility of current response for the oxidation and stability of amitraz. However findings in this study showed that 10 µM amitraz dissolved in 20 % DMSO precipitated under alkaline conditions. No precipitation of 10 µM amitraz dissolved in 20 % acetonitrile occurred under a range of pH conditions.

Based on this data it can be concluded that the ideal solvent to use with regards to amitraz stability, dissolution, CV current and potential reproducibility would be 20 % acetonitrile. These findings concur with those found in literature with regards to choice of solvent for the dissolution of amitraz (Korta *et al.* 2003). Ibrahim *et al.* 2001 had utilised 20 % ethanol to dissolve amitraz; however, these authors make no mention of the stability of amitraz, or its complete dissolution in this solvent.

3.4.2 Choice of supporting electrolyte

Figure 3.3 summarises the difference in current strength and shift in potential for amitraz analysis for three buffers compared to analysis conducted in 0.2 M BR buffer of equivalent pH. The buffers used in the comparative study were 0.2 M sodium acetate buffer (pH 5.5), 0.2 M phosphate buffer (pH 8.0) and 0.2 M sodium carbonate buffer (pH 10.5).

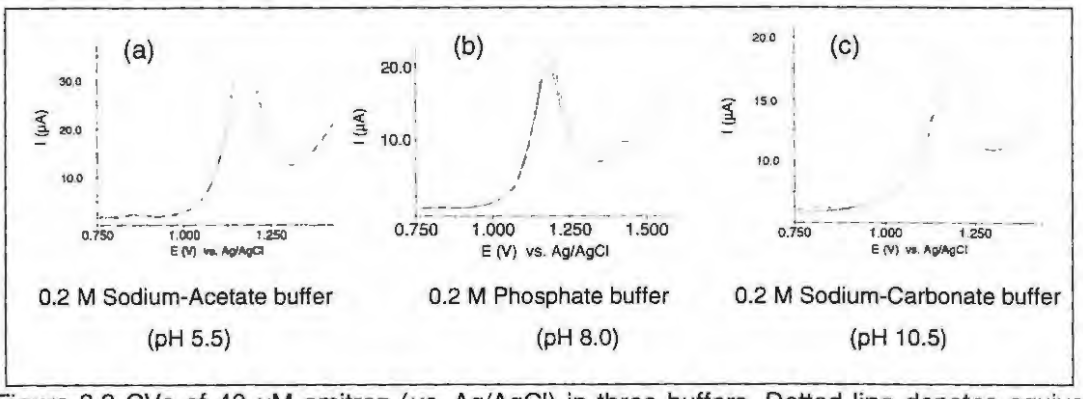

Figure 3.3 CVs of 40 µM amitraz (*vs.* Ag/AgCl) in three buffers. Dotted line denotes equivalent analyses of amitraz in 0.2 M BR buffer of same pH. Scan rate: 100 mV/s.

As shown in figure 3.3, the current strength of amitraz in the presence of 0.2 M sodium acetate buffer (a), yielded a greater response in comparison to analyses in 0.2 M sodium carbonate buffer (c) and 0.2 M phosphate buffer (b), in keeping with the dependence of amitraz current response on pH (detailed further in chapter 3.4.3).However, relative sensitivity of amitraz detection compared to analysis performed in 0.2 M BR buffer was significantly lower. The current response of amitraz in the presence of 0.2 M phosphate buffer (b), yielded an anodic peak of comparative magnitude to that in 0.2 M BR buffer of equivalent pH. The current strength of amitraz in 0.2 M sodium carbonate buffer (c), is substantially less than the equivalent in 0.2 M BR buffer (dotted line). In addition, a shift in potential to less anodic potentials compared to the amitraz peak in 0.2 M BR buffer was observed.

Of the buffers studied the highest sensitivity for amitraz analysis was observed in 0.2 M BR buffer, 0.2 M phosphate buffer could be the alternative choice of supporting electrolyte to BR buffer given the comparable reproducibility and sensitivity of the current response during amitraz oxidation. However, BR buffer had been selected by Ibrahim *et al.* 2001 as the supporting electrolyte for electrochemical analyses due to the

broad pH range over which it can be employed, and was chosen as the optimal supporting electrolyte to use in this study.

3.4.3 The effect of pH

Figure 3.4 (a) and (b) illustrate the role pH plays in detection of amitraz in 0.2 M BR buffer over the pH range 2 – 10. Acidic media generated the greatest amplitude in the current response for amitraz. However the reproducibility of this current response is not reliable due to the direct hydrolysis of amitraz to 2,4-DMA at pH 2 (as discussed in chapter 7). The hydrolysis of amitraz under acidic conditions has been observed by Bernal *et al.* 1997, Pierpoint *et al.* 1997, Corta *et al.* 1999, and Korta *et al.* 2003. The primary oxidation peak for amitraz shifted to more positive potentials with an increase in acidity.

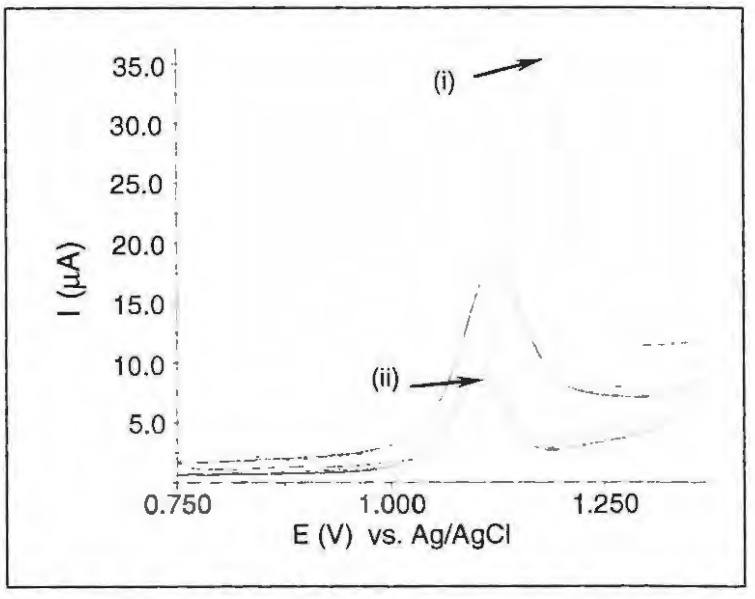

Figure 3.4 (a) Scan showing the shift in oxidation potential and change in current response of 15 µM amitraz in 0.2M BR from i) pH 2, (ii) pH 10. Scan rate: 100 mV/s. Peak shown is the primary oxidation peak for amitraz.

Current response for the oxidation of amitraz at every pH value investigated is shown in figure 3.4 (b). The amplitude of current response for amitraz oxidation at pH 2 was considered to be the highest and assigned a value of 100 %. Current response for the oxidation of amitraz at each subsequent pH was plotted as a percentage of the current amplitude for amitraz oxidation at pH 2.

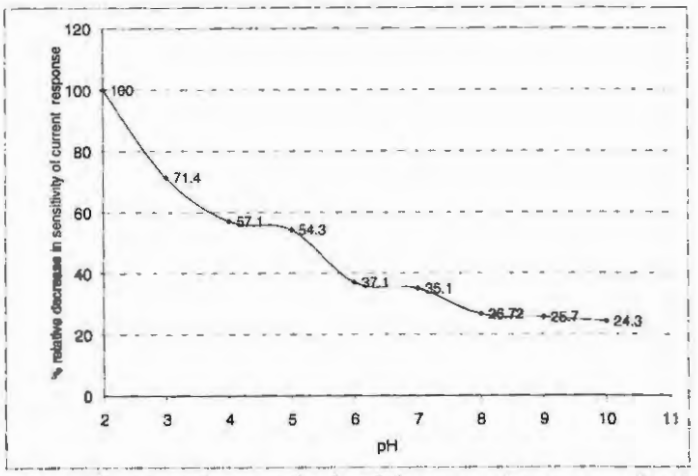

Figure 3.4 (b) Percentage decrease in magnitude of the current response for the oxidation potential peak of 25 µM amitraz relative to the current response observed at pH 2.

It can be seen from figure 3.4 (b) that under acidic conditions, the difference in current amplitude is greater. A decrease of 28.6 % in current amplitude for the oxidation of amitraz was noted between pH 2 and pH 3, and 14.3 % difference was noted between pH 3 and pH 4. From pH 5 to pH 7 a 19.2 % decrease in current amplitude for amitraz oxidation was observed. Under alkaline conditions, pH 8 to pH 10, a 2.42 % decrease in current amplitude was noted.

Figure 3.4 (c) shows the shift in oxidation potential for the amitraz peak with pH in relation to current response.

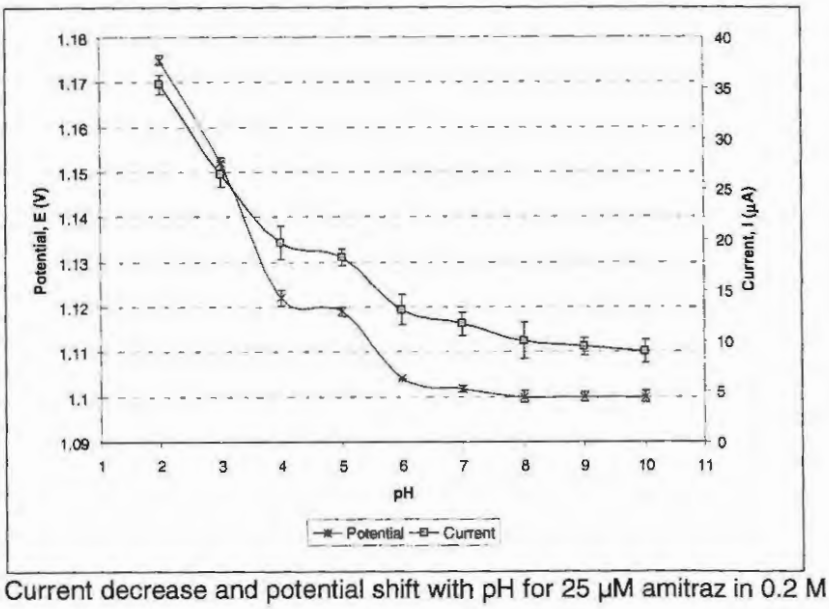

Figure 3.4 (c) Current decrease and potential shift with pH for 25 µM amitraz in 0.2 M BR buffer.

In figure 3.4 (c) current response for amitraz oxidation is observed to decrease with increasing alkalinity [shown as percentages in figure 3.4 (b)]. In addition, a shift in the oxidation potential for amitraz towards less anodic potentials is observed to occur with increasing alkalinity.

3.4.4 Effect of working electrode surface fouling between CV scans

The degree of fouling of the GCE surface was assessed. This was done by performing multiple anodic scans without cleaning the GCE surface between scans in a quiescent solution. The degree of GCE surface fouling was calculated as outlined in chapter 1.2. Figure 3.5 (a) shows the effect of fouling of the GCE under acidic conditions.

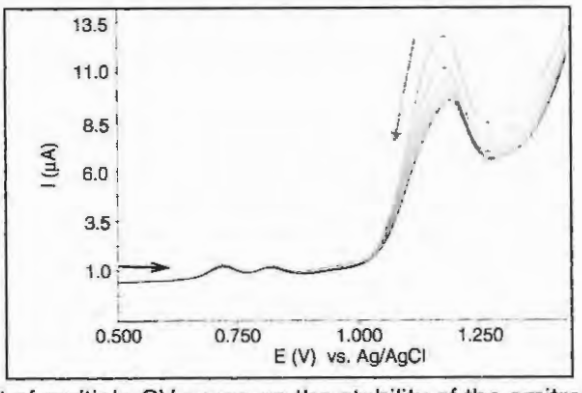

Figure 3.5 (a) The effect of multiple CV scans on the stability of the amitraz (9 µM) oxidation peak current response at pH 2. Supporting electrolyte: 0.2 M BR buffer. Scan rate: 100 mV/s.

Figure 3.5 (b) shows the effect of GCE surface fouling at neutral pH.

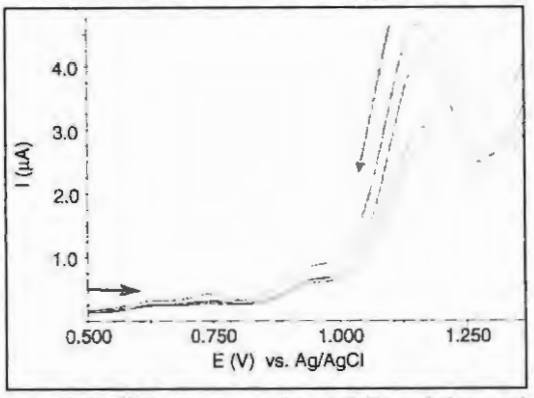

Figure 3.5 (b) The effect of multiple CV scans on the stability of the amitraz (9 µM) oxidation peak current response at pH 7. Scan rate: 100 mV/s.

Figure 3.5 (c) shows the effect of GCE surface fouling under alkaline conditions.

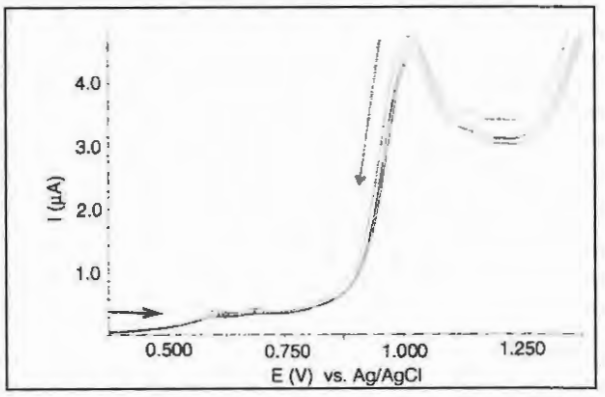

Figure 3.5 (c) The effect of multiple CV scans on the stability of the amitraz (9 µM) oxidation peak current response at pH 10. Supporting electrolyte: 0.2 M BR buffer. Scan rate: 100 mV/s.

Figure 3.5 (d) summarises the effect multiple scans have on the amplitude of the current response under acidic, neutral and alkaline conditions. The first scan for each study was assigned a value of 100 % and the decrease in current amplitude with subsequent oxidation scans were calculated as a percentage of the first scan.

From figure 3.5 (d) it is evident that under more acidic conditions the strength of the current response of the amitraz oxidation peak with multiple scans decreases more significantly compared to that at pH 7 and 10. This is attributed to a higher degree of GCE surface fouling. This phenomenon is most likely a concentration effect, owing to the irreversible adsorption of the oxidised amitraz at the electrode.

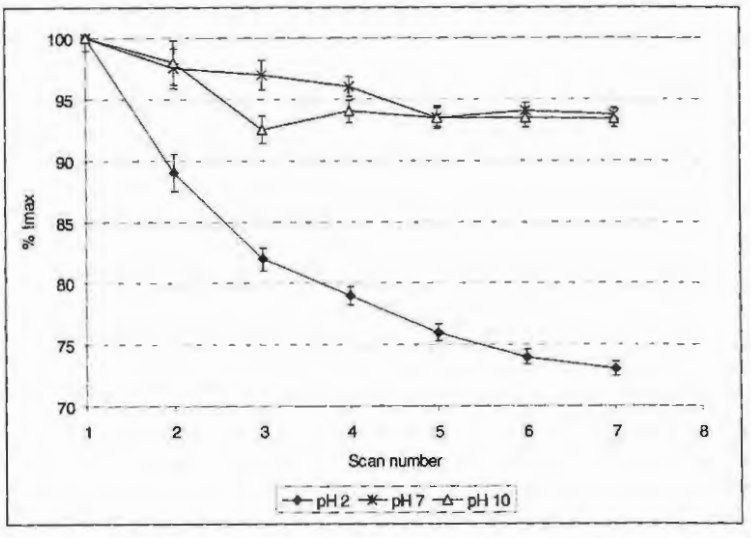

Figure 3.5 (d) The effect of multiple CV scans on the stability of the amitraz (3.5 µM) oxidation peak current response at pH 2, 7 and 10.

After several consecutive scans, minimal working electrode surface regeneration occurred and the number of active sites on the working electrode surface decreased until baseline current amplitude was observed. The poisoning of the electrode by a film of 'spent' analyte is a major disadvantage in the design and fabrication of electrodes for environmental monitoring.

3.4.5 The effect of scan rate on current response

The effect scan rate has on the oxidation peak for amitraz was determined by CVs of amitraz in a quiescent solution at different scan rates (mV/s): 25, 50, 100, 200 and 400.

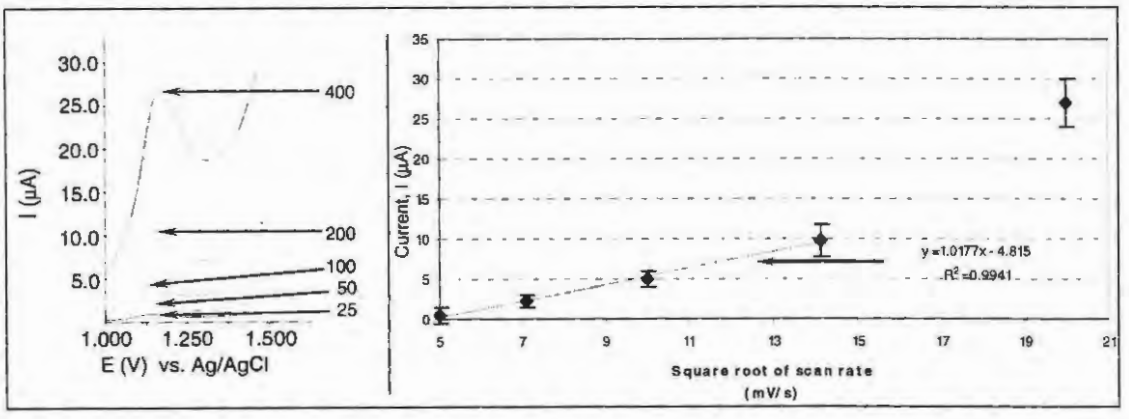

Figure 3.6 (a) CVs of 20 µM amitraz in 0.2 M BR buffer (pH 7) at a range of scan rates between 25 mV/s and 400 mV/s. (b) Linear curve of current, I (µA) vs. square root of scan rate.

From figure 3.6 (a and b) it is evident that a plot of square root of the scan rates yields a linear increase in the current response only between 25 mV/s and 200 mV/s. A deviation from linearity was observed at scan tares above 200 mV/s. A linear relation between current and square root of the scan rate indicates a diffusion controlled process between 25 mV/s and 200 mV/s, in a quiescent solution.

3.4.6 Generation of standard curves for amitraz in 0.2 M BR buffer under different pH conditions

CV of amitraz oxidation at a range of concentrations were performed at pH values of 3, 4, 5, 6, 7, 8, 9 and 10. Figures 3.7 (a,b), 3.8 (a,b) and 3.9 (a,b) represent the CVs and standard curves, under acidic (pH 3) neutral (pH 7) and alkaline (pH 10) conditions, respectively at a range of amitraz concentrations

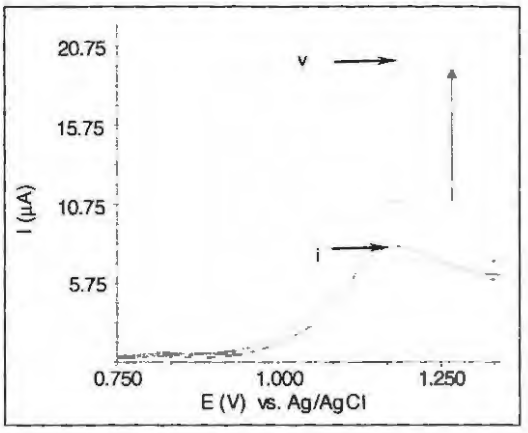

Figure 3.7 (a) CVs showing the increase in current response with increase in amitraz concentration in 0.2 M BR buffer (pH 3). Amitraz concentrations range between 5 µM (i) and 13 µM (v). Scan rate: 100 mV/s.

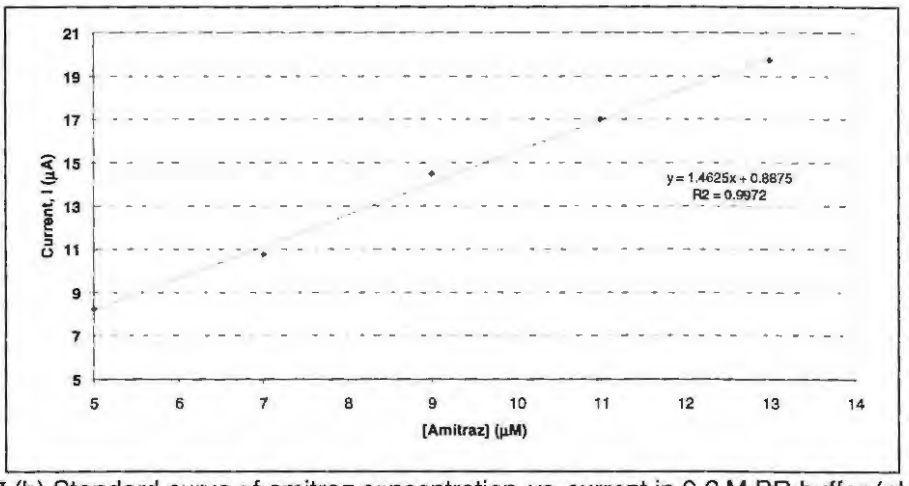

Figure 3.7 (b) Standard curve of amitraz concentration *vs.* current in 0.2 M BR buffer (pH 3). $R^2 = 0.9972$.

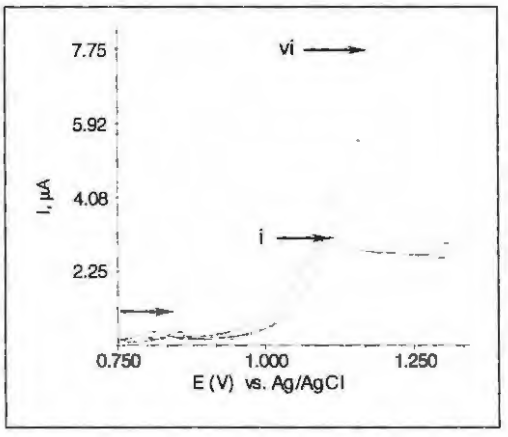

Figure 3.8 (a) CVs showing the increase in current response with increase in amitraz concentration in 0.2 M BR buffer (pH 7). Amitraz concentrations range between 5 µM amitraz (i) and 13 µM amitraz (v). Scan rate: 100 mV/s.

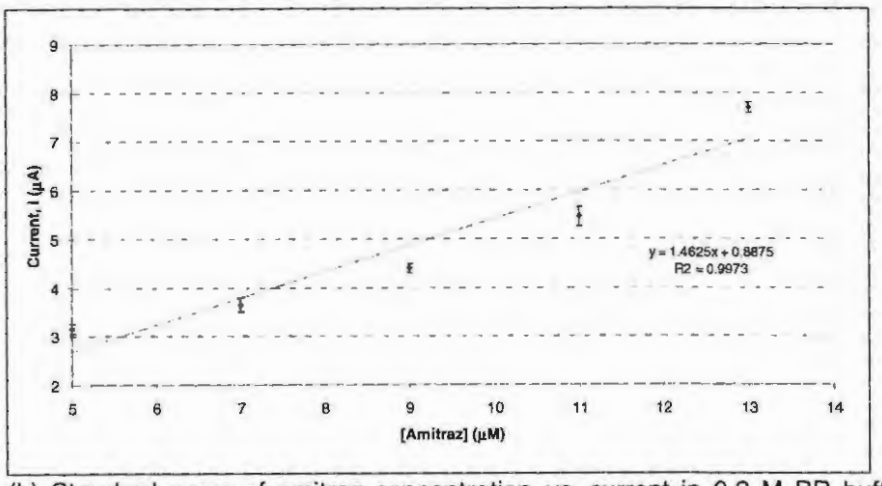

Figure 3.8 (b) Standard curve of amitraz concentration *vs.* current in 0.2 M BR buffer (pH 7). $R^2 = 0.9973$.

Figure 3.9 (a) shows the representative CVs used for the set up of a standard curve for amitraz quantification at pH 10, with the linear curve shown in figure 3.9 (b).

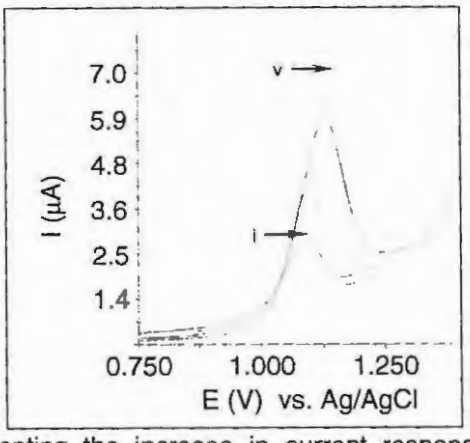

Figure 3.9 (a) CVs representing the increase in current response with increase in amitraz concentration in 0.2 M BR buffer (pH 10). Amitraz concentrations range between 5 µM (i) and 13 µM (v). Scan rate: 100 mV/s.

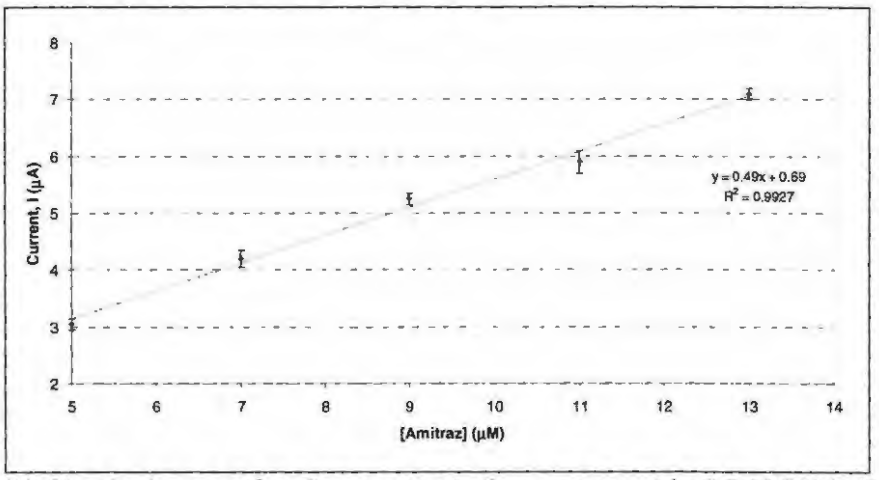

Figure 3.9 (b) Standard curve of amitraz concentration *vs.* current in 0.2 M BR buffer (pH 10). $R^2 = 0.9927$.

Figure 3.10 shows the standard curves of amitraz concentration *vs.* current at pH 3 through pH 10. The standard curves at more acidic pH conditions yield a greater current response, with a steeper gradient.

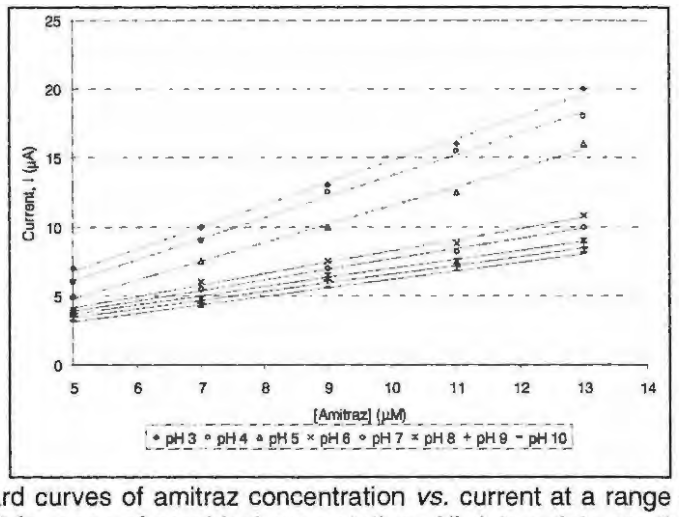

Figure 3.10 Standard curves of amitraz concentration *vs.* current at a range of pH values. Error bars were excluded for ease of graphical presentation. All data points are the mean of triplicate scans.

The reproducibility, accuracy and sensitivity of amitraz detection and quantification in 0.2 M BR buffer over the pH range 3-10 can be examined by a comparison of correlation coefficient and standard deviation between scans, as in table 3.2.

Table 3.2. Comparative study showing differences in key factors between standard curves for the quantification of amitraz at different pH.

pH	R^2	AVERAGE REPRODUCIBILITY (%)*
3	0.9972	92.63
4	0.9994	93.05
5	0.9947	92.91
6	0.9957	92.90
7	0.9973	94.68
8	0.9922	89.48
9	0.9900	91.18
10	0.9927	89.22

* Reproducibility calculated as outlined in chapter 1.2.

The generation of standard curves for amitraz in the pH range 3-10 shows that the average reproducibility of multiple runs of the same concentration of amitraz fluctuates over the concentration range, but is predominantly higher than average under acidic to neutral conditions. Linear regression curves show correlation coefficients nearer 1 in pH 3, 4 and 7. The average reproducibility of the current response of the primary oxidation curve is greatest at studies conducted at pH 7.

An extrapolated limit of detection of 2×10^{-8} M was determined for CV analysis of amitraz as outlined in chapter 2.2. By using differential pulse voltammetry, an experimental limit of detection for amitraz in 0.2 M BR buffer pH 7, was determined as 8.5×10^{-8} M.

3.5 CONCLUSION

Table 3.3 summarises the ideal conditions for amitraz analyses.

Table 3.3 Summary of key operational parameters for qualitative and quantitative amitraz analysis

PARAMETER	OPTIMAL CONDITION
Solvent	20 % acetonitrile
Supporting electrolyte	0.2 M Britton-Robinson buffer
pH	7
Fouling	Regeneration of GCE surface Required between scans

Analysis of pure amitraz on a laboratory scale is possible when the amitraz is dissolved in 20 % acetonitrile and stored in a dark container at 4 °C when not in use. However, prior to analyses using stock solutions of amitraz, the integrity of the amitraz must be checked.

Of the supporting electrolytes examined, oxidation of amitraz in 0.2 M BR buffer was more reproducible and sensitive; pH 7 was selected as the optimal pH, taking into account that good reproducibility, relative stability and sensitivity were obtained for amitraz analyses at this pH.

Electro-oxidation of amitraz leads to the formation of oxidised amitraz on the surface of the electrode, hindering the passage of electrons to the electrode. The extent of electrode passivation could be attributed to concentration of the analyte as well as its chemical structure. Passivation of GCE by amitraz is expected given the irreversible oxidation peak noted. Therefore, the working electrode surface must be cleaned and polished prior to each electrochemical analysis.

Amitraz standard curves can be generated at all pH values between 3 and 10, with acceptable linearity expressed as R^2 values greater than 0.99. Good reproducibility of identical analyses was observed.

CHAPTER 4

OPTIMISATION OF OPERATIONAL PARAMETERS FOR THE CHARACTERISATION AND ANALYSES OF 2,4-DIMETHYLANILINE

4.1 INTRODUCTION

2,4-DMA is an aromatic hydrocarbon with an amine group and two methyl groups in the *ortho* and *para* positions.

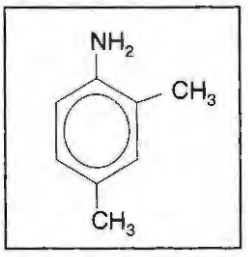

Figure 4.1 Structure of 2,4-dimethylaniline (2,4-DMA)

2,4-DMA is categorized as a class 3 carcinogen, with $LD_{50(rat)(oral)}$ = 467 mg/kg and $LD_{50\ (rat)(inhalation)}$ = 1.53 mg/L (4h). Humans exposed to 2,4-DMA for relatively short periods of time are subject to slight skin and eye irritation, blue skin, blue lips or finger nails, dizziness, nausea, shortness of breath, confusion, convulsions, unconsciousness or abdominal pain (Eastmond 2000, Whysner 2000, Osano *et al.* 2002, Bogdanov *et al.* 2003).

However, humans subjected to prolonged exposure (days) are prone to the formation of methaemoglobin in their blood supply, which effectively reduces the oxygen carrying capacity of the bloodstream and could rapidly result in death (methaemoglobin anaemia). The substance is particularly toxic to aquatic organisms, which is due to the impediment of the 2,4-DMA on the oxygen carrying capacity of the blood supply, thus effectively suffocating the aquatic organism ($LC_{50\ (golden\ orfe)}$ = 196 mg/l, 48h) (Eastmond 2000, Whysner 2000, Osano *et al.* 2002, da Silva *et al.* 2004).

Continual prolonged exposure to 2,4-DMA could potentially be carcinogenic, teratogenic, genotoxic and neurotoxic (Osano *et al.* 2002).

At present, 2,4-DMA is analysed using chromatographic techniques (HPLC and GC-MS) (Robinson & Osteryoung 1980, Seymour *et al.* 2002, Roy *et al.* 2004). While chromatographic techniques are amongst the most sensitive and reliable, no current chromatographic technique allows for on site evaluation of 2,4-DMA levels in real time with minimal (if not negligible) sample pre-treatment.

This section assesses the feasibility of utilising electrochemistry for the analysis of 2,4-DMA. In addition, the fundamental operational parameters are determined.

4.2 AIMS

The purpose of this section is to optimise key parameters in 2,4-DMA detection and quantification. To achieve the overall outcome, the following aims were addressed:

1. Assessment of the stability of 2,4-DMA in different solvents, and evaluation of the effect of solvent type on the magnitude and reproducibility of the electrochemical detection of 2,4-DMA.
2. Determination of the supporting electrolyte for accurate and reproducible 2,4-DMA detection.
3. Investigation of the behaviour of 2,4-DMA under different pH conditions. Assessment of the optimal pH for effective voltammetric analysis in terms of sensitivity, reproducibility and stability of 2,4-DMA.
4. Investigation of the effect of fouling. Assessment of the behaviour of 2,4-DMA at a GCE surface in sequential scans.
5. Investigation of the effect of scan rate on CV analysis of 2,4-DMA.
6. Assessment of the effect of pH on linearity and reproducibility of CV analyses for 2,4-DMA by standard curve generation.

4.3 METHODOLOGY

General methods performed in this section are outlined in chapter 2.
Specific methodology is outlined below:

4.3.1 The effect of solvent type

The methodology for determining effect of solvent on the electrochemical analysis of 2,4-DMA was followed identically to that for amitraz, as per section 3.3.1.

4.3.2 The choice of supporting electrolyte

The choice of supporting electrolyte was determined as described in section 3.3.2.

4.3.3 The effect of pH

The effect of pH on the electrochemical analysis of 2,4-DMA was followed as outlined in section 3.3.3.

4.3.4 Effect of fouling of GCE

The effect of fouling on the electrochemical response for 2,4-DMA was followed as outlined in section 3.3.4.

4.3.5 Effect of scan rate on 2,4-DMA

The methodology outlined in section 3.3.5 was followed.

4.3.6 Standard curves – pH 3–10

Standard curves were set up as outlined in section 3.3.6.

4.4 RESULTS AND DISCUSSION

From chapter 2.3.3 the characterisation of 2,4-DMA under neutral pH conditions yielded a double anodic peak between the range of 0.40 V and 0.80 V. For CV analyses of 2,4-DMA, only the secondary oxidation peak, pa_2, was used, with the exception that at pH 2 and 3, pa_1 was utilised. The reason for this is clarified in section 4.2.3.

4.4.1 The choice of solvent

2,4-DMA was dissolved in four solvents namely, 20 % acetonitrile, 20 % DMSO, 20 % methanol and 20 % ethanol. In turn, the effect the solvent had on the magnitude of the current response, the stability of the 2,4-DMA as well as the reproducibility of current response were compared using cyclic voltammetry. Figure 4.2 shows the CVs obtained for the oxidation of 2,4-DMA in the solvents examined with the primary (pa_1) and secondary (pa_2) waves as described in Chapter 2.3.3.

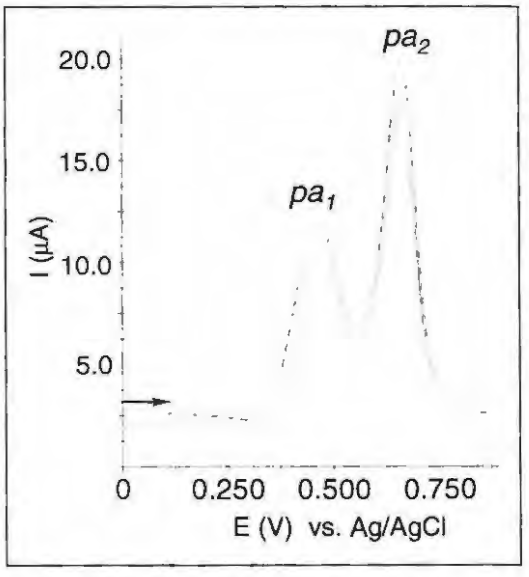

Figure 4.2 CVs generated for (30 μM) 2,4-DMA diluted with each of 20 % acetonitrile, 20 % ethanol, 20 % methanol and 20 % DMSO. *Legend*: green = 20 % DMSO, red = 20 % methanol, blue = 20 % ethanol, black dotted = 20 % acetonitrile, pa_1 = primary anodic peak, pa_2 = secondary anodic peak. Scan rate: 100 mV/s.

From figure 4.2 it is evident that 2,4-DMA dissolved in 20 % acetonitrile yields the greatest current response for pa_2. Dissolved in 20 % methanol, a lower detection of 2,4-DMA is observed. Stability of 2,4-DMA was examined in all the solvent samples.

Table 4.1 shows comparative data generated from the oxidation of 2,4-DMA in the presence of each of the four solvents.

Table 4.1 Comparison between current response and oxidation potential range for 2,4-DMA detection in different solvents.

SOLVENT	CURRENT, Ipa_2 (μA)	POTENTIAL, (V)
20 % acetonitrile	19.850 (± 0.450)	0.710 (± 0.005)
20 % ethanol	17.800 (± 0.320)	0.710 (± 0.009)
20 % methanol	17.700 (± 0.610)	0.730 (± 0.005)
20 % DMSO	19.760 (± 0.690)	0.700 (± 0.004)

Note: Current and potential values shown are the mean of 5 scans. Approximate error margins were calculated as the degree of deviation from the mean over 5 scans, shown in brackets.

As shown in table 4.1, in terms of reproducibility and sensitivity of the anodic detection of 2,4-DMA, 20 % acetonitrile was considered the ideal solvent for the electrochemical analysis of 2,4-DMA. Standard deviation of current was however the lowest for the analysis in 20 % ethanol solution. In chapter 3.4.1, 20 % acetonitrile was selected as the optimum solvent for amitraz analysis based on the criteria of current response and standard deviation, and in order to maintain homogeneity in these studies, 20 % acetonitrile was selected as the ideal solvent for 2,4-DMA analysis.

4.4.2 The choice of supporting electrolyte

Table 4.2 shows the comparison between the current response, oxidation potential shift as well as the reproducibility for the detection of 15 μM 2,4-DMA in each buffer examined. BR buffer has been used in many voltammetric analytical studies as a supporting electrolyte for electrochemical analyses, and given its broad pH spectrum, it was used in this study as a comparison with other potential supporting electrolytes.

Table 4.2 Comparative data for different supporting electrolytes for the detection of 15 μM 2,4-DMA in acetonitrile.

SUPPORTING ELECTROLYTE	pH	Ipa_2 (μA)	Epa_2 (V)
sodium acetate buffer	4.5	9.000 (± 1.020)	0.730 (± 0.007)
Britton-Robinson buffer	4.5	11.200 (± 0.500)	0.700 (± 0.005)
sodium carbonate buffer	10	9.200 (± 0.660)	0.550 (± 0.006)
Britton-Robinson buffer	10	13.600 (± 0.820)	0.490 (± 0.006)
phosphate buffer	7.5	14.600 (± 0.320)	0.710 (± 0.003)
Britton-Robinson buffer	7.5	12.300 (± 0.300)	0.680 (± 0.002)

From table 4.2 it is evident that when the feasibility of using 0.2 M sodium acetate buffer as the supporting electrolyte for 2,4-DMA analysis was investigated, a decrease of at least 20 % in the current strength of the anodic peaks of 2,4-DMA is observed when compared 2,4-DMA analysis in 0.2 M BR buffer at equivalent pH. In addition, 2,4-DMA analysis in 0.2 M sodium acetate buffer is substantially less reproducible than the equivalent analysis in 0.2 M BR buffer, given the two fold increase in standard deviation. The comparison of 2,4-DMA analysis in 0.2 M sodium carbonate buffer with that performed in 0.2 M BR buffer of equivalent pH shows that at least a 30 % decrease in the sensitivity of the anodic peaks for 2,4-DMA is observed when 0.2 M sodium carbonate buffer is used as the supporting electrolyte, as compared to 0.2 M BR buffer. In addition, the standard deviation of 2,4-DMA analysis in 0.2 M sodium carbonate buffer is marginally lower than that in 0.2 M BR buffer.

When the sensitivity of the current response for 2,4-DMA analysis was compared between 0.2 M phosphate buffer and 0.2 M BR buffer of equivalent pH, the observation was made that the magnitude of the current response was at least 15 % lower for 0.2 M BR buffer than that of 0.2 M phosphate buffer, with a negligible difference in standard deviation of current and potential.

From these results it can be deduced that 0.2 M BR buffer does act as an ideal supporting electrolyte when compared to 0.2 M sodium acetate buffer and 0.2 M sodium carbonate buffer in terms of sensitivity. 0.2 M phosphate buffer could be used as an alternative supporting electrolyte for the analysis of 2,4-DMA in aqueous solution at the pH investigated. However, 0.2 M BR buffer was selected as the ideal supporting electrolyte due to the reproducibility of current response and broad pH spectrum.

4.4.3 The effect of pH

Figure 4.3 (a) and (b) shows CVs for 10 µM 2,4-DMA (stock solution dissolved in 20 % acetonitrile) over the pH range of 2 to 10 with 0.2 M BR buffer acting as the supporting electrolyte.

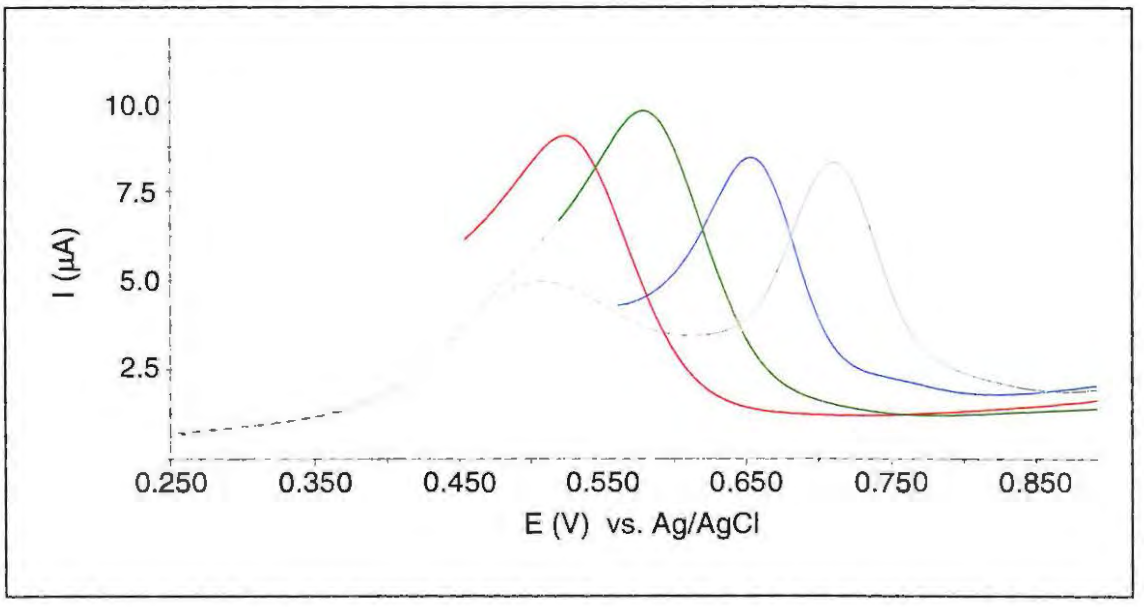

Figure 4.3 (a) CVs of 10 µM 2,4-DMA in 0.2 M BR buffer under alkaline conditions. Dotted line is the primary anodic wave, pa_1, solid line shows the secondary anodic wave, pa_2. Black = pH 6, blue = pH 7, green = pH 8 and red = pH 9. Scan rate: 100 mV/s

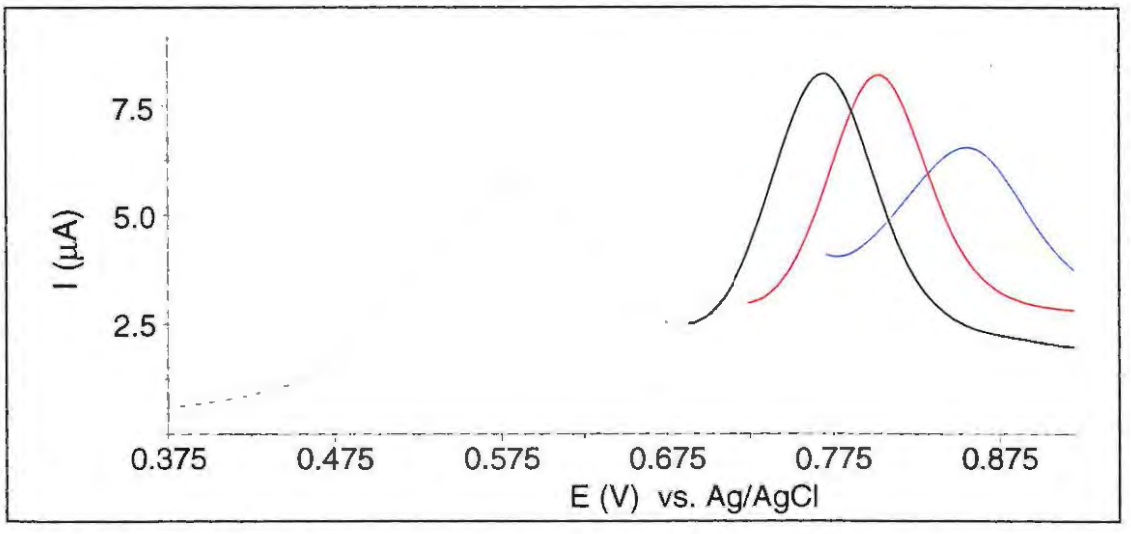

Figure 4.3 (b) CVs of 10 µM 2,4-DMA in 0.2 M BR buffer under acidic conditions. Dotted line is the primary anodic wave, pa_1, solid line shows the secondary anodic wave, pa_2. Green = pH 2, blue = pH 3, red = pH 4 and black = pH 5. Scan rate: 100 mV/s

In figure 4.3 (a) the effect of neutral and alkaline conditions on current response and potential shift for the 2,4-DMA anodic couple is shown. At pH 6 both the primary and secondary peaks are observed, with the secondary oxidation peak showing a more prominent current response. With an increase in alkalinity, the peaks shift toward less anodic potentials, as shown. The potential shift for the secondary anodic peak is greater than that of the primary anodic peak, and at pH 8 and 9 masking of the primary anodic wave by the secondary wave is observed.

At pH 2 and 3 the primary oxidation peak (pa_1) is dominant, whereas at pH 4–5 the secondary oxidation peak (pa_2) is prominent. For studies at neutral to alkaline conditions, the secondary anodic wave (pa_2) was used for quantification purposes, while the primary anodic wave (pa_1) was used for acidic conditions where the primary wave was prominent.

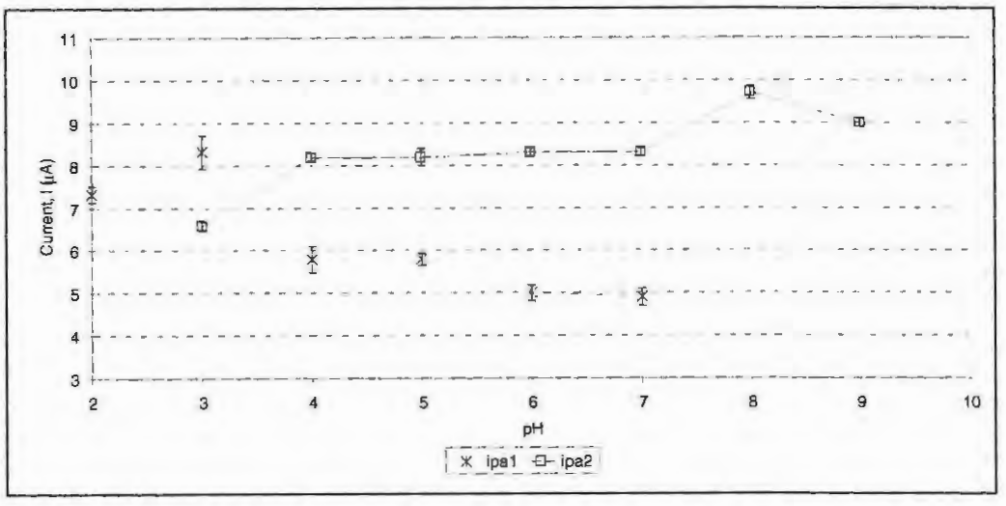

Figure 4.4 (a) Effect of pH on current response for the primary (pa_1) and secondary anodic waves (pa_1) for 10 μM 2,4-DMA with pH.

Figure 4.4 (a) shows the change in current strength of the primary and secondary anodic waves for 2,4-DMA with pH. The primary anodic wave, pa_1, generally decreases with alkalinity while the secondary wave, pa_2, values increase.

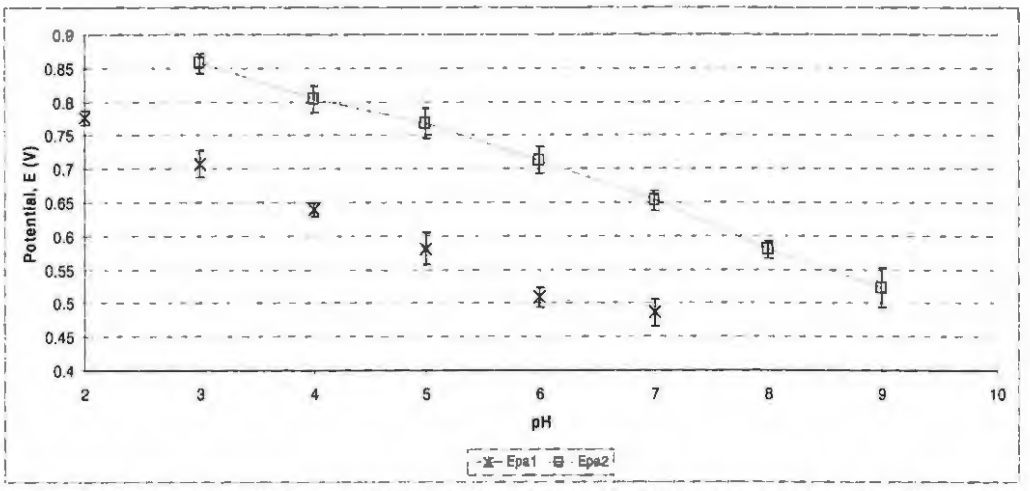

Figure 4.4 (b) Effects of pH on potential for the primary (pa_1) and secondary anodic waves (pa_2) for 10 µM 2,4-DMA

Figure 4.4 (b) shows the shift in potential for the primary and secondary anodic waves for 2,4-DMA with pH. For both primary and secondary waves, a shift towards more positive values is observed with increase in acidity.

As described in chapter 2, Mizoguchi *et al.* 1962 report that the oxidation of N,N'-DMA involves the oxidation of the amine to produce a cation intermediate which reacts with unoxidised DMA to form tetramethylbenzidine (TMB). As proposed by these authors, TMB then oxidizes to produce a quinine diimine, TMBox. This is further reiterated by Suatoni *et al.* 1961 who state that the irreversible oxidation reaction of 2,4-DMA involves the removal of an electron to yield a highly reactive free radical. The free radical is prone to dimerization with unoxidised 2,4-DMA.

Marques *et al.* 1997 in their studies on 2,3-; 2,5-; 2,6-; 3,4- and 3,5-DMA, shifts in anodic waves towards positive potentials with increase in acidity of the electrolyte solution was also observed.

4.4.4 Effect of working electrode surface fouling between CV scans

Figure 4.5 CVs showing the effect of multiple anodic scans in 0.2 M BR buffer pH 2, without cleaning the electrode between scans.

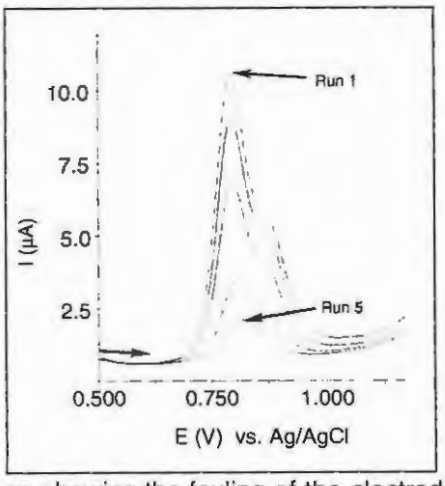

Figure 4.5 Multiple anodic scans showing the fouling of the electrode surface by 20 μM 2,4-DMA in 0.2 M BR buffer pH 2. The electrode surface was not cleaned between runs. Scan rate: 100 mV/s.

A substantial decrease in the current response of the electrode for 2,4-DMA was observed at pH 2, indicating that 2,4-DMA oxidation products adsorb onto the electrode surface irreversibly. However, at pH 7 (shown by figure 4.6), an increase in current response is observed, owing to the electrodeposition of charged 2,4-DMA onto the electrode's surface. In addition, the electrodeposition of 2,4-DMA does not poison the electrode's surface, but rather mediates the diffusion of electrons to the surface of the electrode, as is evident by the increase in current observed in figure 4.6.

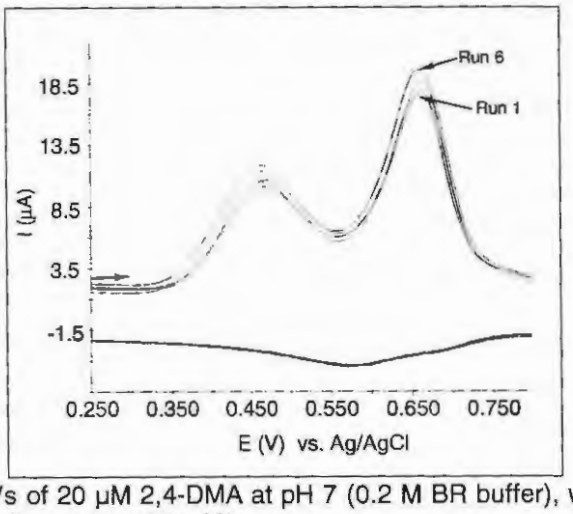

Figure 4.6 Successive CVs of 20 μM 2,4-DMA at pH 7 (0.2 M BR buffer), without cleaning of the electrode between scans. Scan rate: 100 mV/s.

The electrochemical polymerization of monomeric and substituted aniline to form a conducting polymer at an electrode has been well studied. Studies of aniline at a glassy

carbon electrode show increasing oxidation and reduction waves owing to the electrodeposition of the polymer at the electrode (Park *et al.* 1999). In this study, successive CVs in the potential windows examined showed increases in peak height also suggesting the electrodeposition of 2,4-DMA at the electrode at neutral pH.

However, as was noted at acidic pH (figure 4.5), under highly alkaline conditions, a decrease in the current strength occurs as a results of electrode surface fouling (figure 4.7). This is evident of adsorption of 2,4-DMA onto the electrode's surface in an irreversible manner. A slight increase in the current strength is observed after four runs. This could be attributed to the possible diffusion of electrons to the electrode surface, mediated by the adsorbed film, or the dissociation of adsorbed 2,4-DMA oxidation product from the electrode surface. Figure 4.7 shows the fouling of the electrode surface at pH 10.

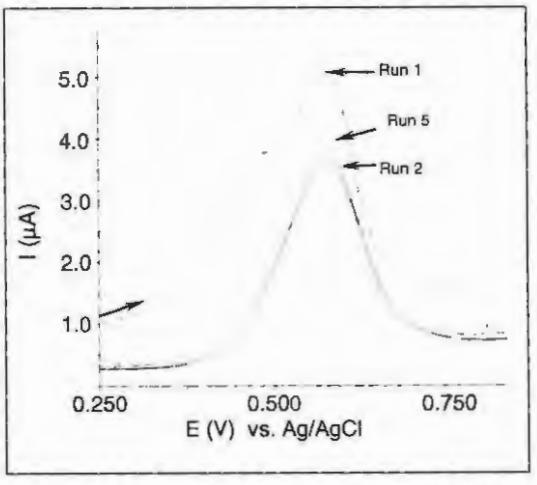

Figure 4.7 Successive CVs of 5 μM 2,4-DMA at pH 10 (0.2 M BR buffer), without electrode cleaning between scans. Scan rate = 100 mV/s.

Figure 4.8 summarises the adsorption or electrodeposition of 2,4-DMA onto the electrode surface under acidic, neutral and alkaline conditions. By setting the current of the first scan at 100 %, fouling for each scan could be presented as a percentage thereof.

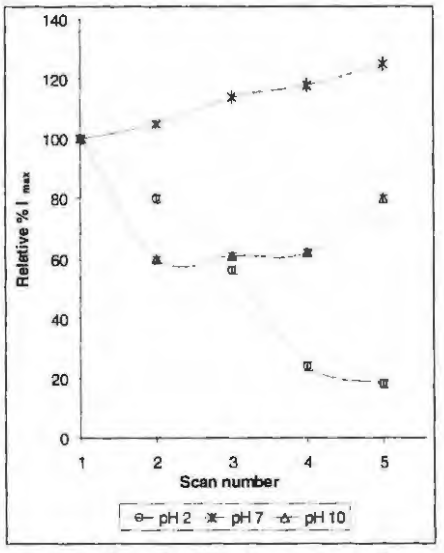

Figure 4.8 Line curves representing the change in current (as a percentage) *vs.* number of successive CV scans of 2,4-DMA as a function of pH.

4.4.5 The effect of scan rate on current response

Representative CVs of 2,4-DMA at a range of scan rates are shown in figure 4.9 at pH 4 (0.2 M BR buffer). Variation in peak current Ipa_1 and Ipa_2 vs. the square root of the scan rate is also shown in figure 4.9. The scan rate range investigated was 50 mV/s to 400 mV/s. The linear relationship between 25 mV/s and 200 mV/s is indicative of a diffusion-controlled process between these scan rates, with a deviation from linearity above 200 mV/s.

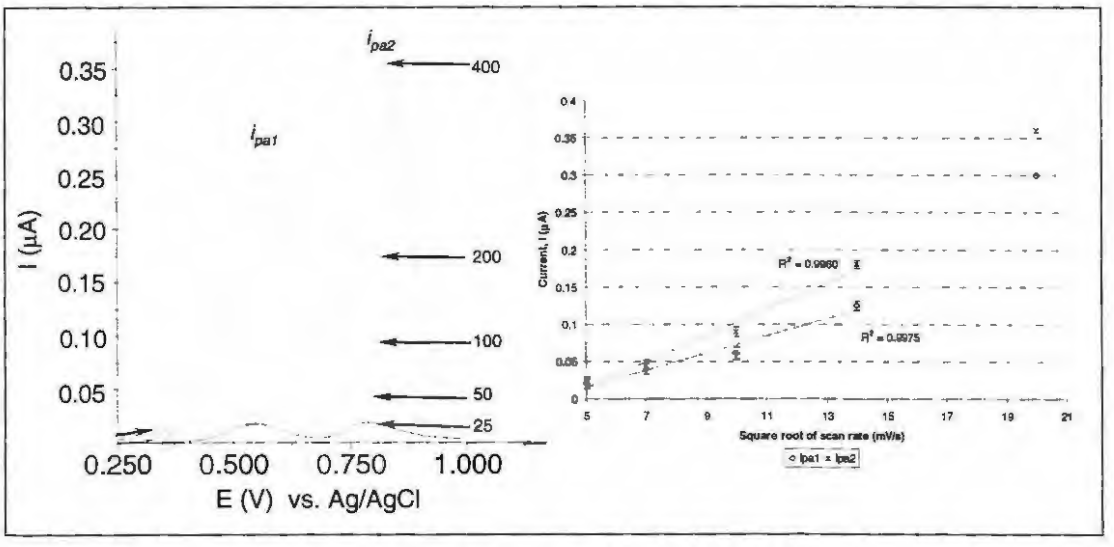

Figure 4.9 Representative CVs and standard curve of 10 µM 2,4-DMA at a range of scan rates (mV/s). Supporting electrolyte: 0.2 M BR buffer pH 7.

4.4.6 Generation of standard curves for 2,4-DMA in 0.2 M BR buffer under different pH conditions

CV of increasing concentration of 2,4-DMA at pH values between 2 and 10 were performed. Representative CV scans and line standard curves at pH 3, 7 and 10 are shown.

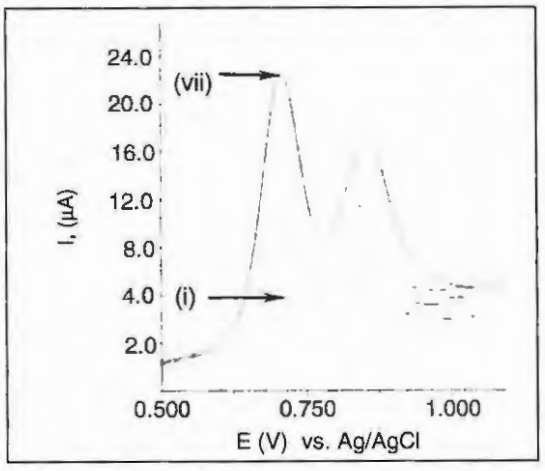

Figure 4.10 (a) Representative CVs of increasing concentration of 2,4-DMA (dissolved in 20 % acetonitrile) between 10 μM and 70 μM in 0.2M BR buffer (pH 3). Scan rate: 100 mV/s.

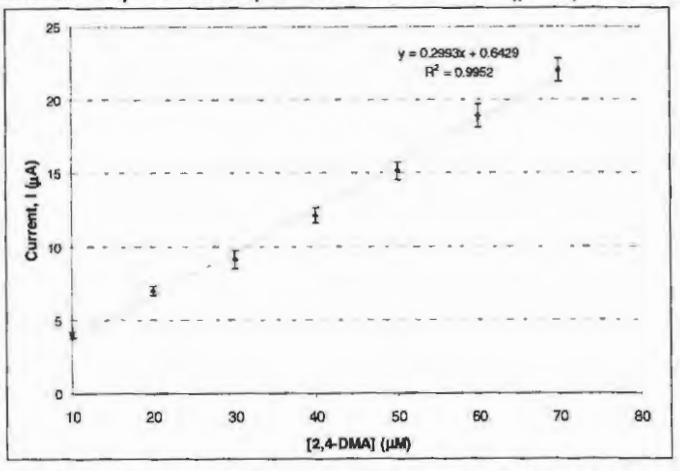

Figure 4.10 (b) Standard curve of current *vs.* concentration of 2,4-DMA (dissolved in 20 % acetonitrile) in 0.2M BR buffer (pH3). Scan rate: 100 mV/s.

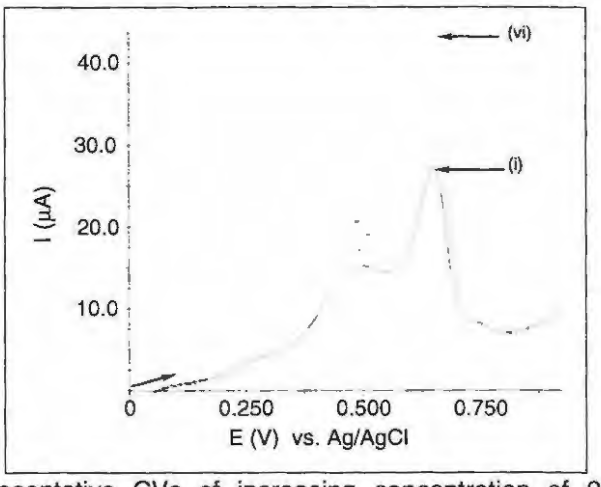

Figure 4.11 (a) Representative CVs of increasing concentration of 2,4-DMA (dissolved in 20 % acetonitrile) in 0.2M BR buffer (pH 7). Scan rate: 100 mV/s.

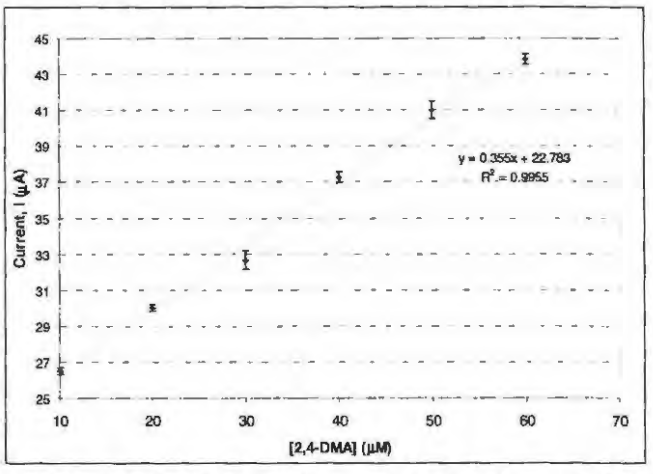

Figure 4.11 (b) Standard curve of current vs. concentration of 2,4-DMA (dissolved in 20 % acetonitrile) in 0.2 M BR buffer (pH 7).

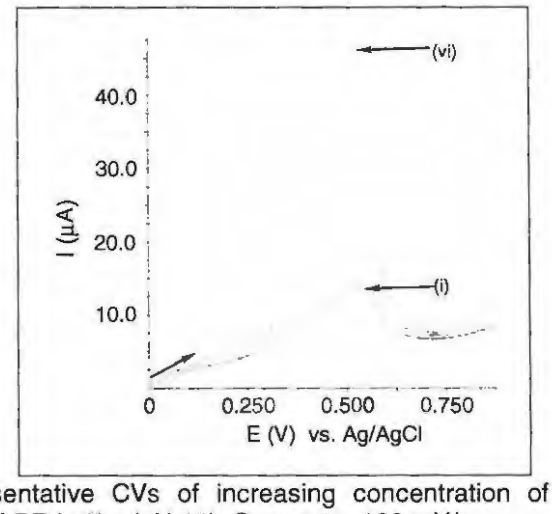

Figure 4.12 (a) Representative CVs of increasing concentration of 2,4-DMA (dissolved in 20 % acetonitrile) in 0.2M BR buffer (pH 10). Scan rate: 100 mV/s.

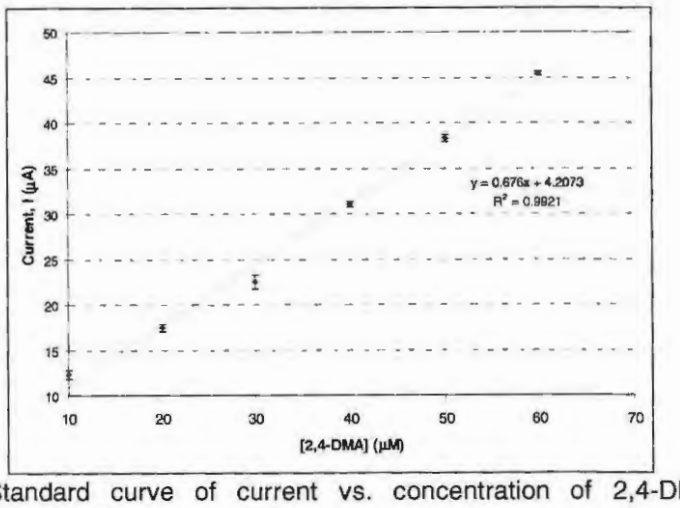

Figure 4.12 (b) Standard curve of current vs. concentration of 2,4-DMA (dissolved in 20 % acetonitrile) in 0.2 M BR buffer (pH 10).

CVs in Figure 4.12 (a) show the increase in current strength with increase in the concentration of 2,4-DMA at pH 10. The masking of the primary oxidation peak appears to be concentration dependent at this pH.

Figure 4.13 shows the line curves obtained for 2,4-DMA from pH 2–10. As shown in section 4.4.3 of this chapter, the greatest sensitivity is obtained at more alkaline conditions.

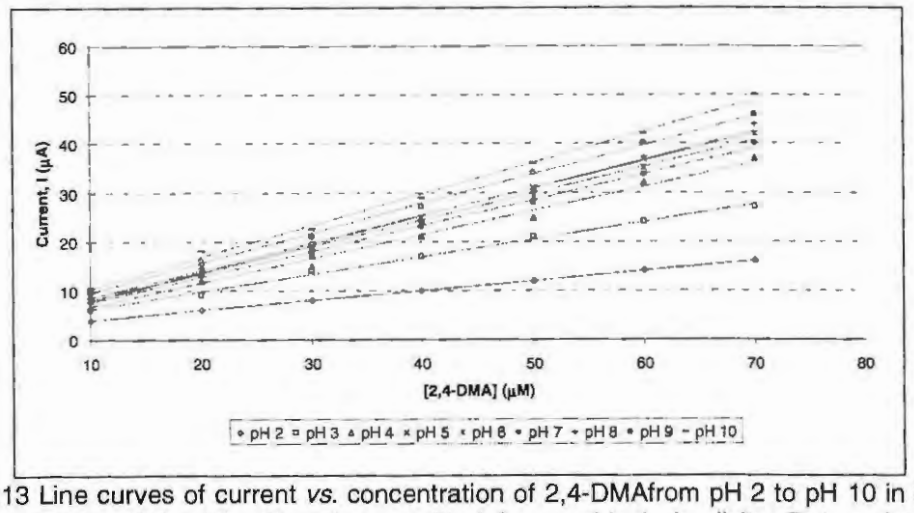

Figure 4.13 Line curves of current *vs.* concentration of 2,4-DMAfrom pH 2 to pH 10 in 0.2 M BR buffer. Scan rate: 100 mV/s. Error bars omitted for graphical simplicity. Data points are the average of three scans.

The reproducibility, accuracy and sensitivity of 2,4-DMA detection and quantification in 0.2 M BR buffer over the pH range 2–10 can be examined by a comparison of the correlation coefficient and average reproducibility between CV scans, as in table 4.3.

Table 4.3 Comparative study showing differences in key factors between standard curves for the quantification of 2,4-DMA at different pH.

pH	R^2	AVERAGE REPRODUCIBILITY (%)*
2	0.9941	95.7
3	0.9952	94.1
4	0.9912	96.1
5	0.9981	94.8
6	0.9946	96.1
7	0.9956	96.6
8	0.9921	96.3
9	0.9985	96.3
10	0.9921	96.6

* Reproducibility calculated as outlined in chapter 1.2.

Good linearity of current response *vs.* concentration was obtained at all pH values with no particular trend observed. Table 4.3 shows that the greatest linearity for 2,4-DMA analysis was observed at pH 9. The average reproducibility of the current response of studies conducted at each pH is on average higher under neutral to alkaline conditions. An extrapolated limit of detection of 1×10^{-8} M was determined for CV analysis of 2,4-DMA. LOD was calculated as outlined in chapter 2.2. By using differential pulse voltammetry, an experimental limit of detection for 2,4-DMA in 0.2 M BR buffer pH 7 was determined as 2.0×10^{-8} M.

4.6 CONCLUSION

Table 4.4 summarises parameters identified as optimal for 2,4-DMA detection and quantification:

Table 4.4 Summary of key operational parameters for qualitative and quantitative 2,4-DMA analysis

PARAMETER	OPTIMAL CONDITION
Solvent	20 % acetonitrile
Supporting electrolyte	0.2 M Britton-Robinson buffer
pH	7 – 9
Fouling	Regeneration of GCE surface required between scans

2,4-DMA analyses could be conducted under acidic, neutral and alkaline conditions. Under acidic conditions, the primary anodic wave was more sensitive than the secondary anodic wave, and may be used for 2,4-DMA analysis at these pH values. Under neutral to alkaline conditions, the secondary anodic wave, pa_2, was more prominent and used for 2,4-DMA analyses at these pH values. In terms of sensitivity, the highest current response was observed under alkaline conditions, the greatest linearity at pH 9 and the highest reproducibility at pH 7 and 10.

Anodic potentials for 2,4-DMA were pH dependent and shifted towards more positive values with increasing acidity. Fouling of the electrode was observed under acidic and alkaline conditions while electrodeposition of 2,4-DMA was observed at pH 7. At pH 7, the linearity of current versus the square root of the scan rate indicated a diffusion controlled process between 25 mV/s and 400 mV/s.

CHAPTER 5

OPTIMISATION OF OPERATIONAL PARAMETERS FOR THE CHARACTERISATION AND ANALYSES OF 3-METHYLCATECHOL

5.1 INTRODUCTION

3-methylcatechol (3-MC) is a polyhydroxyaromatic, versatile electroactive species (Davies *et al.* 1998, Bazzicalupi *et al.* 1998) that has been used as a ligand for the detection of heavy metals electrochemically by adsorption onto the electrode. Catechol polymerisation onto electrode surfaces is relatively easy and is useful as an electrode modifier in that catechol readily mediates the electron transfer between the oxidised and reduced forms of nicotinamide adenine dinucleotide (NAD^+ and NADH) (Athwale *et al.* 1999, Seymour *et al.* 2002, Korbi *et al.* 2004).

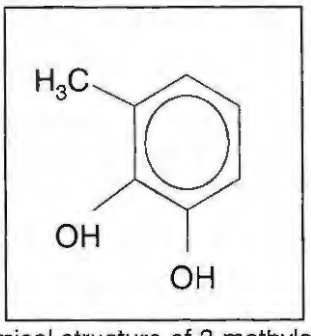

Figure 5.1 Chemical structure of 3-methylcatechol (3-MC).

Electrochemistry of 3-methylcatechol

3-MC consists of a benzene ring with two *ortho* hydroxyl groups and a single methyl group in the *meta* position. The electrochemical oxidation of 3-MC is well understood. Cyclic voltammetry of 3-MC in the presence of a supporting electrolyte, such as 0.15 M phosphate buffer (pH 7.2), exhibits an anodic and cathodic peak couple that corresponds to the quasi-reversible two electron transformation of 3-MC to 3-methyl-*o*-benzoquinone, and vice versa. A peak – current ratio, *pa/pc* of near unity is observed for the oxidation of 3-MC (Nematollahi *et al.* 2002, Fakhari *et al.* 2005).

Scheme 5.1 illustrates the formation of a quinone derivative when 3-methylcatechol is oxidised.

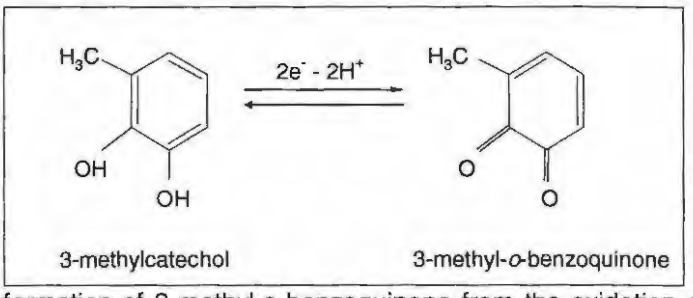

Scheme 5.1. The formation of 3-methyl-o-benzoquinone from the oxidation of 3-methylcatechol (Fakhari *et al.* 2005).

In a methanol solution, 3-MC can undergo methoxylation according to an ECECE (electrochemical, chemical) or ECE mechanism with the utilisation of 6 or 4 electrons per molecule. If no methoxylation of the *ortho* methyl group occurs, the electrode process obeys a simple E mechanism. The resultant product is a methoxy-*o*-benzoquinone. In the presence of ethanol, 3-MC undergoes ethoxylation by an ECECE mechanism to afford 4,5-diethoxy-*o*-benzoquinone (Nematollahi *et al.* 2002, Fakhari *et al.* 2005).

Authors such as Habibi *et al.* 2005 have shown in their previous studies that catechols can be hydrolysed to 1,2-benzoquinone. The *o*-quinones that are generated in *situ* are relatively reactive, and react readily with an array of nucleophiles such as 4-hydroxycoumarin, barbituric acids and acetylacetone, methanol, ammonia, chloride and sulfhydryl groups.

The relatively high degree of reactivity of catechols makes them targets for assisting in the synthesis of new compounds, such as pyrimidines, which are an important class of heteroaromatic compounds that are known to have antitumour and antimicrobial activities.

5.2 AIMS

The purpose of this section is to optimise key parameters in 3-MC detection and quantification. These parameters include:

1. Investigation of the behaviour of 3-MC under different pH conditions. Assessment of the optimal pH for effective voltammetric analysis in terms of sensitivity, reproducibility and stability of 3-MC.
2. Investigation of the effect of fouling. Assessment of the behaviour of 3-MC at a GCE surface in sequential scans.
3. Investigation of the effect of scan rate on CV analysis of 3-MC.
4. Assessment of the effect of pH on linearity of CV analyses for 3-MC by standard curve generation.

5.3 METHODOLOGY

3-MC is soluble in water. Therefore all dilutions of 3-MC were done in aqueous solution and no solvent comparison was required. For 2,4-DMA and amitraz analysis, Britton-Robinson (BR) buffer was determined to be the optimal buffer for electrochemical analyses, and 3-MC was analysed in the same supporting electrolyte.

The investigation of the effect of pH on the potential shift and the strength of the current response was performed as outlined in chapter 2. Reproducibility studies were performed with and without cleaning of the electrode surface, as outlined in chapter 2. Scan rate studies and the quantification of 3-MC as before were performed according to the procedure outlined in chapter 2.

5.4 RESULTS AND DISCUSSION

A CV characterising 3-MC was shown in chapter 2.3.4.

5.4.1 The effect of pH

The quasi-reversible peak couple for 3-MC can be ascribed to the oxidation of 3-MC to a related quinone, 3-methyl-*o*-benzoquinone (3-MBQ), and subsequent homogenous cathodic regeneration of 3-MC on the return scan. This is graphically presented in figure 5.2 (a). The analysis of 3-MC over the pH spectrum 2 to 10 yielded 3 different behavioural patterns. At pH 2, an anodic peak is observed at 0.48 V (*vs.* Ag/AgCl), which is accompanied by a return cathodic wave at 0.45 V (*vs.* Ag/AgCl).

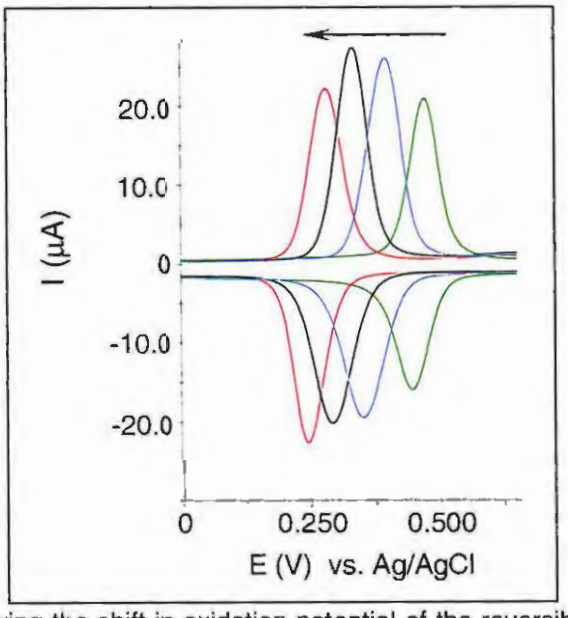

Figure 5.2 (a) CVs showing the shift in oxidation potential of the reversible peak couple of 3-MC (30 µM) with pH change between 2 (green) and 5 (red). Supporting electrolyte: 0.2 M BR buffer, scan rate: 100 mV/s.

With a shift to less acidic pH, a uniform shift in the oxidation wave to less anodic potentials is observed, with a slight increase in the peak current ratio, as seen in figure 5.2 (a). The increase in current response from pH 2 to 4 could be attributed to an increase in the apparent number of electrons transferred, from the limits of n = 2 to 4 electrons per molecule (Nematollahi *et al.* 2002).

At neutral pH (6–7) a behavioural change in the peak potentials is observed, where CV of the electro-oxidation of 3-MC yields the formation of a secondary oxidation peak at higher anodic potentials. The current strength of the secondary oxidation peak increases from pH 6 to 7, with a uniform decrease in the primary oxidation peak owing to the oxidation of 3-MC. Nematollahi and Hesari 2005 attribute the secondary anodic peak to the dimerization of anionic or dianionic forms of 3-MC with *o*-benzoquinones. The authors further elucidate that the rate of the catechol–benzoquinone dimerization reaction is pH dependent and is amplified by a pH shift towards more alkaline conditions. The results of this study concur with these findings, and are presented in figure 5.2 (b).

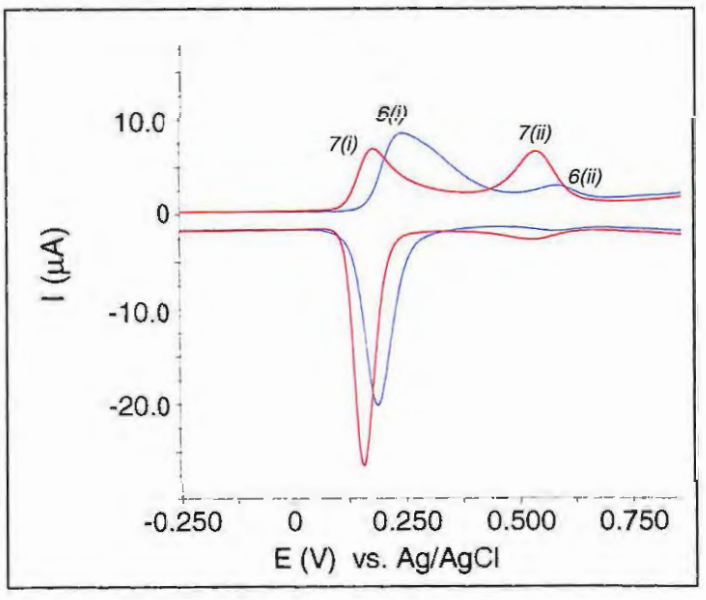

Figure 5.2 (b) CVs showing the shift in oxidation potential of the oxidation peak for 3-MC (30 µM) at pH 6 and 7. Supporting electrolyte: 0.2 M BR buffer, scan rate: 100 mV/s.

In figure 5.2 (b), the decreasing primary oxidation peak of 3-MC is shown at pH 6 and 7, with a secondary peak ascribed to 3-methyl-*o*-benzoquinone (3-MBQ) dimer formation shown to increase with alkalinity.

With an increase in alkalinity of the solution, the primary oxidation peak is significantly reduced while that attributed to formation of the 3-MBQ dimer is substantially enhanced, as shown in figure 5.2 (c). In addition, the peak current ratio is shown to be less than unity, and decreasing further with an increase in pH value. This finding concurs with those of Nematollahi and Hesari 2005.

Figure 5.2 (c) shows the CVs for 30 µM 3-MC at pH 8, 9 and 10.

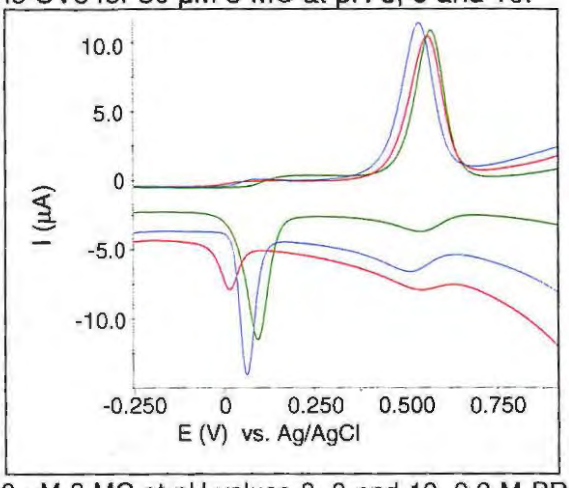

Figure 5.2 (c) CVs for 30 µM 3-MC at pH values 8, 9 and 10. 0.2 M BR buffer was used as the supporting electrolyte. Scan rate = 100 mV/s. *Legend:* green line = pH 8, blue line = pH 9, red line = pH 10.

Figure 5.2 (d) compares the forward scan of a CV of 3-MC at pH 4, 7 and 10; The figure shows at pH 4 the peak attributed to the oxidation of 3-MC to 3-MBQ, and the formation of the second anodic peak under more basic conditions attributed to the formation of a dimer between 3-MC and the 3-MBQ species.

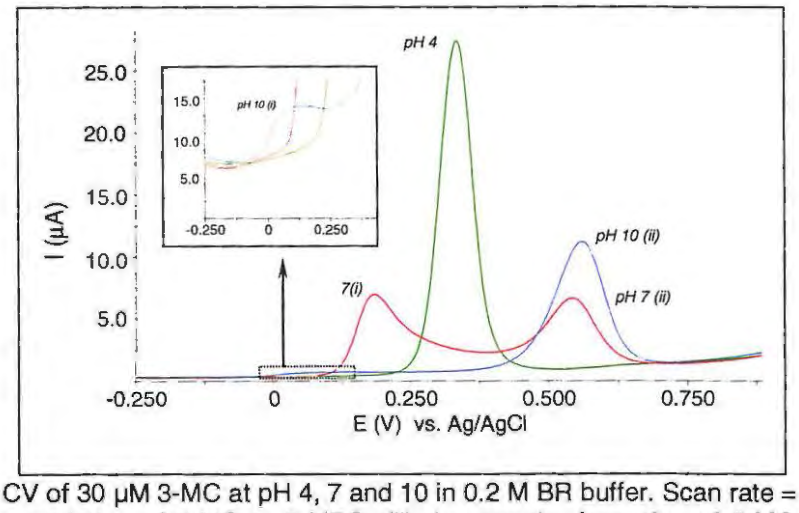

Figure 5.2 (d) CV of 30 µM 3-MC at pH 4, 7 and 10 in 0.2 M BR buffer. Scan rate = 100 mV/s. (i) denotes the oxidation of 3-MC to 3-MBQ. (ii) denotes the formation of 3-MC-3-MBQ dimer. Inset is an enlarged area showing the weak oxidation of 3-MC observed at pH 10.

5.4.2 Effect of working electrode surface fouling

Nematollahi *et al.* 2002 and Fakhari *et al.* 2005 concur that at acidic pH, the oxidised 3-MC is reduced in the cathodic return scan. This homogenous regeneration of 3-MC under acidic conditions leads to the regeneration of the electrodes surface, so no fouling

would be expected. If any fouling did occur it would be attributed to electro-adsorption. Successive CVs of 3-MC without electrode cleaning are shown in figure 5.3 (a). The increasing current response with scan number is indicative of the electrodeposition of 3-MC onto the electrode surface under acidic conditions. These results concur with the findings of Nematollahi *et al.* 2002 and Fakhari *et al.* 2005. In addition, these authors state that under neutral to basic pH conditions, where dimerization of 3-MC occurs with 3-MBox, the peak current ratio decreases, and a non-corresponding return cathodic wave is observed. In this state, the homogenous regeneration of 3-MC does not occur, and the dimerized species adsorbs to the electrode, hindering the passage of electrons to the electrode surface. The fouling of the electrode at neutral to alkaline pH is shown in figure 5.3 (b), corresponding with the findings of the above mentioned authors.

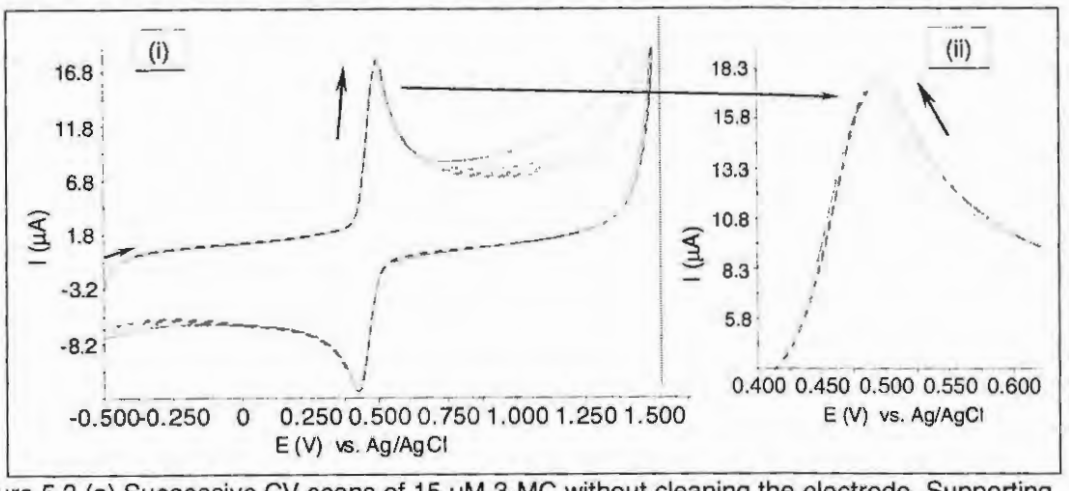

Figure 5.3 (a) Successive CV scans of 15 µM 3-MC without cleaning the electrode. Supporting electrolyte: 0.2 M BR buffer pH 4.The solid line is the first run, with the dotted lines representing subsequent scans without electrode cleaning.

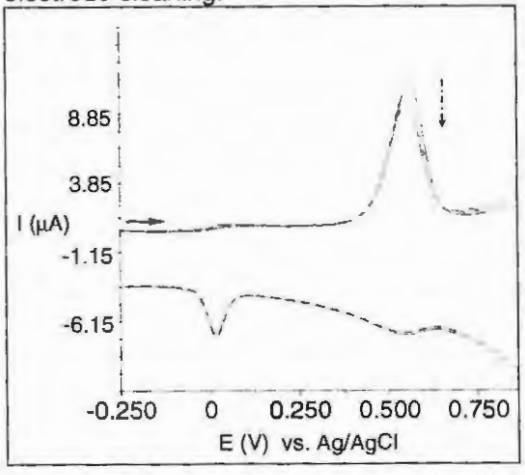

Figure 5.3 (b) Successive CV scans of 40 µM 3-MC at pH 10, 0.2 M BR buffer, without electrode cleaning. Scan rate = 100 mV/s.

A decrease in the current response with subsequent scans is observed in figure 5.3 (b), indicative of adsorption of oxidised species onto the electrode. A decrease in the return cathodic wave at pH 10 shows the inability of the oxidised species to dissociate from the electrode.

5.4.3 The effect of scan rate on current response

Representative CVs of 3-MC at a range of scan rates are shown in figure 5.4 (a) at pH 4. Variation in peak current *vs.* the square root of the scan rate is shown in figure 5.4 (a). The scan rate range investigated was 50 mV/s to 400 mV/s. The linear relationship shown on figure 5.4 (b) is indicative of a diffusion controlled reaction occurring in the electrochemical cell, at these scan rates.

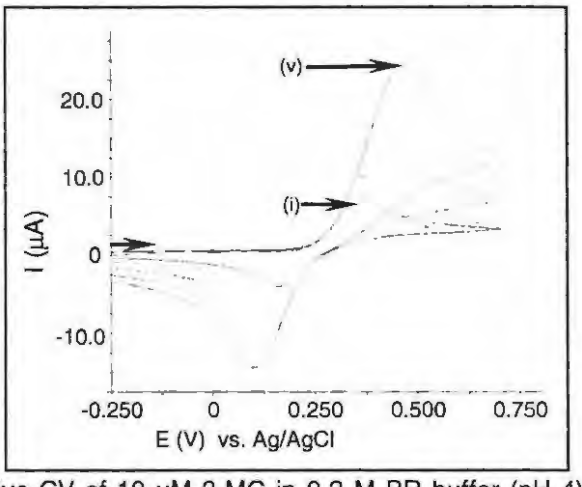

Figure 5.4 (a) Successive CV of 10 μM 3-MC in 0.2 M BR buffer (pH 4). Scan rate increments (mV/s): 25 (i), 50, 100, 200 and 400 (v).

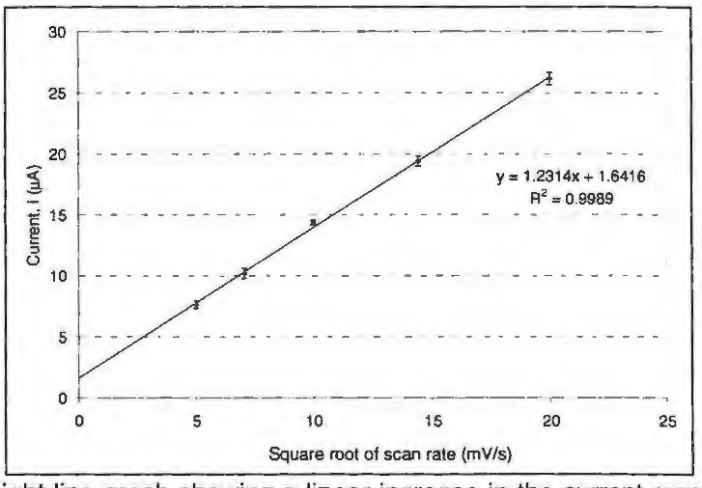

Figure 5.4 (b) Straight line graph showing a linear increase in the current response of 3-MC with an increase in scan rate.

From figure 5.4 (b) it is evident that a linear relationship exists between the square root of the scan rate and current response for 3-MC. This is indicative of a diffusion controlled process. However, quasi-reversible systems are characterised by non-linear current responses, which requires mass transport of the electrons to the electrode. A diffusion controlled process in quasi-reversible systems could be attributed to the ionic strength of the supporting electrolyte.

5.4.4 Generation of standard curves for 3-MC in 0.2 M BR buffer under different pH conditions

Standard curves for 3-MC at pH 4 and 10 showed a linear response as shown in figures 5.5 and 5.6. At pH 4, the primary anodic wave at lower potentials was used for analyses while the secondary anodic wave was used for analyses at pH 10.

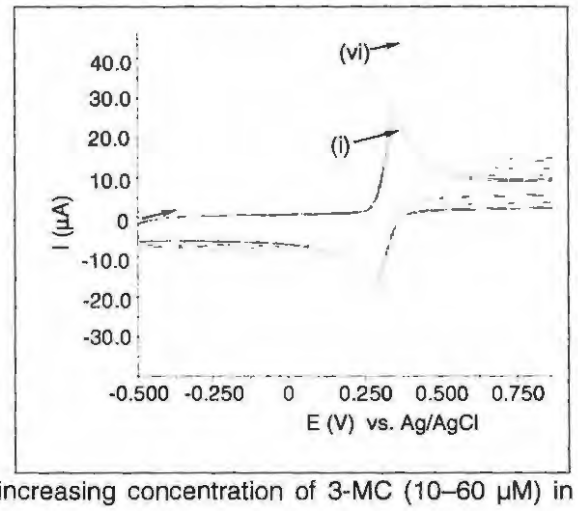

Figure 5.5 (a) CVs of increasing concentration of 3-MC (10–60 µM) in 0.2M BR buffer (pH 4). Scan rate = 100 mV/s.

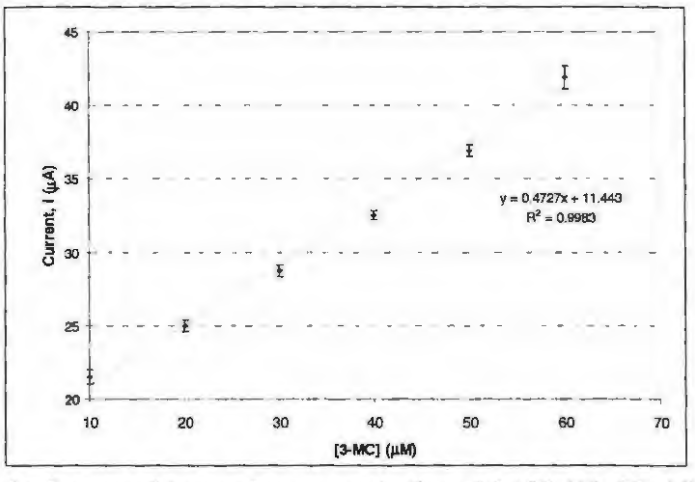

Figure 5.5 (b) Standard curve of increasing concentration of 3-MC (10–60 µM) in 0.2M BR buffer (pH 4).

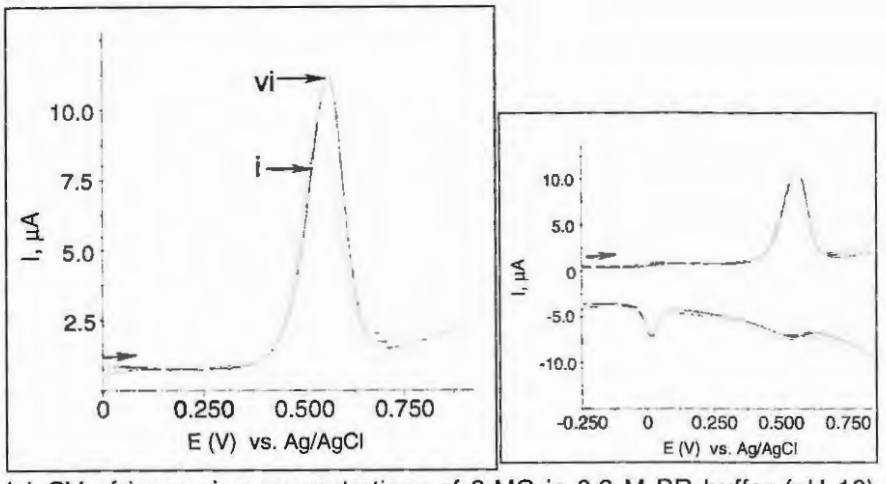

Figure 5.6 (a) CV of increasing concentrations of 3-MC in 0.2 M BR buffer (pH 10). The inset shows anodic and cathodic waves obtained. Scan rate: 100 mV/s.

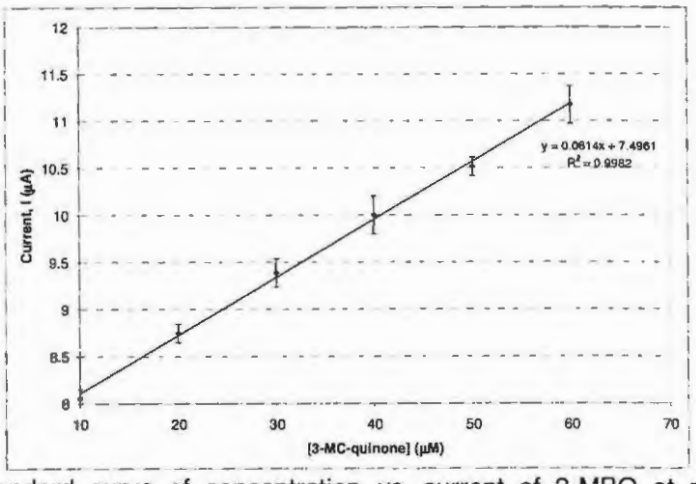

Figure 5.6 (b) Standard curve of concentration *vs.* current of 3-MBQ at pH 10. Supporting electrolyte: 0.2 M BR buffer.

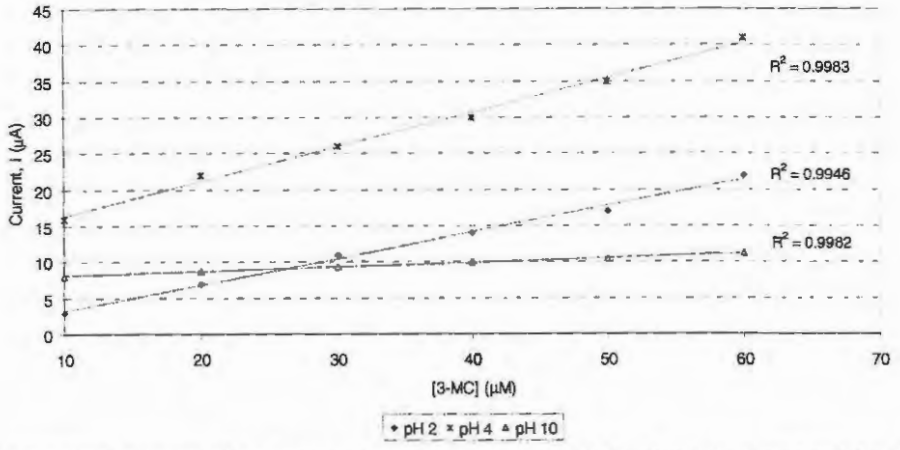

Figure 5.7 Standard curves of concentration *vs.* current of 3-MC at pH 2, 4 and pH 10. Error bars are excluded for ease of visualisation.

In figure 5.7, good linearity is observed for 3-MC quantification at pH 2 and 4, with R^2 values of 0.9983 and 0.9947, respectively. At pH 10, while good linearity of concentration *vs.* current response was observed, substantial decrease in sensitivity was evident at pH 10.

5.5 CONCLUSION

CV studies showed a quasi-reversible couple for oxidation of 3-MC to 3-MBQ at pH 2–5. The anodic potential was dependent on the pH of the solution. A secondary irreversible couple with a decreasing peak-current ratio was observed to occur at neutral pH. The secondary oxidation peak attributed to formation of a 3-MC-3MBQ dimer which increased in current response with an increase in alkalinity, while the primary oxidation peak decreased.

Under acidic conditions, the primary anodic couple for 3-MC shows electrodeposition at the electrode surface following multiple scans. Under neutral to alkaline conditions, fouling was observed. The oxidation of the secondary oxidation peak at high pH is irreversible, leading to a decreased current response due to electrode surface fouling. Scan rate studies showed that the transport of 3-MC to the electrode is a diffusion controlled process at pH 4. The electrochemical behaviour of 3-MC is well understood, and the findings of this study concur with findings in literature by Golabi and Nematollahi 1997, Nematollahi *et al.* 2002, Fakhari *et al.* 2005 and Nematollahi and Hesari 2005.

CHAPTER 6

TESTING THE EFFICACY OF USING ELECTROCHEMISTRY FOR ENVIRONMENTAL MONITORING OF AMITRAZ AND ITS DEGRADANTS

6.1 INTRODUCTION

There exists a risk that amitraz used on livestock can absorb into the meat as well as be found in residual concentrations in milk. In addition, amitraz has been used in beehives to control the mite, *Varroa jacobsoni* (Corta *et al.* 1999, Martel & Zeggane 2002). Studies performed by Corta *et al.* 1999 have shown that even though amitraz hydrolyses in the acidic conditions of honey, 2,4-DMA is stable in this medium and can be found in residual concentrations in the honey.

Honey is consumed by humans, and also used in the production of mead. Stewart *et al.* 1999 states that at least 33 % of fatal cases of poisoning attributed to traditional remedies in South Africa are a direct cause of agri-chemicals. In soil, amitraz is hydrolysed through biodegradation, however 2,4-DMA is believed to be recalcitrant in the environment.

Amitraz is an effective control pesticide for *Boophilus microplus* (Canestrini) on cattle (George *et al.* 1998) as well as controlling mange on livestock and is used for the eradication of insects in agronomy and horticulture (Abu-Basha *et al.* 1999). The actions of amitraz are thought to be mediated by octopamine receptors (Evans & Gee 1980, Singh *et al.* 1990, Hashemazadeh *et al.* 1985, Roder 1995). When amitraz is administered orally to mammals, it is "rapidly absorbed, distributed, metabolized and eliminated primarily via urine" (Abu-Basha 1999).

Amitraz can aggravate the cause of (amongst others) hyperglycaemia, central nervous system depression, bradycardia, polyuria and coma in humans. Many cases of fatal amitraz toxicity have been reported (Kennel *et al.* 1996, Jorens *et al.* 1997, Aydin *et al.* 1997). In addition, amitraz and 2,4-DMA have an effect on the secretion of insulin and glucagon from the pancreas (Abu-Basha 1999).

Further studies have shown that residual amitraz is found in the milk of cattle to which amitraz was topically administered, however at low concentrations of 0.07 ppm. In addition, 2,4-DMA was found in much higher concentrations than amitraz in cattle meat along with intermediates such as DMF and DMP, which are known toxins. At least 3.7 ppm of 2,4-DMA has been found to accumulate in cattle to which amitraz has been topically administered. Therefore a real risk exists for human ingestion of residual 2,4-DMA. Even though the lethal dosage of 2,4-DMA is high, the accumulation of 2,4-DMA over time is cause for concern (Bolognesi 2003).

A common form of amitraz administration is through plunge dipping or spraying of livestock. Both of these techniques are subject to shortcomings in terms of dosing livestock at the correct concentrations. The plunge dipping method in particular is problematic, as dip water is frequently re-used for further dosing of animals, with users adding additional pesticide to water that may contain unknown residual amounts of pesticide, or potentially harmful degradation products. There is much room for error in maintaining effective dosages if residual concentrations of pesticides are unknown. Researchers have shown that incorrect dosing of amitraz has lead to ticks and mites gaining resistance to the pesticide (Jonsson *et al.* 2000).

The potential for pesticide resistance coupled with the toxicity of amitraz and 2,4-DMA to humans, livestock and the environment has led to a demand for a portable analytical device that can relay information regarding the concentration of active pesticides on-site and in real time. The detection and monitoring of toxic analytes in complex matrices with extensive sample preparation such as milk, spent cattle dip and honey by using HPLC and GC-MS has been difficult given that the matrices contain an array of possible interferents.

Conventionally, high performance liquid chromatography (HPLC) and gas chromatography (GC) have been employed as the analytical techniques for amitraz and 2,4-DMA analysis (Corta *et al.* 1999). These techniques are, however, not readily adapted for on-site use. While water samples from livestock dipping tanks can be sent to laboratories for analysis, this leads to delays in the relay of analytical results and potential inaccuracies as the pesticide composition of the dipping tanks is subject to alteration during long analysis times.

Electrochemistry has the potential to detect analytes of interest in a complex matrix with negligent interference from analytes in the sample and with minimal sample preparation.

No studies have been conducted on the voltammetric analysis of amitraz and 2,4-DMA in the complex matrix of a livestock dipping tank, honey and milk. Korta *et al.* 2003 state that amitraz and 2,4-DMA cannot be detected in honey using GC-MS, only residues of DMF could be detected. In this study we explore the cyclic voltammetric behaviour of amitraz and 2,4-DMA at a glassy carbon electrode, in spent cattle dip, honey and milk.

6.2 AIMS

Assess the feasibility of detecting amitraz and 2,4-DMA in spent cattle dip, milk and honey.

6.3 METHODOLOGY

6.3.1 Detection of amitraz and 2,4-DMA in spent cattle dip

Amitraz and 2,4-DMA were prepared fresh as outlined in chapter 2.2. The pH of the spent cattle dip was determined by using a pH meter (chapter 2.2). Electrochemical studies of the analyte in 0.2 M BR buffer of the same pH was used as a comparison. Electrochemistry was performed in the spent cattle dip obtained from Cold Springs farm in Grahamstown. No sample preparation was performed. A CV of spent cattle dip with residual concentrations of amitraz and 2,4-DMA was used as a baseline. Thereafter, the spent cattle dip sample was spiked with amitraz, or where 2,4-DMA was quantified, the spent cattle dip was spiked with 2,4-DMA.

6.3.2 Characterisation of amitraz and 2,4-DMA in spent cattle dip, milk and honey

A sample of spent cattle dip to which no amitraz had been applied was obtained and its pH determined. A CV of this sample was performed in the absence and presence of amitraz and 2,4-DMA. For milk, the pH was determined and 0.2 M BR buffer of equivalent pH was used as a comparison. A CV of milk in the absence of amitraz and 2,4-DMA was used as a baseline. Milk samples were spiked with amitraz or 2,4-DMA and electrochemical analyses performed. For honey, the pH was determined, and given its viscosity, was mixed with 0.2M BR buffer of the same pH at a ratio of 0.2 M BR

buffer: honey (50:50) (v/v). A CV of 0.2 M BR buffer: honey (50:50) (v/v) in the absence of amitraz or 2,4-DMA was used as a baseline. Thereafter, the samples were spiked with amitraz or 2,4-DMA, respectively and electrochemistry performed. The CV scans were performed 5 times in order to determine the degree of standard deviation.

6.3.3 Standard curve generation for amitraz and 2,4-DMA in spent cattle dip, milk and honey.

Standard curves were set up for amitraz and 2,4-DMA in each of the environmental samples by recording CV of increasing concentrations of amitraz and 2,4-DMA.

6.4 RESULTS AND DISCUSSION

6.4.1. Detection of amitraz and 2,4-DMA in spent cattle dip (pH 3)

A sample of spent cattle dip was obtained from a dipping tank to which amitraz had been applied. A CV of this sample, figure 6.1 (a), shows an anodic peak at 1.18 V (± 0.04 V), which concurs with the anodic wave for amitraz as characterised in chapter 2. This was confirmed by spiking the sample with 10 µM amitraz, as is represented by the blue line in figure 6.1 (a). A slight shift towards less anodic potentials is noted for the amitraz peak when the dip was spiked with amitraz.

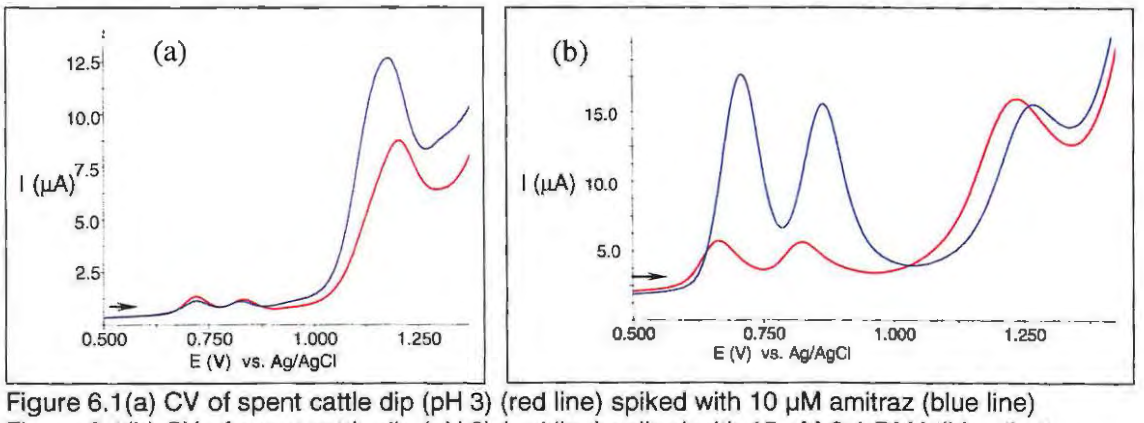

Figure 6.1(a) CV of spent cattle dip (pH 3) (red line) spiked with 10 µM amitraz (blue line)
Figure 6.1(b) CV of spent cattle dip (pH 3) (red line) spiked with 15 µM 2,4-DMA (blue line)

The anodic couple at 0.66 V (± 0.05 V) and 0.83 V (± 0.05 V) in figure 6.1 (b) concurs with the characterisation of 2,4-DMA shown in chapter 2.3.3, and confirmed by spiking the spent cattle dip sample with 15 µM 2,4-DMA.

6.4.2. Detection of amitraz in environmental samples

13 µM Amitraz was added to each of spent cattle dip (pH 3) (to which no amitraz had been applied), honey:BR buffer (50:50) (v/v) (pH 4) and milk (pH 7). Figure 2 show CVs where the comparison in current strength in amitraz detection in spent cattle dip, honey and milk to analyses in 0.2 M BR buffer of equivalent pH and amitraz concentration was made.

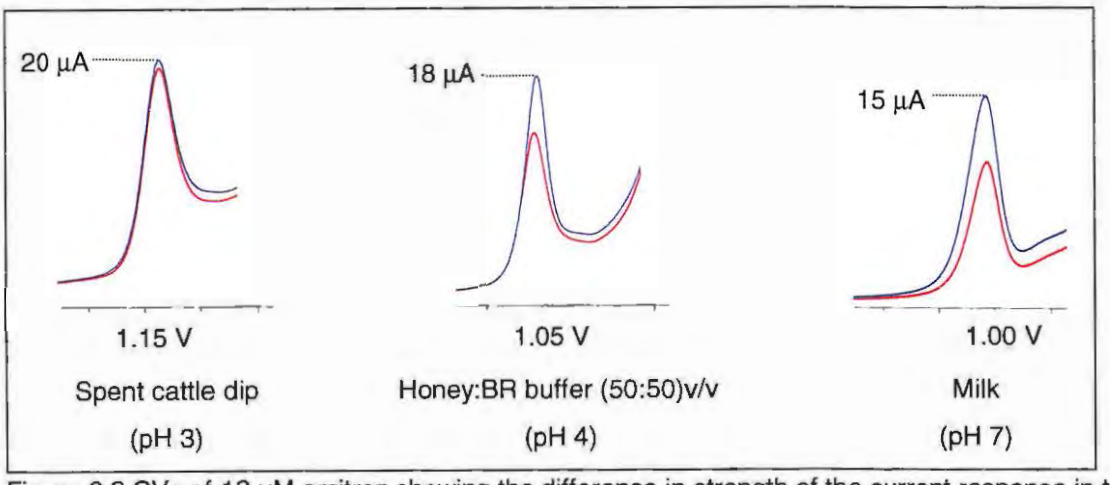

Figure 6.2 CVs of 13 µM amitraz showing the difference in strength of the current response in the relevant sample [spent cattle dip (no amitraz), honey or milk] as compared to the current response obtained in 0.2 M BR buffer of the same pH. Legend: red line = amitraz in environmental sample, blue line = amitraz in 0.2 M BR buffer of equivalent pH. Scan rate: 100 mV/s.

For analyses in spent cattle dip, minimal current strength decrease and potential shift was observed, when compared to that in 0.2 M BR buffer. In the honey:BR buffer (50:50) (v/v) mixture the amitraz peak exhibited a 24.3 % decrease in the current strength, as compared to the analysis of amitraz in 0.2 M BR buffer of equivalent pH.

In milk, a 37.5 % decrease in current strength was observed. Table 6.1 summarises these results for amitraz detection in spent cattle dip, honey and milk.

Table 6.1 Data obtained for amitraz detection and quantification in spent cattle dip, honey and milk, as compared to identical analyses in 0.2 M BR buffer of equivalent pH.

SAMPLE	CURRENT pa_1 (µA)	POTENTIAL E (V)	RELATIVE SENSITIVITY** (%)	REPRODUCIBILITY (%)
Spent cattle dip	19.52 (20)*	1.18 (1.175)*	97.6	93.09
Honey:BR buffer (50:50) (v/v)	13.45 (18)*	1.04 (1.050)*	74.7	78.17
Milk	9.38 (15)*	0.98 (1.000)*	62.5	76.81

*Values in brackets are those obtained for amitraz in 0.2 M BR buffer of equivalent pH values.

**Relative sensitivity compares the current obtained in the environmental sample with that obtained in 0.2 M BR buffer sample.

Comparison of the current strength of 13 µM amitraz in spent cattle dip, honey and milk, shows that the highest current response obtained was that in spent cattle dip, with the lowest in milk. This is in keeping with expected results, as shown in chapter 3, where current response for amitraz is dependent on pH.

However, the relative sensitivity for each compound compared to the equivalent analyses in 0.2 M BR buffer of the same pH, shows that additional factors for the decrease in sensitivity are involved. The decrease in current strength observed for amitraz in milk and honey could be attributed to low ionic strength of these media.

Reproducibility of 93.09 % for analysis of amitraz in spent cattle dip was favourable, compared to 78.17 % in honey and 76.81 % in milk.

6.4.3 Standard curve generation for amitraz in environmental samples.

Figures 6.3 (a,b,c) show the standard curves generated in: a) spent cattle dip, b) honey:BR buffer (50:50) (v/v) and c) milk.

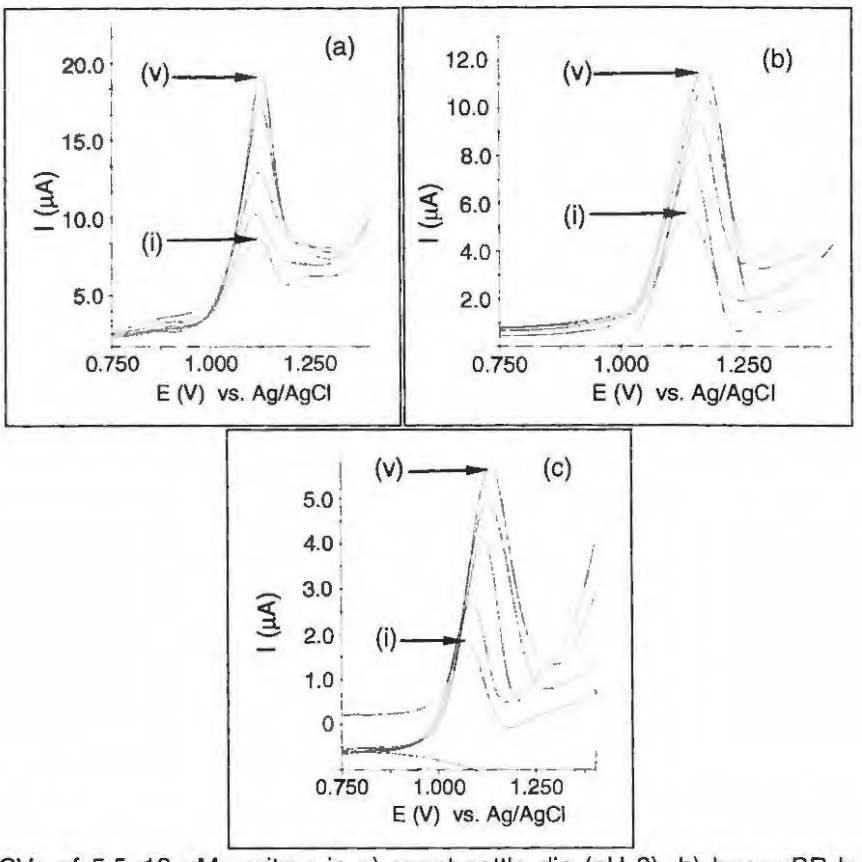

Figure 6.3 CVs of 5.5–13 μM amitraz in a) spent cattle dip (pH 3), b) honey:BR buffer (50:50) (v/v) (pH 4) and c) milk (pH 7). Scan rate = 100 mV/s.

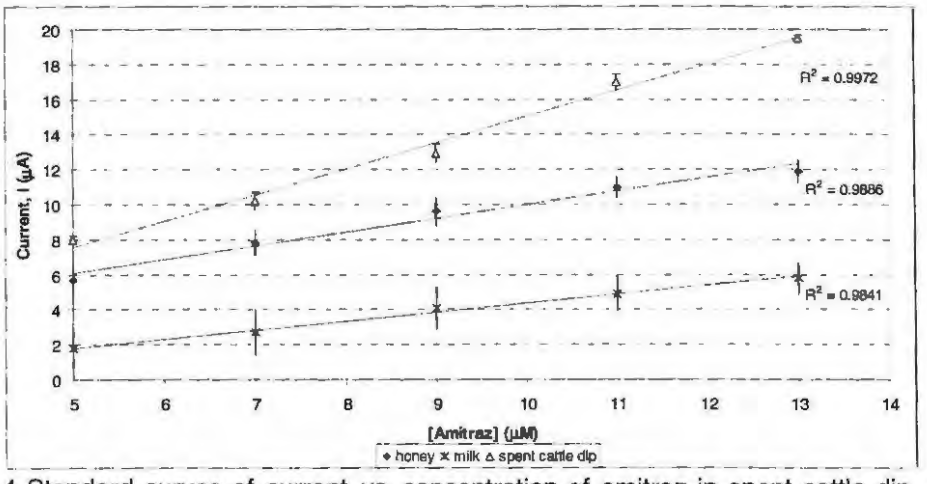

Figure 6.4 Standard curves of current *vs.* concentration of amitraz in spent cattle dip, milk and honey. Correlation coefficients are shown on the graph.

A comparison of the correlation coefficients for each straight line curve in figure 6.4 show that the most linear standard curve for amitraz was obtained in spent cattle dip ($R^2 = 0.9972$), with the least linear being that in milk ($R^2 = 0.9841$). Table 6.2 shows the comparisons between the R^2 values obtained in each of the complex matrices as compared to the respective standard curves generated in 0.2 M BR buffer of equivalent pH. As shown, the R^2 value for amitraz in spent cattle did not vary from a comparative regression curve in 0.2 M BR buffer at the same pH, while that in honey and milk differed significantly from the analyses in 0.2 M BR control at equivalent pH. For honey the deviation from linearity could be attributed to the viscosity of the solution, while in milk the decrease in linearity could be interference from milk constituents.

Table 6.2 Difference between the R^2 values obtained in the environmental samples as compared to 0.2 M BR buffer of equivalent pH for amitraz quantification.

SAMPLE	pH	R^2
Spent cattle dip	3.0	0.9972
0.2 M BR buffer	3.0	0.9972
Honey:BR buffer (50:50) (v/v)	4.0	0.9886
0.2 M BR buffer	4.0	0.9994
Milk	7.0	0.9841
0.2 M BR buffer	7.0	0.9973

While further optimisation of parameters for analysis of amitraz in honey and milk is required, given the deviation from linearity, the above data indicate the feasibility of using electrochemical methods for analysis of amitraz in these environmental samples and with minimal sample preparation.

6.4.4 Detection of 2,4-DMA in environmental samples

Figure 6.5 (a, b, c) compares the current strength of 2,4-DMA in each of a) spent cattle dip to which no amitraz had been applied (pH 3), b) honey:BR buffer (50:50) (v/v) (pH 4) and c) milk (pH 7). The CVs obtained were compared to a control CV of 10 µM 2,4-DMA in 0.2 M BR buffer of the same pH, as before in section 6.4.2.

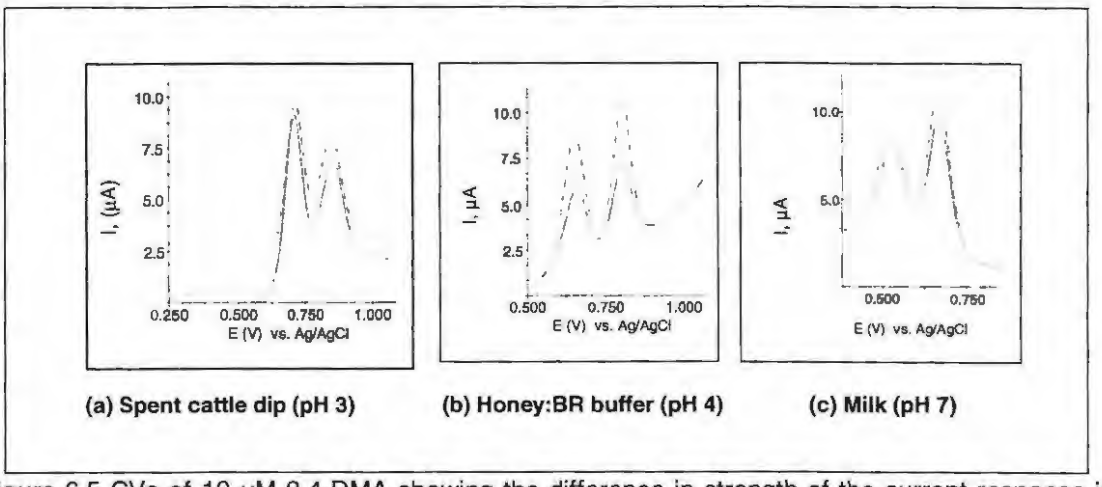

Figure 6.5 CVs of 10 μM 2,4-DMA showing the difference in strength of the current response in the relevant sample: a) spent cattle dip to which no amitraz had been applied (pH 3). b) honey:0.2 M BR buffer (50:50) (v/v) (pH 4). c) milk (pH 7). The dotted line represents the detection of 2,4-DMA in 0.2 M BR buffer of equivalent pH. Primary anodic peak, pa_1, used for analyses at pH 3. Scan rate: 100 mV/s.

2,4-DMA was detected in all environmental samples compared to analyses in 0.2 M BR buffer. Decreases in anodic peak strength for all environmental samples compared to analyses in 0.2 M BR buffer were accompanied by slight potential shifts, as shown in table 6.3. The relative sensitivity of 2,4-DMA as compared to an equivalent analysis in 0.2 M BR buffer in spent cattle dip was 91.0 %, followed by honey, 56.4 % and milk, 82.6 %. The decrease in current strength can be attributed to lower ionic strength in the milk and honey environmental samples as compared to the spent cattle dip, and 0.2 M BR buffer. Reproducibility of the current response was similar to that for amitraz, 95.60 % in spent cattle dip, 75.68 % in honey and 71.61 % in milk.

Table 6.3 Comparative data for the detection of 2,4-DMA in spent cattle, honey and milk.

SAMPLE	CURRENT, I (μA)	POTENTIAL, E (V)	RELATIVE SENSITIVITY** (%)	REPRODUCIBILITY (%)
Spent cattle dip	pa_1: 9.1 (10.0)*	0.687 (0.695)*	91.0	95.60
Honey:BR buffer (50:50)	pa_2: 6.2 (11.0)*	0.813 (0.821)*	56.4	75.68
Milk	pa_2:9.0 (10.9)*	0.665 (0.662)*	82.6	71.61

*The value in brackets in table 6.2 are those obtained for 2,4-DMA in 0.2 M BR buffer of the same pH.

**Relative sensitivity compares the current obtained in the environmental sample with that obtained in 0.2 M BR buffer.

6.4.5 Standard curve generation for 2,4-DMA in spent cattle dip, milk and honey.

Figure 6.6 (a, b, c) shows the CVs of increasing concentrations of 2,4-DMA in each of the complex matrices: a) spent cattle dip (pH 3), b) honey:0.2 M BR buffer (50:50) (v/v) (pH 4) and c) milk (pH 7). Standard curves of current *vs.* concentration derived are shown in figure 6.7.

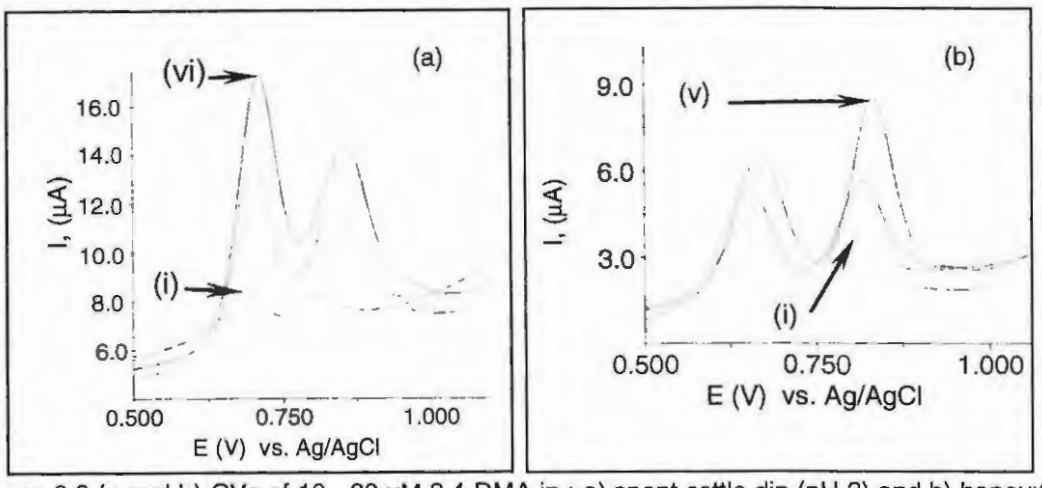

Figure 6.6 (a and b) CVs of 10 - 60 μM 2,4-DMA in : a) spent cattle dip (pH 3) and b) honey:0.2 M BR buffer (50:50) (v/v) (pH 4). Scan rate: 100 mV/s.

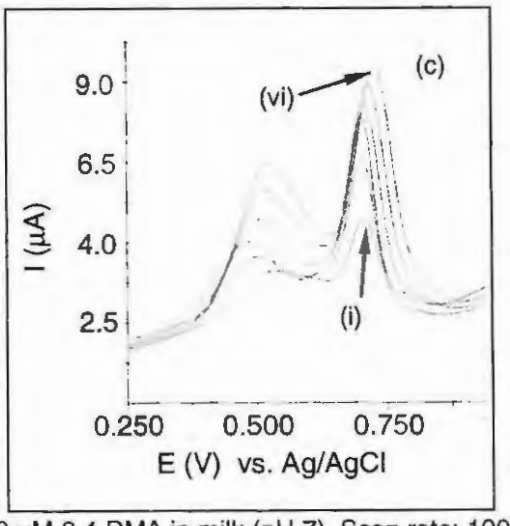

Figure 6.6 (c) CVs of 1.0–10 μM 2,4-DMA in milk (pH 7). Scan rate: 100 mV/s.

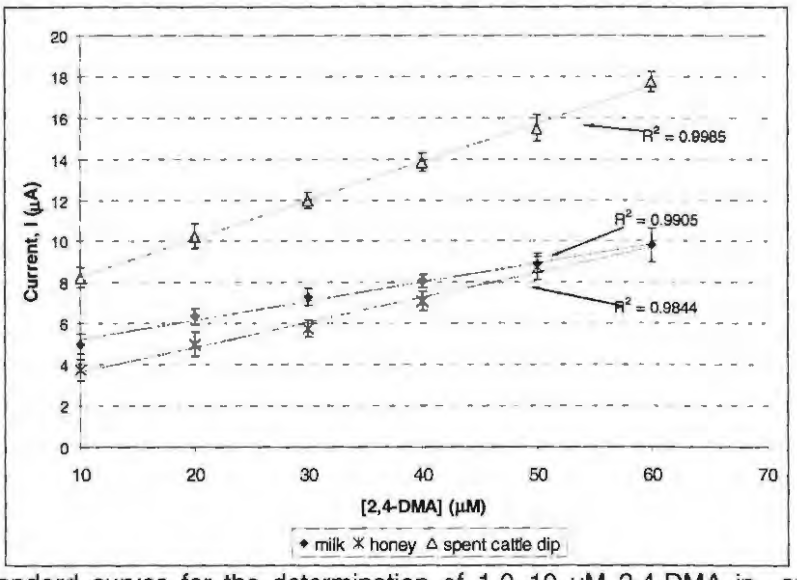

Figure 6.7 Standard curves for the determination of 1.0–10 μM 2,4-DMA in spent cattle dip (pH 3), honey:0.2 M BR buffer (50:50) (v/v) (pH 4) and milk (pH 7).

A comparison of the linearity of the standard curves generated for 2,4-DMA shows that the most linear curve, with R^2 = 0.9959, was obtained in spent cattle dip. The standard curve generated in milk (pH 7) yielded a favourable R^2 of 0.9905 (figure 6.7), whereas the standard curve generated in honey:0.2 M BR buffer (50:50) (v/v) (pH 4) [figure 6.6 (c)] yielded the lowest R^2 value of 0.9844 (figure 6.7). Reproducibility of current response was as before with 95 % in spent cattle dip, 72 % in honey and 76 % in milk. Table 6.4 shows comparative data for the correlation coefficients (R^2) obtained in the analysis of 2,4-DMA in the environmental samples and the respective data obtained for 0.2 M BR buffer at the same pH.

Table 6.4 Difference between the R^2 values obtained in the environmental samples as compared to 0.2 M BR buffer of equivalent pH for 2,4-DMA quantification.

SAMPLE	pH	R^2
Spent cattle dip	3.0	0.9985
0.2 M BR buffer	3.0	0.9952
Honey:BR buffer (50:50) (v/v)	4.0	0.9844
0.2 M BR buffer	4.0	0.9912
Milk	7.0	0.9905
0.2 M BR buffer	7.0	0.9956

6.5 CONCLUSIONS

The detection of amitraz and 2,4-DMA in spent cattle dip, milk and honey could be performed with minimal interference. In terms of sensitivity and reproducibility, analyses of amitraz and 2,4-DMA, the best results were obtained in spent cattle dip. The highest linearity of the current response was also obtained in spent cattle dip. Weaker current and reproducibility observed in milk and honey could be attributed in low ionic strength. The viscosity of honey provides interference in that it hinders the free passage of ions to the electrode surface. This suggests that factors such as ionic strength of the buffer introduced could improve analyses in this medium.

CHAPTER 7

THE EFFECT OF pH ON AMITRAZ STABILITY, AND STUDY OF THE BIODEGRADATION OF 2,4-DMA

7.1 INTRODUCTION

Amitraz Hydrolysis

Hydrolysis of amitraz poses two prominent problems. The decrease in concentration of amitraz for example in cattle dip vats, allows the opportunity for pests (such as *Boophilus microplus*) to obtain resistance against the pesticide, either through metabolic detoxification or enzootic stability (Foil *et al.* 2004). Secondly, the hydrolysis of amitraz produces intermediate and final breakdown products that are recalcitrant in the environment and of toxicological importance to plants, livestock and humans (Corta *et al.* 1999).

Amitraz is hydrolysed under both chemical and biological conditions. Cosolvents, such as methanol, ethanol and *n*-hexane, used to dissolve amitraz in laboratory analyses have been shown by Bernal *et al.* 1997 to affect the stability of amitraz. These authors conclude that due to the hydrolytic properties of cosolvents, stock solutions of amitraz need to be prepared fresh prior to analyses, as within minutes of preparation, a decrease in the amitraz concentration due to hydrolysis is noted. The same authors showed that sunlight (UV exposure) and temperature (25 °C) affect the stability of amitraz. In their studies, amitraz concentrations decreased by 20 % when kept at room temperature in the dark and under alkaline conditions, whereas at 4 °C, a 5 % decrease was noted. In addition, samples of amitraz exposed to UV light had an accelerated rate of hydrolysis as compared to samples retained in the dark.

The biological degradation of amitraz has been well studied. Baker and Woods 1977 showed that amitraz was hydrolysed in a dipping vat by *Escherichia coli* and *Pseudomonas* species (spp). Pierpoint *et al.* 1997, Bernal *et al.* 1997, Corta *et al.* 1999, and Tseng *et al.* 1999 have shown that amitraz stability is affected by pH conditions.

However there remains uncertainty as to the degradation pathway of amitraz due to factors such as pH.

Pierpoint *et al.* 1997 showed through using HPLC that under acidic conditions (pH < 3), amitraz hydrolyses to 2,4-dimethylphenylformamide (DMF) and then to 2,4-DMA. Corta *et al.* 1999 comment on this finding by describing the rapid and direct hydrolysis of amitraz to 2,4-DMA under very acidic conditions without formation of intermediate compounds first.

Pierpoint *et al.* 1997, further state that the amitraz daughter degradants eventually hydrolyse to a stable 2,4-DMA. Corta *et al.* 1999, further showed that amitraz hydrolyses to two intermediate products, DPMF and DMF, both of which (depending on the pH of the aqueous solution), break down to the stable 2,4-DMA molecule.

The addition of slaked lime to a dipping vat is commented on by many authors as being a method of stabilising amitraz. Pierpoint *et al.* 1997 state that the intermediate hydrolysis products of amitraz (DMF and 2,4-DMA) are acid stable, and will only hydrolyse further when the pH of the dipping vat is made more alkaline (addition of slaked lime). Corta *et al.* 1999 questioned the findings of Pierpoint *et al.* 1997 and follow up by finding that more than one pathway for amitraz hydrolysis (based on pH) exists.

Corta *et al.* 1999 used HPLC, GC-MS and spectrophotometry and found that under pH conditions < 3, amitraz hydrolyses directly to 2,4-DMA in less than an hour (Scheme 7.1).

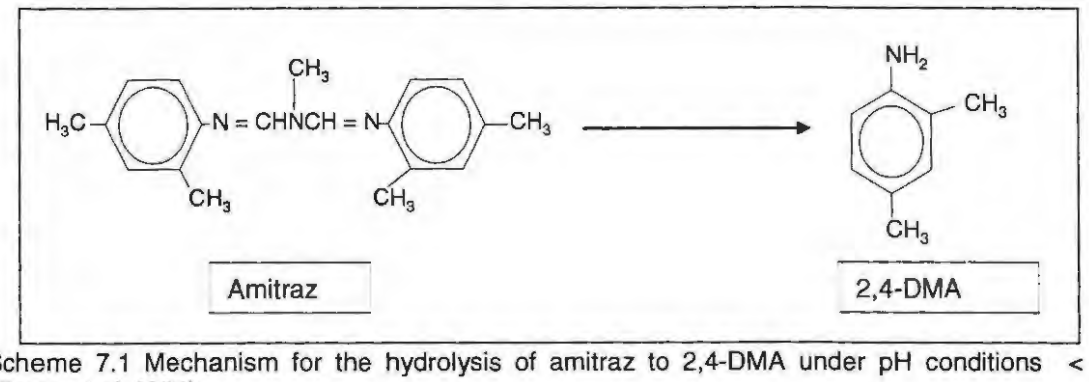

Scheme 7.1 Mechanism for the hydrolysis of amitraz to 2,4-DMA under pH conditions < 3. (Corta *et al.* 1999).

Under pH conditions from 3 – 6, Corta *et al.* 1999 found that amitraz hydrolyses to equivalent concentrations of the intermediates 2,4-dimethyphenylformamide (DMF) and 2,4-dimethyphenylformamidine (DPMF), after which the formamide hydrolyses to 2,4-DMA within 2 – 3 days, while the formamidine hydrolyses to 2,4-DMA in 5 days (Scheme 7.2).

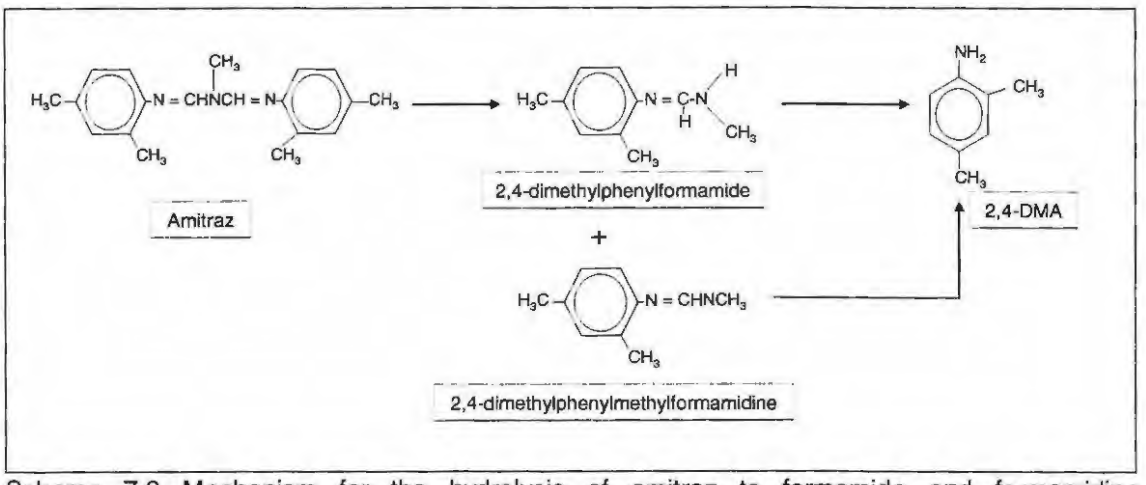

Scheme 7.2 Mechanism for the hydrolysis of amitraz to formamide and formamidine intermediates prior to hydrolysis to 2,4-DMA under pH conditions 3 – 6 (Corta *et al.* 1999).

Under alkaline pH conditions (pH > 7), Corta *et al.* 1999 showed that amitraz hydrolysed at a slower rate, but the major intermediate hydrolysis product is DMF, which has a half life of 300 days at pH 9.12 (as calculated by Pierpoint *et al.* 1997) before hydrolysing to 2,4-DMA (Scheme 7.3).

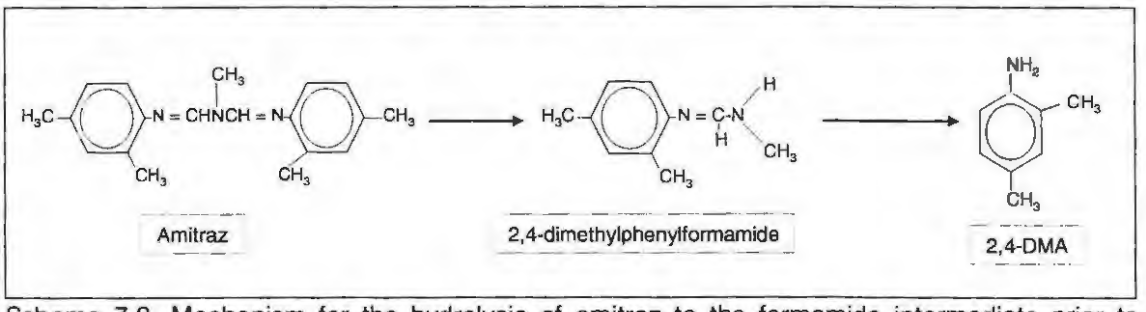

Scheme 7.3. Mechanism for the hydrolysis of amitraz to the formamide intermediate prior to hydrolysis to 2,4-DMA under pH conditions > 7 (Corta *et al.*1999).

2,4-Dimethylaniline breakdown

2,4-DMA is stated by many authors to be the end product of amitraz hydrolysis and is said to be stable in the environment. The recalcitrance of 2,4-DMA in the environment is cause for concern given its high degree of toxicity to plants, animals and humans.

Corta *et al.* 1999 conclude that 2,4-DMA has toxicological importance, and could be found as a product of amitraz degradation on food and in surface water samples.

Aniline-based derivatives are not only found as components of acaricide pesticides, but are important starting components in both the pharmaceutical and chemical industries (John & Nair 2004). 2,4-DMA is an important raw material in the production of pesticides as well as in dye manufacture. Azo dyes are the largest and most versatile class of synthetic dyes, with applications ranging from textile, leather, paper and food dyes, to pharmaceutical and cosmetic industries (Peres *et al.* 1998, Nachiyar & Rajakumar 2003, El-Naggar *et al.* 2004, Purwaningsih *et al.* 2004).

Microorganisms source bioavailable sources of carbon and nitrogen that are easily metabolised. Generally, the most favoured source of carbon is found in glucose, while ammonia provides a simple form of nitrogen. If carbon and nitrogen are not available in simple forms, a microorganism is required to adapt and metabolise more complex forms of carbon and nitrogen in order to survive. Certain microorganisms are capable of metabolising toxic and recalcitrant compounds that can accumulate in water, soil and plants, and extracting the necessary carbon and nitrogen required for their cellular anabolic processes. Bacteria such as *Pseudomonas* strains are capable of metabolising recalcitrant anilines as either a carbon or nitrogen source (or a combination thereof), or as part of the metabolism of more readily available sources of energy, otherwise known as cometabolism (Stamper *et al.* 1998, Kargi & Eker 2004, Rozkov *et al.* 1999, Wackett & Herschberger, 2001).

Pseudomonas strains have been shown to be capable of metabolising aniline-based derivatives both through cometabolism and direct utilisation as a source of energy. Bell *et al.* 2003, Kao *et al.* 2005, El-Naggar *et al.* 2004, Foster *et al.* 2004 and Kulkarni and Chaudhari 2005 all report on the utilisation of *Pseudomonas* strains for the bioremediation of soil and water polluted by toxic recalcitrant compounds.

El-Naggar *et al.* 2004 and Kulkarni & Chaudhari 2005 report that the complete mineralization of aniline-based derivatives is only possible if the reductive cleavage of the azo bond is performed under anaerobic conditions, followed by aerobic oxidation of amines formed in the reductive steps. However, Nachiyar & Rajakumar 2004 found that

aniline-based derivatives can be metabolised by *Pseudomonas* strains under aerobic conditions by oxidative deamination, leading to the formation of a catechol derivative. Through *ortho* pathway reactions, the ring structure of the catechol derivative can be cleaved, forming α-ketoadipic acid, which completely mineralises in the tricarboxylic acid (TCA) cycle (Nachiyar & Rajakumar 2004).

Under aerobic conditions El-Naggar *et al.* 2004 propose that 2,4-DMA can be degraded to 3-methylcatechol (3-MC) by *Pseudomonas* strains. The mineralization of 3-MC is thought to follow similar breakdown pathways to aniline-based derivatives of desulphonated azo dyes (Nachiyar & Rajakumar 2004). 3-MC contains two hydroxyl groups in the *ortho* position, which through *ortho* pathway reactions involving carboxylation and hydroxylation, facilitate ring cleavage, leading to the formation of a semialdehyde that enters the TCA cycle resulting in the release of aniline carbon as CO_2 (Nachiyar and Rajakumar, 2004). This is corroborated by the findings of Park *et al.* 1999 who identified the formation of semialdehyde derivatives from aniline-based compounds.

Scheme 7.4. represents the proposed pathway for the mineralization of 2,4-DMA derivatives by *Pseudomonas* strains, under aerobic conditions based on studies of other aniline derivatives.

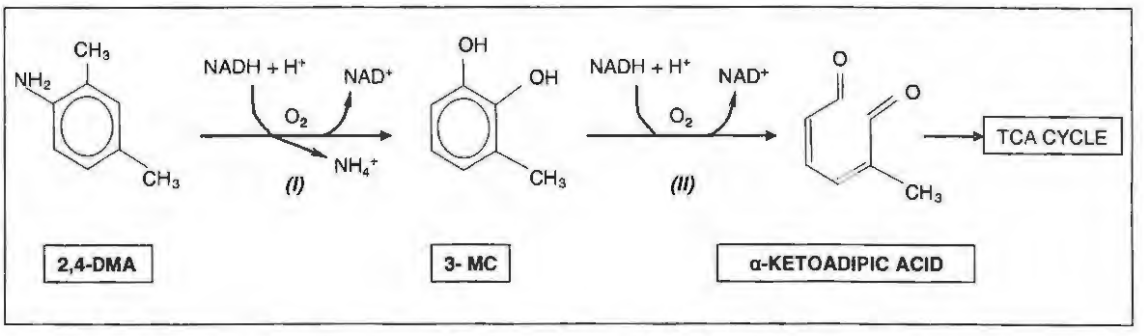

Scheme 7.4 Proposed pathway of biodegradation of 2,4-DMA by *Pseudomonas* spp.
Legend: (I)=dioxygenase,(II)=catechol-2,3-dioxygenase, 3-MC (*Adaptation*: Nachiyar & Rajakumar 2004).

Discrepancies exist as to the mechanism of hydrolysis of amitraz. In addition, little reference to the biodegradation of 2,4-DMA is available. The pathway as well as the mechanism of biodegradation of 2,4-DMA by *Pseudomonas* spp. is not yet fully understood. Numerous studies show that *Pseudomonas* spp. degrade amitraz and aniline based derivatives (Amat *et al.* 2004) This study does not seek to identify, but rather to utilise already existing consortia isolated from spent cattle dip vats to prove the

mechanism by which amitraz and 2,4-DMA are degraded by these microorganisms. In addition, electrochemical methods are explored to provide clarity with regards to the breakdown mechanisms that occur.

7.2 AIMS

This study therefore sets out:

1. To better understand the hydrolysis mechanisms of amitraz under highly acidic, acidic-neutral and alkaline conditions.
2. To compare the rate of amitraz hydrolysis under highly acidic, acidic-neutral and alkaline conditions.
3. To isolate *Pseudomonas* spp. (that are capable of degrading 2,4-DMA) from spent cattle dip.
4. To determine the degree of toxicity of 2,4-DMA to *Pseudomonas* spp.
5. To assess the ability of *Pseudomonas* spp. to metabolise 2,4-DMA as a source of energy (carbon and nitrogen).
6. To monitor degradation of 2,4-DMA using electrochemical methods.
7. To study the pathway of 2,4-DMA metabolism by *Pseudomonas* spp.

7.3 MATERIALS AND METHODS

7.3.1 Chemical hydrolysis of amitraz

Amitraz stock was prepared fresh as outlined in chapter 2.2 and added to 0.2 M BR buffer (pH 2.0) to yield a final concentration of 1 µM amitraz. Cyclic voltammetry (CV) was performed as outlined in chapter 2.2. Cyclic voltammetry was repeated at 5 minute intervals. The identical protocol was followed for the analysis of amitraz hydrolysis at pH 3.0. For amitraz hydrolysis at pH 7.0, CV readings were performed on an hourly basis, and for pH 10.0, readings were performed on a daily basis for a total of 25 days.

7.3.2 Biological degradation of 2,4-DMA

Isolation and enrichment of Pseudomonas spp. from spent cattle dip.

Pseudomonas spp. was isolated from spent cattle dip by plating dilutions onto MacConkey purple agar (Difco) plates to which 0.1 µM 2,4-DMA solubilised with 0.2 M NaOH was added. The plates were incubated at 37°C overnight.

Colonies were picked and transferred into conical flasks containing nutrient broth. The flasks were placed in a gyrator shaker (Labcon) (120 RPM) and incubated at 37°C. The growth of the *Pseudomonas* spp. was monitored spectrometrically at an OD of 600 nm. The *Pseudomonas* spp. were harvested by centrifugation using a Beckman JA14 rotor (10 000 x g) when the cells were in exponential growth phase, and resuspended in saline solution and stored at 4°C. Identification of isolates from the enrichment culture was performed in accordance with identification protocols described in *Bergey's Manual of Systemic Bacteriology* (Garrity *et al.* 2002).

Toxicity of 2,4-DMA to Pseudomonas spp.

The degree of toxicity of 2,4-DMA to *Pseudomonas* spp. was assessed. This was done by growing the *Pseudomonas* spp. cells in the presence of different concentrations of 2,4-DMA. Batch flasks of nutrient broth inoculated with harvested *Pseudomonas* spp. cells were prepared, each containing a different concentration of 2,4-DMA. The concentrations of 2,4-DMA used ranged between 0.1 µM and 5 µM. The flasks were incubated at 37 °C on a gyrator shaker (120 RPM) and samples were removed aseptically on an hourly basis. The effect of 2,4-DMA on the growth of the *Pseudomonas* spp. cells was monitored using UV-VIS spectroscopy at OD_{600nm}. All flasks and readings were performed in triplicate.

Assessment of 2,4-DMA as a carbon or nitrogen source.

2,4-DMA stock was prepared fresh as outlined in chapter 2.2. Fifty (50) ml of autoclaved nitrogen and carbon-free minimal salts medium was added to 250 ml conical flasks. The mineral salts medium consisted of (per litre of distilled water): 1.0 g H_2PO_4, 0.6 g NaH_2PO_4, 0.2 g $MgSO_4 \cdot 7H_2O$, 0.2 g KCl, 2 mg yeast extract (Difco) and 1 ml of trace element solution containing 0.05 mg H_3BO_3, 0.2 mg $CaSO_4$, 0.1 mg $CoSO_4$, 0.2 mg $CuSO_4$, 3 mg $FeSO_4$, 0.02 mg $MnCl_2$ and 0.03 mg $ZnSO_4 \cdot 7H_2O$ (Park *et al.* 1999). Once

added to the batch flasks, 2,4-DMA was aliquoted into each to yield a final concentration of 1 µM 2,4-DMA. Four batch flask studies were prepared in triplicate. Table 7.1 summarises the experimental setup.

Table 7.1 Parameters used for the assessment of whether *Pseudomonas* spp. can utilise 2,4-DMA as an alternate carbon or nitrogen source, or both.

FLASK SET	POTENTIAL CARBON COURCE		POTENTIAL NITROGEN SOURCE	
1	No glucose	2,4-DMA	NH_4Cl	2,4-DMA
2	Glucose	2,4-DMA	No NH_4Cl	2,4-DMA
3	No glucose	2,4-DMA	No NH_4Cl	2,4-DMA
4	Glucose	2,4-DMA	NH_4Cl	2,4-DMA

Pseudomonas spp. was inoculated into flasks containing the carbon and nitrogen sources outlined in table 7.1. A final concentration of 1 µM 2,4-DMA was used. *Pseudomonas* spp. cell viability and growth state was assessed by UV-VIS spectroscopy at OD_{600nm}. Cell viability was confirmed by serial dilution and plating of broth containing *Pseudomonas* cells onto autoclaved minimal salts agar containing 1 µM 2,4-DMA solubilised by the addition of 0.1 M NaOH, and incubated at 37 °C.

The decrease in 2,4-DMA concentration due to its biodegradation was monitored electrochemically by cyclic voltammetry. 100 µl of each sample was added to 0.2 M BR buffer pH 7.0 and cyclic voltammetry performed as outlined in chapter 2.2. Sampling was performed at two hour intervals for the first 24 hours, and then at ten hour intervals thereafter.

Spiking of carbon- and nitrogen-free flasks with 2,4-DMA

In a second batch flask experiment where both the carbon and nitrogen source were replaced by 2,4-DMA, the breakdown of 2,4-DMA was assessed and monitored by cyclic voltammetry for 120 hours (at 2 hour intervals for the first 20 hours, and then at 10 hour intervals). After 120 hours, the batch flasks were spiked with 2,4-DMA to obtain a final concentration of 1 µM 2,4-DMA. The breakdown of 2,4-DMA was monitored initially at 2 hour intervals for 20 hours and then at 10 hour intervals. The rate of 2,4-DMA breakdown was assessed by cyclic voltammetry, and the growth of the *Pseudomonas* spp. cells analysed by UV-VIS spectroscopy at OD_{600nm}.

7.4 RESULTS AND DISCUSSION

7.4.1 Chemical hydrolysis of amitraz

CVs in figure 7.1 show the hydrolysis of amitraz at pH 3, to an intermediate compound, identified as DMF, which is further hydrolysed to 2,4-DMA. From Figure 7.1 it is evident that within 10 minutes the concentration of amitraz decreased by nearly 50 %. No literature could be found on the electrochemical analysis of amitraz hydrolysis. However, these findings concur with those of Bernal *et al.* 1997 and Corta *et al.* 1999 where HPLC and GC-MS were utilised by these authors.

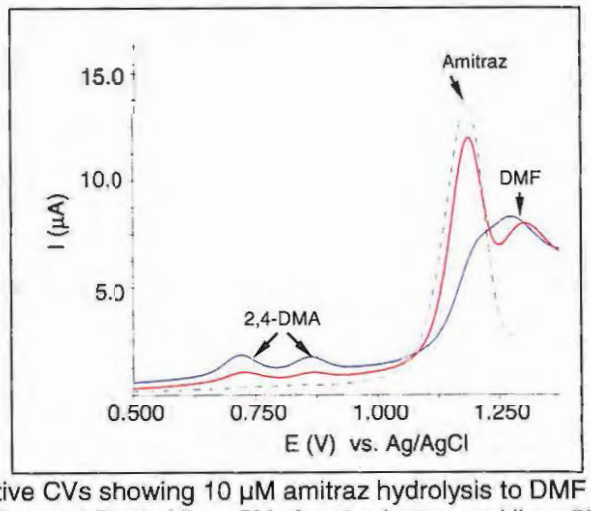

Figure 7.1 Representative CVs showing 10 µM amitraz hydrolysis to DMF and then to 2,4-DMA in 0.2 M BR buffer pH 3. *Legend*: Dotted line: CV after 0 minutes, red line: CV after 10 minutes, blue line: CV after 15 minutes.

From figure 7.1 it can be seen that amitraz hydrolyses to an intermediate, DMF and then 2,4-DMA. This concurs with what Corta *et al.* 1999 and Pierpoint *et al.* 1997 observed. It is also evident from figure 7.1, that the transition from the intermediate hydrolysis products of amitraz to 2,4-DMA is rapid at this pH.

Figure 7.2 represents the hydrolysis of amitraz directly to 2,4-DMA under highly acidic conditions (pH < 3) without formation of DMF. Within 10 minutes a 50 % decrease in the concentration of amitraz is noted with increase in anodic waves attributed to 2,4-DMA over time. Scheme 7.1 shows the pathway for the direct hydrolysis of amitraz to 2,4-DMA under highly acidic conditions.

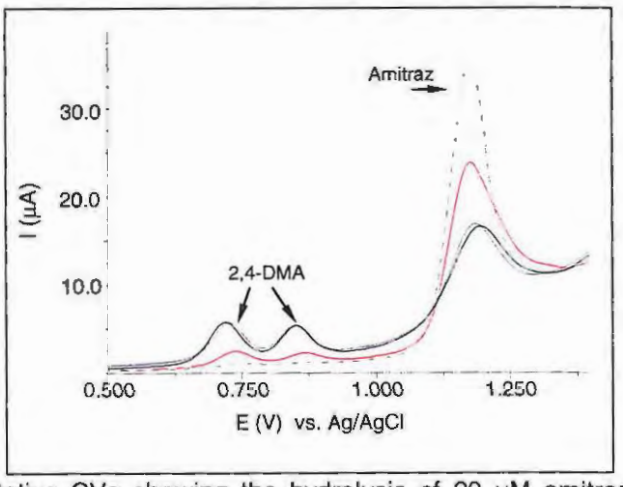

Figure 7.2 Representative CVs showing the hydrolysis of 20 µM amitraz directly to 2,4-DMA under pH conditions < 2. *Legend*: dotted line: CV at 0 minutes, red line: CV at 10 minutes, blue line: CV at 15 minutes, green line: CV at 20 minutes, black line: amitraz at 25 minutes.

Pierpoint *et al.* 1997, observed the formation of two intermediates, a formamidine (DMPF) and a formamide (DMF), in their studies of amitraz hydrolysis at pH < 3 but make no mention of further hydrolysis of these transition compounds to 2,4-DMA. Instead, Pierpoint *et al.* 1997 state that the intermediates are acid stable, and only degrade to DMA once the pH of the aqueous medium has been raised to alkaline levels. Corta *et al.* 1999 elucidate that this is not the case, but rather that amitraz undergoes rapid hydrolysis at pH < 3 directly to 2,4-DMA with no intermediate compound formation. The results obtained in figure 7.2 correspond with the observations of Corta *et al.* 1999.

Rate of amitraz hydrolysis

The rate at which pH - dependent amitraz hydrolysis occurs is graphically presented in figure 7.3. These studies were conducted over the pH range 2, 3, 7 and 10.

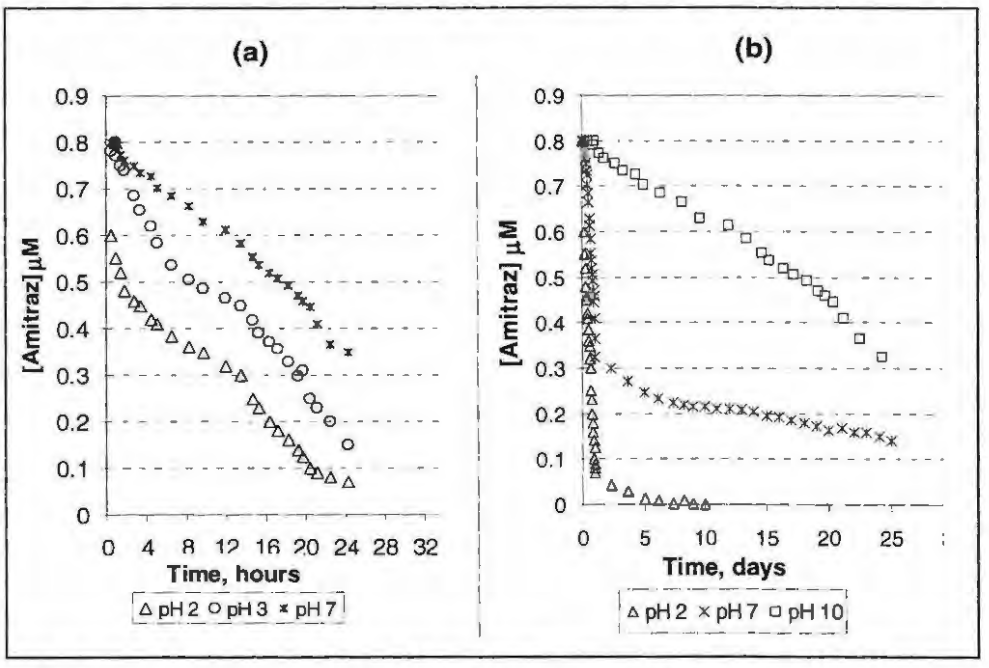

Figure 7.3 Rate of amitraz hydrolysis at pH 2, 3, 7 and 10. Supporting electrolyte: 0.2 M BR buffer. Figure 7.3 (a) shows the hydrolysis of amitraz at pH 2, 3 and 7 in 24 hours. Figure 7.3 (b) shows the hydrolysis of amitraz at pH 2, 7 and 10 over 25 days.

As seen in Figure 7.3, and concurring with the findings of Bernal *et al.* 1997 the rate of amitraz hydrolysis is more rapid under acidic conditions than under neutral and alkaline conditions respectively. For example, at pH 2, the concentration of amitraz decreased by 87.5 % after 24 hours, and after 10 days amitraz concentration reduced by 98 %, being undetectable by day 13. In contrast at pH 10, a 60 % decrease in amitraz concentration was observed only after 25 days.

7.4.2 Biological degradation of 2,4-DMA

Isolation and enrichment of Pseudomonas spp. from spent cattle dip.

The identity of the *Pseudomonas* colonies isolated and grown was confirmed by a Gram stain, where gram negative rod shaped bacteria were observed.

Toxicity of 2,4-DMA to Pseudomonas spp.

Figure 7.4 shows the absorbance readings for the growth of *Pseudomonas* spp. in minimal salts batch flask culture, in concentrations of 2,4-DMA between 1 µM and 5 µM.

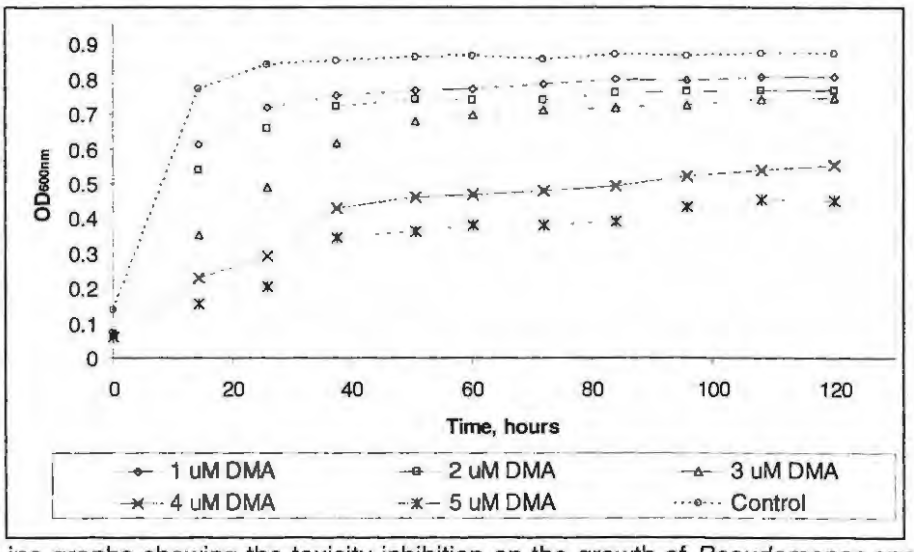

Figure 7.4 Line graphs showing the toxicity inhibition on the growth of *Pseudomonas* spp. in the presence of concentrations of 2,4-DMA ranging between 1 and 5 µM as determined using UV-VIS spectroscopy at OD_{600nm}. Error bars were removed for graphical simplicity. All analyses were performed in triplicate.

In figure 7.4 the control study shows growth of *Pseudomonas* spp. in absence of 2,4-DMA, as illustrated by an increase in optical density. Decrease in optical density in the presence of 2,4-DMA, shown in figure 7.4, indicates that this toxin does inhibit the growth of *Pseudomonas* spp. When compared to the control, 1 µM 2,4-DMA yielded the lowest degree of inhibition, and this concentration was used for all studies of 2,4-DMA metabolism by *Pseudomonas* spp. analyses.

Assessment of 2,4-DMA utilisation as a carbon or nitrogen source by Pseudomonas spp.

The utilisation of 2,4-DMA by *Pseudomonas* spp. as a carbon, nitrogen source, or a combination thereof was assessed. Figure 7.5 (a – d) shows the alteration in 2,4-DMA concentration under the conditions stated.

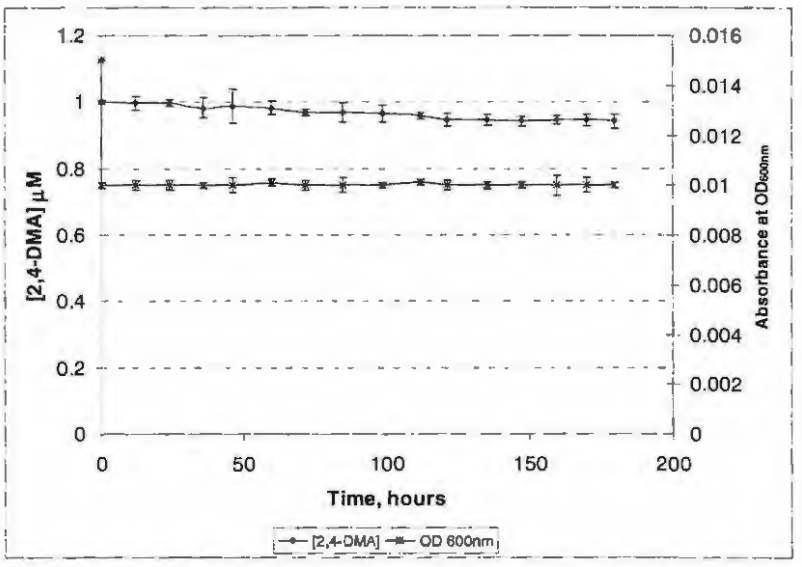

Figure 7.5 (a) Examination of 2,4-DMA utilisation as a carbon source by *Pseudomonas* spp. in the presence of 1 µM 2,4-DMA and NH_4Cl.

For ease of visual comparison, the scale for figures 7.5 (a) – 7.5 (d) are the same. The study shown in figure 7.5 (a) assessed the feasibility of using 2,4-DMA as a carbon source for *Pseudomonas* spp. with NH_4Cl present as the readily available nitrogen source. The readily available carbon source in the form of glucose was excluded in this study. Figure 7.5 (a) shows a minimal decrease in the concentration of 2,4-DMA over 180 hours, indicating that 2,4-DMA was not readily degraded by *Pseudomonas* spp.

Low absorbance values for *Pseudomonas* spp. at OD_{600nm}, figure 7.5 (a) suggest lysis of the *Pseudomonas* spp. cells, indicating cell death in the absence of a readily available carbon source. Both a carbon and nitrogen source is required for bacterial cell growth. NH_4Cl provided a readily available source of nitrogen, however the lack of growth indicates that the *Pseudomonas* spp. was unable to utilise 2,4-DMA as a source of carbon, hence the cell death and minimal decrease in 2,4-DMA concentration.

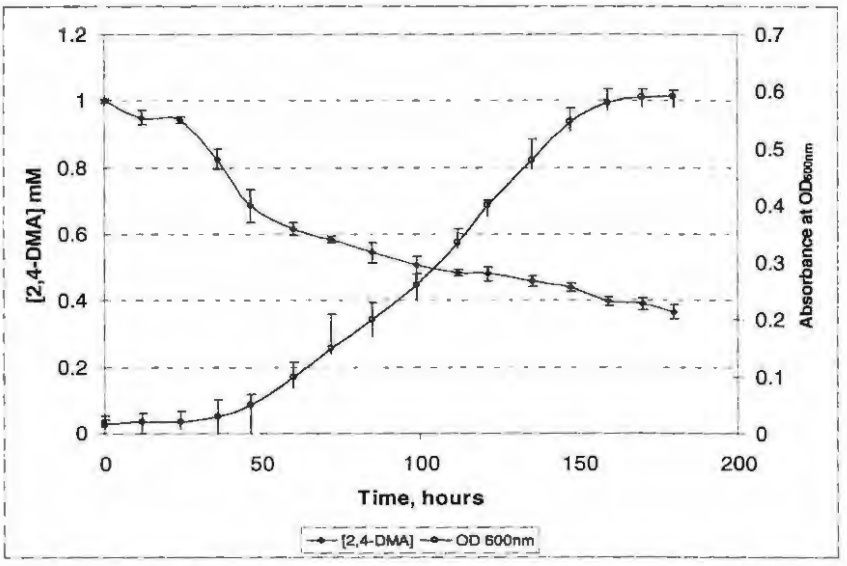

Figure 7.5 (b) Examination of 2,4-DMA utilisation as a nitrogen source by *Pseudomonas* spp. in the presence of 1 µM 2,4-DMA and glucose.

The utilisation of 2,4-DMA as a potential nitrogen source is presented in figure 7.5 (b), where glucose is readily available as a primary carbon source, and the only source of nitrogen available to the *Pseudomonas* spp. was 2,4-DMA. It can be seen from figure 7.5 (b) that after 48 hours, a substantial decrease in the concentration of 2,4-DMA is noted, with a 60% decrease in the concentration of 2,4-DMA observed after 180 hours, and the optical density at 600 nm found to be 0.58.

This proves that in order for the *Pseudomonas* spp. to survive, it would have to make use of the 2,4-DMA amine group as a nitrogen source. This ready utilisation of 2,4-DMA as a nitrogen source suggests that the initial step in the breakdown of 2,4-DMA by *Pseudomonas* spp. could be deamination under aerobic conditions.

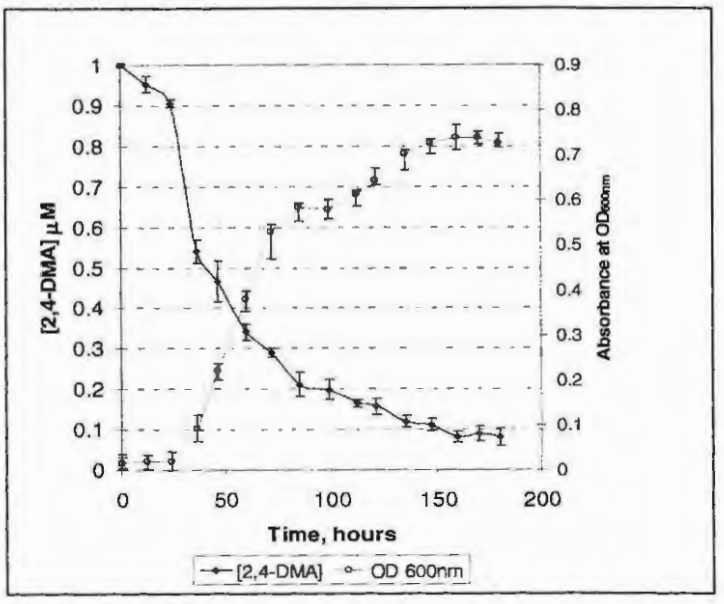

Figure 7.5 (c) Examination of 2,4-DMA utilisation as both a carbon and nitrogen source by *Pseudomonas* spp. in the presence of 1 µM 2,4-DMA.

In figure 7.5 (c), the readily available carbon and nitrogen sources were substituted with 2,4-DMA. In order to grow, the *Pseudomonas* spp. would have to metabolise 2,4-DMA to utilise it as both a carbon and nitrogen source. From the line curve it is evident that 2,4-DMA decreased in concentration in the presence of *Pseudomonas* spp. while the OD increases, indicating that the microorganism utilised the 2,4-DMA as both a carbon and nitrogen source in order to grow.

The decrease in 2,4-DMA concentration is greater when the carbon and nitrogen sources are substituted by 2,4-DMA, as graphically presented in Figure 7.5 (c), than when only the nitrogen source is substituted by 2,4-DMA, as shown in figure 7.5 (b). In the presence of a readily available carbon source (glucose), *Pseudomonas* spp. preferentially utilises it as a carbon source instead of 2,4-DMA. This can explain why the 2,4-DMA concentration only decreases to a certain point as shown in figure 7.5 (b). The decrease in 2,4-DMA in figure 7.5 (c) compared to figure 7.5 (b) thus shows the ability of *Pseudomonas* spp. to utilise it as both a carbon and nitrogen source.

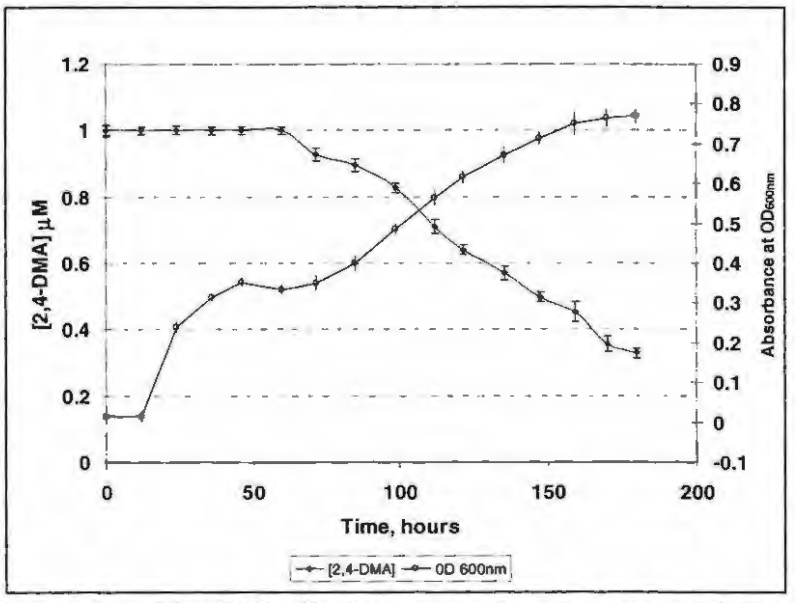

Figure 7.5 (d) Examination of 2,4-DMA utilisation as an alternate carbon and nitrogen source by *Pseudomonas* spp. in the presence of 1 µM 2,4-DMA, NH_4Cl and glucose.

In figure 7.5 (d) readily accessible carbon and nitrogen sources were available to *Pseudomonas* spp. in the form of glucose and ammonia, in the presence of 2,4-DMA. For 60 hours no decrease in the concentration of 2,4-DMA was noted. The *Pseudomonas* spp. was able to utilise glucose and ammonia for growth given the increase in the absorbance at 600 nm. After 60 hours, the readily available carbon and nitrogen sources were exhausted as indicated by the lag in the growth phase. At this point, the concentration of 2,4-DMA began decreasing, indicating its use as a carbon and nitrogen source by the *Pseudomonas* spp. followed by the associated increase in growth of the *Pseudomonas* spp.

A plausible scenario exists where the sequence of 2,4-DMA degradation by *Pseudomonas* spp. can be deduced as follows:

The initial step in the degradation of 2,4-DMA by *Pseudomonas* spp. would have to be removal of the amine group, which has been proposed by Nachiyar & Rajakumar 2004 to be a result of oxidative deamination by ortho cleavage of the amine. Subsequent hydroxylation occurs due to enzymatic function of hydroxylases, with the outcome being the formation of a catechol derivative. Ring cleavage from this point is easier and carbon utilised readily, by the bacteria, as proposed in scheme 7.4.

The following section assessed the rate of 2,4-DMA degradation by *Pseudomonas* spp. that have acclimatised to utilising 2,4-DMA as a carbon and nitrogen source.

Figure 7.6 shows the decrease in 2,4 –DMA concentration in the presence of *Pseudomonas* spp. with time in the absence of alternative sources of carbon and nitrogen. Growth of the *Pseudomonas* spp. is shown by an increase in OD_{600nm}.

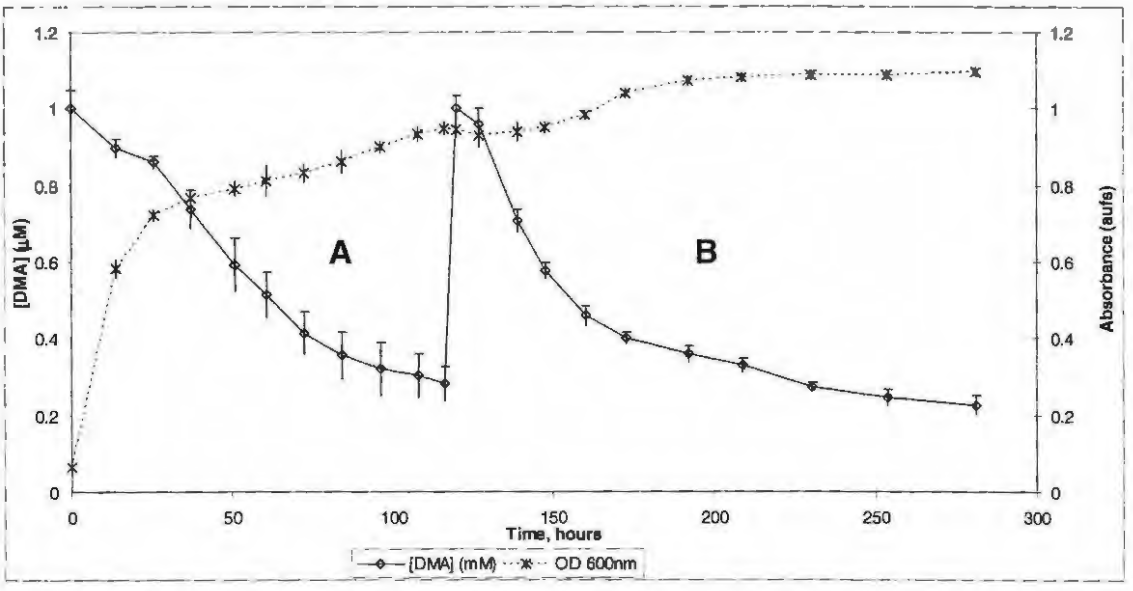

Figure 7.6 The breakdown of 2,4-DMA by *Pseudomonas* spp. and spiking of the batch culture with 2,4-DMA to yield a final concentration of 1 µM 2,4-DMA. The diauxic growth curve for *Pseudomonas* spp. is shown by the broken line.

When 70 % of the 2,4-DMA was utilised, spiking this culture with additional 2,4-DMA after 120 hours induced a second phase of 2,4-DMA breakdown (B).

At time = 12 hours, after spiking with 2,4-DMA, a more elevated decrease in the concentration of 2,4-DMA was noted. At time = 24 hours, a 40% decrease in the 2,4-DMA concentration was observed whereas in the first phase (A), a 40 % decrease was observed after only 50 hours. This phenomenon occurs as the *Pseudomonas* spp. was already acclimatised to utilising 2,4-DMA as a source of carbon and nitrogen. The OD_{600nm} readings confirm the utilisation of 2,4-DMA as a carbon and nitrogen source by *Pseudomonas* spp. as the organism enters a second exponential growth phase, as shown by the diauxic curve, A and B, shown in figure 7.6.

Based on this evidence in which *Pseudomonas* spp. readily accessed 2,4-DMA as a nitrogen source, in the absence of a more readily available nitrogen source, and the lack of 2,4-DMA utilisation as a carbon source in the presence of a more readily available carbon source, it is evident that a pathway in which the amine group of 2,4-DMA is degraded as the initial step is plausible. Given however that the *Pseudomonas* spp. was capable of utilising 2,4-DMA as both a carbon and nitrogen source, it follows that oxidative deamination yields an intermediate which can readily be accessed as a carbon source. The pathway proposed by Nachiyar & Rajakumar 2004 thus seems plausible. According to these authors, *ortho* ring cleavage of the catechol derivative in the second step yields an intermediate as indicated which can readily be degraded further.

Figure 7.7 shows CV studies on the breakdown of 2,4-DMA to 3-MC.

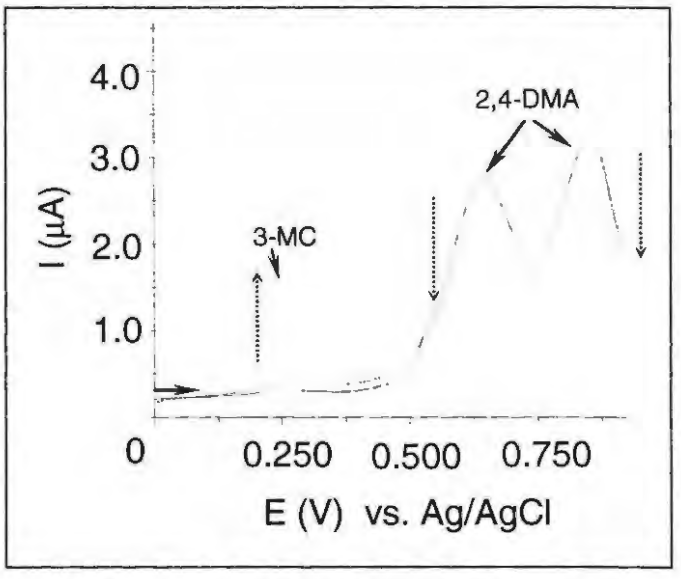

Figure 7.7 CVs showing the breakdown of 2,4-DMA by *Pseudomonas* spp. and the formation of 3-MC between 48 hours and 60 hours. *Legend:* black = 48 hours, blue = 54 hours, red = 60 hours.

To test this theory, CVs of a solution in which 2,4-DMA was utilised as the sole carbon and nitrogen source by *Pseudomonas* spp. was performed over time (figure 7.7). The anodic couple between 0.6 V and 0.8 V (indicated in figure 7.7) is attributed to 2,4-DMA and the oxidation peak at 0.25 V to formation of 3-MC, as per the characterisation of 3-MC shown in chapter 2.2. With time, the oxidation peaks attributed to 2,4-DMA decrease as that of the 3-MC increases, indicative of metabolism of 2,4-DMA to 3-MC by *Pseudomonas* spp. While it is evident that the concentration of 2,4-DMA decreases as

the concentration of 3-MC increases, a direct correlation between the decrease in 2,4-DMA concentration and 3-MC increase in concentration is difficult, given that 3-MC is further mineralised. However these observations provide conclusive evidence for the proposed degradation of 2,4-DMA to a catechol intermediate.

7.5 CONCLUSIONS

Under very acidic conditions, this study showed that amitraz hydrolyses directly to 2,4-DMA, without the formation of the intermediate, DMF. In addition, only at pH 2 and below is the instantaneous hydrolysis of amitraz to 2,4-DMA observed.

At pH 3, it is evident that the hydrolysis of amitraz occurs via the intermediate, DMF, which hydrolyses further to 2,4-DMA. The rate of amitraz hydrolysis was observed to decrease with an increase in pH to more alkaline.

Pseudomonas spp. experience stunted growth in the presence of 2,4-DMA concentrations of 5 µM. Optimal *Pseudomonas* spp. growth was noted at 0.1 µM 2,4-DMA.

The studies show that the *Pseudomonas* spp. can utilise 2,4-DMA as both a carbon and nitrogen source. In addition, these results propose that the degradation of 2,4-DMA by *Pseudomonas* spp. results first in the *ortho* cleavage of the amine group through oxidative deamination, which is thought to be due to the catalytic action of catechol dioxygenases and hydroxylases (Park *et al.* 1999). Cleavage of the amine group yields an intermediate which is a readily available carbon source for bacterial utilisation.

Given this outcome, the DMA breakdown pathway proposed by Nachiyar & Rajakumar 2004 is feasible, where the initial step in DMA degradation could be removal of the amine group by oxidative deamination, followed by catechol formation and subsequent ring cleavage leading to more accessible carbon.

The breakdown of 2,4-DMA to 3-MC was proven electrochemically, where a decrease in the 2,4-DMA double anodic wave is complemented by an increase in the previously identified 3-MC oxidation peak. It should be noted that the hydrolysis of 3-MC occurs

rapidly, and its formation cannot be correlated to the decrease in 2,4-DMA concentration.

CHAPTER 8

OVERALL CONCLUSIONS AND FUTURE RECOMMENDATIONS

8.1 CONCLUSIONS

This thesis examined the electrochemical analysis of amitraz and its major degradants, and sought to identify and monitor the pathways of its chemical and biological degradation.

Specifically, the thesis showed that it was possible to differentiate between amitraz and its degradants, DMF, 2,4-DMA and 3-MC using voltammetric methods. Studies presented in chapter 2 characterised the anodic and cathodic waveforms by cyclic voltammetry. For the major analytes under investigation, their reproducibility and sensitivity in a range of solvents, buffer media, at a range of pH values, scan rates, concentrations, and in environmental samples were investigated.

With regards to the stability of amitraz in different solvents, the outcome was amitraz is most stable in 20 % acetonitrile. In addition, voltammetric analyses of amitraz were most reproducible in 20 % acetonitrile. 2,4-DMA was found to be stable in all the solvents investigated, however 20 % acetonitrile was selected for dissolving 2,4-DMA. In the presence of methanol or ethanol, 3-MC tends to be methylated or ethylated, respectively, which leads to the formation of an undesired methoxy-catechol derivative. 3-MC is soluble in water, and was opted for use in dissolving 3-MC.

Choice of supporting electrolyte

Reproducible and sensitive detection of amitraz was obtained by using 0.2 M Britton-Robinson (BR) buffer as the supporting electrolyte. Linearity in current response with increasing scan rate was observed for all the analytes, indicating the ease of electron migration to the electrode in BR buffer. In addition, 0.2 M BR buffer can be employed over a broad pH range (2 – 10). For the analyses of amitraz, DMF, 2,4-DMA and 3-MC, 0.2 M BR buffer was selected as the supporting electrolyte.

pH optima

Amitraz detection could be performed over a broad pH range (2 – 10). Current strength increased with acidity as oxidation potentials shifted to more positive values. However, at pH 2 – 5, hydrolysis of amitraz occurs rapidly (within minutes). In terms of current response linearity, sensitivity and reproducibility of current response, amitraz detection is best performed at pH 7. Double anodic waves attributed to 2,4-DMA oxidation were pH dependent. For analyses at pH 2 – 3, the first (primary) anodic wave was selected for analyses while the secondary wave at pH 4 – 9 was selected.

The general trend for 2,4-DMA analyses at a range of pH values was an increase in sensitivity and a shift in oxidation potentials to less anodic potentials with a shift towards more alkaline conditions. It is deduced that with regards to sensitivity and reproducibility of 2,4-DMA analyses, pH 4 – 8 is the ideal pH working range.

For 3-MC analyses regarding pH, under acidic conditions (pH 2 – 5), uniform current response was observed with a shift in oxidation potentials to less anodic potentials with increasing acidity. The oxidation wave may be attributed to oxidation of 3-MC to 3-methyl-*o*-benzoquinone (3-MBQ). At pH 6 and 7 the formation of a second anodic wave was attributed to dimer formation between 3-MBQ and 3-MC. This second wave became more dominant comrade to the first wave with an increase in alkalinity.

Linear increases in current response with regards to the square root of scan rate for amitraz, 2,4-DMA and 3-MC suggest that the migration to the electrode is diffusion controlled in a quiescent solution between the scan rates of 25 mV/s and 200 mV/s for amitraz, and 25 mV/s and 400 mV/s for 2,4-DMA and 3-MC.

Fouling of the working electrode surface

Without cleaning the electrode surface between scans, it was found that for amitraz the highest degree of electrode fouling occurred at low pH, with the rate of fouling decreasing with alkalinity.

Under acidic and alkaline conditions, adsorption of 2,4-DMA oxidation products led to passivation of the electrode surface. However, at neutral pH, increased electrodeposition of this aniline based compound occurs. Due to the formation of 3-MBQ under alkaline

conditions, fouling of the electrode was observed, attributed to irreversible adsorption of the oxidised species onto the electrode. Thus in order to obtain reproducible and sensitive results for each of the analytes, cleaning of the electrode surface is recommended between electrochemical scans.

Generation of standard curves for the analytes at pH optima

Extrapolated limits of detection for amitraz and 2,4-DMA were found to be 2.0×10^{-8} M and 1.0×10^{-8} M, respectively. Experimental limits of detection using differential pulse voltammetry were found to be 8.5×10^{-8} M for amitraz and 2.0×10^{-8} M for 2,4-DMA.

Linear standard curves of current *vs.* concentration were produced for amitraz between pH 3 and 10. For 2,4-DMA, linear standard curves were generated over a broad pH range (2 – 10), and for 3-MC linear standard curves were generated at pH 2 and 4, and pH10 for 3-MBQ.

Environmental monitoring of the analytes

Amitraz and 2,4-DMA were readily detected in spent cattle dip with minimal interference. In addition, amitraz and 2,4-DMA was detected in honey and milk. A decrease in sensitivity for amitraz, 2,4-DMA and 3-MC detection was noted in honey and milk, however standard curves could be generated of comparable linearity to studies in 0.2 M BR buffer of equivalent pH. The degree of fouling of the electrode surface by the analytes was identical to that of the pure samples of the analytes. The decrease in sensitivity for the analytes in honey and milk could be attributed to the low ionic strength of the matrices as opposed to interferents, suggesting that further optimisation could enhance analyses.

Chemical hydrolysis of amitraz

Amitraz was shown to hydrolyse readily to DMF at pH 3 and directly to 2,4-DMA at pH 2.0. In addition, the hydrolysis rate of amitraz at pH 2 and 3 has a half life of 20 minutes. These observations support those found in literature.

In addition, the breakdown of 2,4-DMA to 3-MC was proven electrochemically, where the decrease in the 2,4-DMA double anodic waves through utilisation by *Pseudomonas* spp. was associated with an increase in the oxidation peaks attributed to 3-MC.

Using electrochemical methods developed in this study, it is plausible to deduce a complete hydrolysis pathway for amitraz and 2,4-DMA. 2,4-DMA is a known recalcitrant; however these findings prove that in the presence of log phase *Pseudomonas* spp. 2,4-DMA is readily hydrolysed as an alternative carbon and nitrogen source. In summation, 2,4-DMA is recalcitrant in the environment, especially in water and on fruit, however the novelty of this study has not only proven that it is possible to rapidly hydrolyse 2,4-DMA by *Pseudomonas* spp. which could be found in cattle dip, but also that cyclic voltammetry can be used to monitor the hydrolysis of both amitraz and 2,4-DMA in a complex matrix, with comparable sensitivity and reproducibility to the more established techniques. The following fundamental pathway is presented:

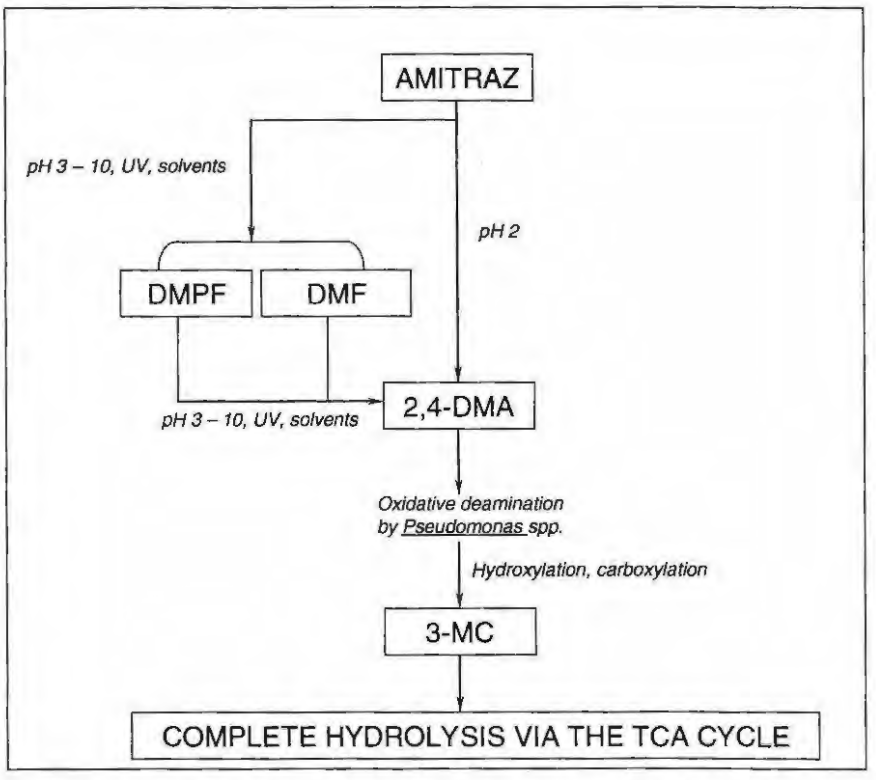

Scheme 8.1 Pathway for the complete hydrolysis of amitraz.

These studies thus pave the way for the utilisation of electrochemical methods for monitoring of pesticides in a range of environments and monitoring of the chemical and biological degradation with minimal interference and sample preparation.

8.2 FUTURE STUDIES

Fouling of the electrode surface during analysis of amitraz, DMPF, 2,4-DMA, 3-MC and 3-MBQ can be addressed through the use of disposable screen-printed electrodes (SPEs). Preliminary studies using a portable potentiostat with graphite SPEs have already commenced, using the PalmSens and screen printed electrodes (SPEs), which have shown comparable sensitivity and reproducibility to the results obtained in this study. In addition, the feasibility of modifying the working electrode surface of the SPEs with chemical modifiers, such as the well utilised metallophthalocyanines, for increased sensitivity could be assessed.

The feasibility of increasing selectivity of the SPEs for amitraz, DMF, 2,4-DMA, 3-MC and 3-MBQ using whole bacterial cells and isolated enzymes was investigated. Further comparison will be drawn on the sensitivity of the detection of the analytes of interest. Future studies regarding the incorporation of a hand-held sensor include adapting its portability and speed of analysis to an on-line monitoring system.

Characterisation of the *Pseudomonas* species isolated in this study, which will be achieved by sequencing highly conserved regions of the *Pseudomonas* genome, amplifying the area by polymerase chain reaction, and comparing it to sequences in databases such as BLAST. The *Pseudomonas* spp. are a potential source of molecules for the development of a microbial-based sensor for 2,4-DMA detection. Isolation of enzymes from this bacteria could also provide the biological component for 2,4-DMA biosensors. Furthermore, investigation of the bacteria as an agent in bioremediation of 2,4-DMA and other analytes found in industrial waste is viable. In achieving this, enzyme screening can be done to determine which enzymes are capable of hydrolysing 2,4-DMA. These enzymes could be isolated and over expressed using in place vector systems, and adopted to accelerated 2,4-DMA biodegradation.

In accordance, the feasibility of adapting the biological breakdown of 2,4-DMA by *Pseudomonas* spp. to industries, such as further breakdown of azo dyes used in textile and leather industries, and the breakdown of recalcitrant aniline derivatives from pharmaceutical industry waste may be assessed. Further concurrence of the breakdown pathway of 2,4-DMA by *Pseudomonas* spp. will be performed using NMR.

REFERENCES

Abell A, Juul S, Bonde JP (2000) Time to pregnancy among female greenhouse workers. *Scand. J. Work. Environ. Health.* 26: 131-136.

Abu-Basha EA, Yibchok-Anun S, Hopper DL, Walter HH (1999) Effects of the pesticide amitraz and its metabolite BTS 27271 on insulin and glucagon secretion from the perfused rat pancreas: involvement of α_{2D}-adrenergic receptors. *Metabolism.* 48: 1461-1469.

Altobelli D, Martire M, Maurizi S, Preziosi P (2001) Interaction of formamidine pesticides with the presynaptic α_2-adreonceptor regulating [^{3}H]noradrenaline release from rat hypothalamic synaptosomes. *Toxicol. Appl. Pharmacol.* 172: 179-185.

Amat AN, Arques A, Bossmann SH, Braun AM, Göb S, Miranda MA, Oliveros E (2004) Oxidative degradation of 2,4-xylidine by photosensitization with 2,4,6-triphenylpyrylium: homogeneous and heterogenous catalysis. *Chemosphere* 57: 1123-1130.

Ameno K, Fuke C, Ameno S, Kiriu T, Shinohara T, Ijiri I (1991) A rapid and sensitive quantitation of amitraz in plasma by gas chromatography with nitrogen-phosphorous detection and its application for pharmacokinetics. *J. Anal. Toxicol.* 15: 116 -118.

Arrebola FJ, Martínez Vidal JL, González-Rodríguez MJ, Garrido-Frenich A, Sánchez Morito N (2003) Reduction of analysis time in gas chromatography Application of low-pressure gas chromatography—tandem mass spectrometry to the determination of pesticide residues in vegetables. *J. Chromatogr. A.* 1005: 131-141.

Athawale AA, Milind BAD, Kulkarni V (1999) Spectroscopy and electrochemical properties of poly(2,5 dimethyl aniline) films. *Mater. Chem. Phys.* 60: 262-267.

Aydin K, Kurtoglu S, Poyrazoglu MH (1997) Amitraz poisoning in children: clinical and laboratory findings in eight cases. *Hum. Exp. Toxicol.* 16: 680-682.

Baker PB, Woods DR (1977) Cometabolism of the ixodicide amitraz. *J. Appl. Bacteriol.* 42: 187-196.

Bard AJ, Faulkner LR (1980) *Electrochemical methods. Fundamentals and applications.* Canada: John Wiley & Sons, Inc, pp 7-44, 86-91, 119-130.

Bell LS, Devlin JF, Gillham RW, Binning PJ (2003) A sequential zero valent iron and aerobic biodegradation treatment system for nitrobenzene. *J. Contam. Hydrol.* 66: 201-217.

Bernal JL, del Nozal M, Jiménez JJ (1997) Influence of solvent storage on the stability of acaricide standard stock solutions. *J. Chromatogr. A.* 765: 109-114.

Bilitewski U, Turner APF (2000) *Biosensors for environmental monitoring.* Netherlands: Harwood academic publishers, pp 6-12, 137-150, 248-277.

Bogdanov S (2003) Current status of analytical methods for the detection of residues in bee products. *Apiacta.* 38: 190-197.

Bogdanov S, Charrier JD, Imdorf A, Kilchenmann V, Fluri P (2002) Determination of residues in honey after treatments with formic and oxalic acid under field conditions. *Apidologie.* 33: 399-409.

Bogdanov S, Kilchenmann V, Imdorf A (1998) Acaricide residues in some bee products. *J. Apic. Res.* 37: 57-67.

Bolognesi C (2003) Genotoxicity of pesticides: a review of human biomonitoring studies. *Mutation Research.* 543: 251-272.

Campbell JK, Needham D (1984) A comparison of the metabolism of 14C-amitraz in rat, mouse, baboon and human. Unpublished report No. METAB/84/1 from FBC Ltd, Chesterford Park Research Station , Saffron Walden, Essex, UK.

Corta E, Bakkali A, Berrueta B, Vicente F (1999) Kinetics and mechanism of amitraz hydrolysis in aqueous media by HPLC and GC-MS. *Talanta* 48: 189-199.

Costa LG, Olibet G, Wu DS (1989) Acute and chronic effects of the pesticide amitraz on alpha 2-adrenoreceptors in mouse brain. *Toxicol. Letters.* 47: 135-143.

da Silva Vaz Jr I, Lermen TT, Michelon A, Ferreira CAS, de Freitas DRJ, Termignoni C, Masuda A (2004) Effect of acaricides on the activity of *Boophilus microplus* glutathione S-transferase. *Vet. Parasitol.* 119: 237-245.

Dearfield KL, McCarroll NE, Protzel A, Stack HF, Jackson MA, Waters MD (1999) A survey of EPA/OPP and open literature data on selected pesticide chemicals tested for mutagenicity: I. introduction and first ten chemicals. *Mutat. Res.* 297: 197-233.

Eastmond DA (2000) Benzene-induced genotoxicity: a different perspective. *J. Toxicol. Environ. Health.* 61: 353-356.

El-Naggar MA, El-Aasar SA, Barakat KI (2004) Bioremediation of crystal violet using air bubble bioreactor packed with *Pseudomonas aeruginosa. Wat. Res.* 38: 4313-4322.

Evans PD, Gee JD (1980) Action of formamidine pesticides on octopamine receptors. *Nature.* 287: 60-62.

Fakhari AR, Nematollahi D, Moghaddam AB (2005) Mechanistic study of electrochemical oxidation of catechols in the presence of 4-hydroxy-1-methyl-2(1H)-quinolone: Application to the electrochemical synthesis. *Electrochim. Acta.* 50 : 5322-5328.

Floris I, Satta A, Garau VL, Melis M, Cabras P, Aloul N (2001) Effectiveness, persistence, and residue of amitraz plastic strips in the apiary control of *Varroa destructor. Apidologie.* 32: 577-585.

Foil LD, Coleman P, Eisler M, Fragoso-Sanchez H, Garcia-Vazquez Z, Guerrero FD, Jonsson NN, Langstaff IG, Li AY, Machila M, Miller RJ, Morton J, Pruett JH, Torr S (2004) Factors that influence the prevalence of acaricide resistance and tick-borne diseases. *J. Vet. Parasitol.* 125: 163-181.

Foster LJR, Kwan BH, Vancov T (2004) Microbial degradation of the organophosphate pesticide, Ethion. *FEMS Micribiol. Lett.* 240: 49-53.

Garrity GM, Boone DR, Castenholz RW (2002) *Bergey's Manual of Systematic Bacteriology.* 2nd ed. Vol 2, Springer-Verlag, New York, pp 23-56

George JE, Davey RB, Ahrens EH, Pound JM, Drummond RO (1998) Efficacy of amitraz (Taktic® 12.5% EC) as a dip for the control of *Boophilus microplus* (Canestrini) (Acari: Ixodidae) on cattle. *Prev. Vet. Med.* 37: 55-67.

Ghazali FM, Rahman RNZA, Salleh AB, Basri M (2004) Biodegradation of hydrocarbons in soil by microbial consortium. *Int. biodeter. biodegradation.* 54: 61-67.

Golabi SM, Nematollahi D (1997) Electrochemical study of catechol and some 3-substituted catechols in the presence of 4-hydroxy coumarin: application to the electro-organic synthesis of new coumestan derivatives. *J. Electroanal. Chem.* 420: 127-134

Habibi D, Nematollahi D, Alizadeh A, Hesari M (2005) Oxidative coupling of in-situ generated o-benzoquinones with 4-hydroxy-6-methyl-2-pyrone. *Hetero. Comms.* 11: 145-148.

Hall JE, Ahluwalia H, Hampson P (1975) A study of the effects of oral administration of a metabolite (BTS 27 271) of amitraz to volunteers. Schering Agrochemicals Ltd. UK.

Hapeman CJ, Pierpoint AC, Torrents A (2002) Deactivation, disposal, and management of amitraz dip-vats. *Am. Chem. Soc.* ENVR 24: 448-451.

Hashemazadeh H, Hollingworth RM, Voliva A (1985) Receptor for ^{3}H-octopamine in the adult firefly light organ. *Life Sci.* 37: 433-440.

Hodgson E, Silver IS, Butler LE, Lawton MP, Levi PE (1991) Metabolism. In: Hayes WJ, Laws ER, eds. *Handbook of Pesticides Toxicology*, San Diego: Academic Press, pp. 106–167.

Hornish R, Clasly M, Nappier JL, Nappier JM, Hoffman GA (1984) Total residue analysis of amitraz. Residues in fruit and soil samples by electron capture gas chromatography. *Agric. Food. Chem.* 32: 1219-1233.

Hsu WK, Kakuk TJ (1984) Effect of amitraz and chlordimeform on heart rate and pupil diameter: mediated by α_2-adrenoreceptors. *Toxicol. Appl. Pharmacol.* 73: 411-415.

Hugnet C, Buronfosse F, Pineau X (1996) Toxicity and kinetics of amitraz in dogs. *Am. J. Vet. Res.* 57: 1506-1510.

Ibrahim MS, El-Maazawi MS, Al-Magboul KM, Kamal MM (2001) Determination of amitraz pesticide by adsorptive stripping voltammetry on the hanging mercury drop electrode. *Mikrochim. Acta.* 137: 215-220.

Iwata Y, Walker GP, O'Neal JR, Barkley JH (1985) Residues of acephate, amitraz, chlorpyrifos and formetanate hydrolchloride on and in fruits after low-volume application to orange trees. *Pestic. Sci.* 16: 172-178.

Jacques RJS, Santos EC, Bento FM, Peralba MCR, Selbach PA, Sá ELS, Camargo FAO (2005) Anthracene biodegradation by *Psuedomonas* sp. Isolated from a petrochemical sludge landfarming site. *Int. biodeter. biodegradation.* 56: 143-150.

Jiménez JJ, Bernal JL, del Nozal MJ, Alonso C (2004) Extraction and clean-up methods for the determination of amitraz total residues in beeswax by gas chromatography with electron capture detection. *Anal. Chim. Acta.* 524: 271-278.

Jiménez JJ, Bernal JL, Nozal MJ, Toribido L (1997) Characterization and monitoring of amitraz degradation products in honey. *J. High Resol. Chromatogr.* 20: 81-84.

John U, Nair KPR (2004) Liquid phase overtone spectral investigations of 2,6-dimethylaniline and 2,4-dimethylaniline—evidence for steric nature of the *ortho* effect and the consequent base weakening. *Spectrochim. Acta.* 60: 2337-2341.

Jonsson NN, Mayer PE, Green PE (2000) Possible risk factors on Queensland dairy farms for acaricide resistance in cattle tick (*Boophilus microplus*) *J. Vet. Parasitol.* 88: 79-92.

Jorens PG, Zandijk E, Belmans L (1997) An unusual poisoning with the unusual pesticide amitraz. *Hum. Exp. Toxicol.* 16: 600-601.

Kagaruki LK (1996) The efficacy of amitraz against cattle ticks in Tanzania. *Onderstepoort J. Vet. Res.* 63: 91-96.

Kao CM, Liu JK, Chen YL, Chai CT, Chen SC (2005) Factors affecting the biodegradation of PCP by *Pseudomonas mendocina* NSYSU. *J. Hazar. Mater.* B124: 68-73.

Kargi F, Eker S (2004) Toxicity and batch biodegradation kinetics of 2,4 dichlorophenol by pure *Pseudomonas pudita* culture. *Enzyme Microb. Technol.* 35: 424-428.

Kennel O, Prince C, Garnier R (1996) Four cases of amitraz poisoning in humans. *Vet. Hum. Toxicology.* 38: 28-30.

Kissinger PT, Heinemann WR (1996) *Laboratory techniques in electroanalytical chemistry,* 2nd edn. New York: Marcel Dekker, Inc, pp 11-48, 52-60, 293-305, 443-466.

Korbi BH, Tapsoba I, Benkhoud ML, Boujel K (2004) Electroxidation of *ortho*-substituted aromatic amines mechanistic investigation. *J. Electroanal. Chem.* 571: 241-246.

Korta E, Bakkali A, Berrueta LA, Gallo B, Vicente F, Bogdanov S (2003) Determination of amitraz and other acaricide residues in beeswax. *Anal. Chim. Acta.* 475: 97-103.

Kulkarni M, Chaudhari A (2005) Biodegradation of *p*-nitrophenol by *P. pudita. Bioresour. Technol.* Article in press.

Li AY, Davey RB, Miller RJ, George JE (2004) Detection of amitraz resistance in the southern cattle tick, *Boophilus microplus* (Acaril Ixodidae). *J. Med. Ent.* 41: 193-200.

Lodesani M, Pellacani A, Bergomi S, Carpana E, Rabitti T, Lasagni P (1992) Residue determination for some products used against *Varroa* infestation in bees. *Apidologie.* 23: 257-272.

Mafatle T, Nyokong T (1997) Use of cobalt(II) phthalocyanine to improve the sensitivity and stability of glassy carbon electrodes for the detection of cresols, chlorophenols and phenol. *Anal. Chim. Acta.* 354: 307-314.

Marques MM, Mourato LLG, Amorim MT, Santos MA, Melchior Jr WB, Beland FA (1997) Effect of substitution site upon the oxidation potentials of alkylanilines, the mutagenicities of N-hydroxyalkylanilines, and the conformations of alkylaniline-DNA adducts. *Chem. Res. Toxicol.* 10: 1266.

Martel A, Zeggane S (2002) Determination of acaricides in honey by high-performance liquid chromatography with photodiode array detection. *J. Chromatogr. A.* 954:173-180.

McConnell LL, Torrents A, Sparling D, Fellers G, Cowman D (2002) Atmospheric transport and deposition of agricultural pesticides to sensitive ecosystems. *S.E. Reg. Am. Chem. Soc.* 439.

Mester Z, Sturgeon R, Pawliszyn J (2001) Solid phase microextraction as a tool for trace element speciation. *Spectrochim. Acta Part B: Atomic Spectroscopy.* 56: 233-260.

Mizoguchi T, Adams RN (1962) Anodic oxidation studies of N,N-dimethylaniline. I. Voltammetric and spectroscopic investigations at platinum electrodes. *J. Am. Chem. Soc.* 84: 2058-2061.

Nachiyar CV, Rajakumar GS (2004) Mechanism of Navitan Fast Blue S5R degradation by *Pseudomonas aeruginosa*. *Chemosphere*. 57: 165-169.

Nachiyar CV, Rajkumar GS (2003) Degradation of tannery and textile dye, Navitan Fast Blue S5R by *Pseudomonas aeruginosa*. *World J. Microbiol. Biotechnol.* 19: 609-614.

Nakamura Y, Hasegawa Y, Tonogai Y, Ito Y (1989) Simultaneous determination of 8 kinds of acaricides in agricultural products by gas chromatography. *Eisei Kagaku*. 35: 466-475.

Nematollahi D, Hesari M (2005) Electrochemical synthesis of amino-substituted 1,2-benzoquinone derivatives. *J. elect. Chem.* 577: 197-203.

Nematollahi D, Rahchamani RA (2002) Electro-oxidation of catechols in the presence of benzenesulfinic acid. Application to electro-organic synthesis of new sulfone derivatives. *J. Electroanal. Chem.* 520: 145-149.

Osano O, Admiraal W, Klamer HJC, Pastor D, Bleeker EAJ (2002) Comparative toxic and genotoxic effects of chloroacetanilides, formamidines and their degradation products on *Vibrio fischeri* and *Chironomus riparius*. *Environ. Pollut.* 119: 195-202.

Park H, Lim S, Chang YK, Livingstone AG, Kim H (1999) Degradation of chloronitrobenzenes by a coculture of *Pseudomonas pudita* and a *Rhodococcus* sp. *Appl. Environ. Microbiol.* 65: 1083-1091.

Peres CM, Naveau H, Agathos SN (1998) Biodegradation of nitrobenzene by its simultaneous reduction into aniline and mineralization of the aniline formed. *Appl. Microbiol.. biotechnol.* 49: 343-349.

Perrin DD, Dempsey B (1974) *Buffers for pH and metal ion control*. London: Chapman and Hall, pp 55-64.

Pierpoint. AC, Hapeman CJ, Torrents A (1997) Kinetics and mechanism of amitraz hydrolysis. *J. Agric. Chem.* 45: 651-654.

Pinheiro HM, Touraud E, Thomas O (2004) Aromatic amines from azo dye reduction: status review with emphasis on direct UV spectrophotometric detection in textile industry wastewaters. *Dyes and Pigments*. 61: 121-139.

Pritchard J, Law K, Vakurov A, Millner P, Higson SPJ (2004) Sonochemically fabricated enzyme microelectrode arrays for the environmental monitoring of pesticides. *Biosens. Bioelectron.* 20: 765-772.

Pugliese P, Moltó JC, Damiani P, Marín R, Cossignani L, Mañes J (2004) Gas chromatographic evaluation of pesticide residue contents in nectarines after non-toxic washing treatments. *J. Chromatogr. A*. 1050:185-191.

Purwaningsih IS, Hill GA, Headley JV (2004) Mass transfer and bioremediation of naphthalene particles in a roller bioreactor. *Water Res.* 38: 2027-2034.

Queiroz MEC, Valadão CAA, Farias A, Carvalho D, Lanças FM (2003) Determination of amitraz in canine plasma by solid-phase microextraction-gas chromatography with thermionic specific detection. *J. Chromatogr. B*. 794: 337-342.

Ralide AF (1992) The epidemiology of poisoning: a monitoring program for developing countries. *Vet. Hum. Toxicol.* 34: 261-263.

Rice LG (1984) Rapid separation of pesticides by high performance liquid chromatography with 3-µm columns. *J. Chromat.* 317: 523-526.

Robinson J, Osteryoung RA (1980) An investigation into the electrochemical oxidation of some aromatic amines in the room-temperature molten salt system aluminium chloride–*n*-butylpyrinium chloride. *Am. Chem. Soc.* 102: 4415-4420.

Roder T (1995) Pharmacology of the octopamine receptor form locust central nervous tissue (OAR3). *Br. J. Pharmacol.* 114: 210-216.

Rojas A, Ojeda ME, Barraza X (2000) Congenital malformations and pesticide exposure. *Rev. Med. Chil.* 128: 399-404.

Rossi S, Dalpero AP, Ghini S, Colombo R, Sabatini AG, Girotti S (2001) Multiresidual method for the gas chromatographic analysis of pesticides in honeybees cleaned by gel permeation chromatography. *J. Chromatogr. A.* 905: 223-232.

Roy PR, Okajima T, Ohsaka T (2004) Simultaneous electrochemical detection of uric acid and ascorbic acid at a poly(*N,N*-dimethylaniline) film-coated GC electrode. *J. Electroanal. Chem.* 561: 75-82.

Rozkov A, Vassiljeva I, Kurvet M, Kahru A, Preis S, Kharchenko A, Krichevskaya M, Liiv M, Käärd A, Vilu R (1999) Laboratory study of bioremediation of rocket fuel-polluted groundwater. *Wat. Res.* 33: 1303-1313.

Rubinstein I (1995) *Physical electrochemistry. Principles, methods and applications.* Marcel Dekker, Inc. New York, pp 27-81.

Rule S, Ianga Z (2005) HSRC client survey 2004. Report to the Understanding of Biotechnology

Seymour EH, Lawrence NS, Beckett EL, Davis J, Comptom RG (2002) Electrochemical detection of aniline: an electrochemically initiated pathway. *Talanta.* 57: 233-242.

Singh GJ, Orchard I, Loughton BG (1990) Octopamine-like actions of formamidines on hormone secretion in the locust *Locusta migratoria. Pest. Biochem. Physiol.* 16: 249-255.

Stamper DM, Tuovinen OH (1998) Biodegradation of the acetanilide herbicides Alachlor, Metachlor, and Propachlor. *Crit. rev. micro.* 24: 1-22.

Stewart MJ, Moar JJ, Steenkamp P, Kokot M (1999) Findings in fatal cases of poisoning attributed to traditional remedies in South Africa. *Forensic Science International.* 101: 177-183.

Suatoni JC, Snyder RE, Clark RO (1961) Voltammetric studies of phenol and aniline ring substitution. *Anal. Chem.* 33: 1894-1897.

Taccheo BM, de Paoli M, Spessotto C (1988) Determination of total amitraz residue in honey by electron capture capillary gas chromatography – a simplified method. *Pest. Sci.* 23: 131-144.

Taylor RF, Schultz JS (2003) *Handbook of chemical and biological sensors.* Bristol: Institute of Physics publishing, pp 123-136.

Torres CM, Picó Y, Mañes J (1996) Determination of pesticide residues in fruit and vegetables. *J. Chromatogr. A.* 754: 301-331.

Tseng S, Chang P, Chou S (1999) Determination of amitraz residue in fruits by high performance liquid chromatography. *J. Food and Drug Analysis.* 7: 225-232.

Wackett LP, Hershberger CD (2001) *Biocatalysis and biodegradation.* Washington D.C: ASM Press, pp 39-45, 115-127.

Wang J (1994) *Analytical Electrochemistry.* New York: VCH, pp 15-42.

Wang J, Mahmoud JS (1986) Stripping voltammetry with adsorptive accumulation for trace measurements of titanium. *J. Electroanal. Chem.* 208: 383-394.

Weissenberger DD, Harrington DS, Armitage JO (1990) B-cell neoplasia - a conceptual understanding based on the normal humoral immune response. *Pathol. Annu.* 25:99-115.

Whysner J (2000) Benzene-induced genotoxicity. *J. Toxicol. Environ.* Health. 61:347-351.

Zahm SH, Ward MH, Blair A (1997) Pesticides and childhood cancer. *Occup. Med. State. Art. Rev.* 12: 269-289.